Eesti Maaülikool
Estonian University of Life Sciences

FUEL SUPPLY SYSTEM OF PISTON ENGINE WORKING ON LIQUID BIOFUELS

VEDELATE BIOKÜTUSTEGA TÖÖTAVA KOLBMOOTORI TOITESÜSTEEM

RISTO ILVES

A Thesis
for applying for the degree of Doctor of Philosophy
in Production Engineering

Väitekiri
Filosoofiadoktori kraadi taotlemiseks
tootmistehnika erialal

Tartu 2014

EESTI MAAÜLIKOOL
ESTONIAN UNIVERSITY OF LIFE SCIENCES

Eesti Maaülikool
Estonian University of Life Sciences

FUEL SUPPLY SYSTEM OF PISTON ENGINE WORKING ON LIQUID BIOFUELS

VEDELATE BIOKÜTUSTEGA TÖÖTAVA KOLBMOOTORI TOITESÜSTEEM

RISTO ILVES

A Thesis
for applying for the degree of Doctor of Philosophy
in Production Engineering

Väitekiri
Filosoofiadoktori kraadi taotlemiseks
tootmistehnika erialal

Tartu 2014

Institute of Technology,
Eesti Maaülikool, Estonian University of Life Sciences

According to verdict No 36 of June 20, 2014, the Doctoral Committee of the Engineering Sciences of the Estonian University of Life Sciences has accepted the thesis for the defence of the degree of Doctor of Philosophy in Production Engineering.

Opponent: **Professor Gvidonas Labeckas**, DSc (Eng)
Power and Transport Machinery Engineering
Institute at Aleksandras Stulginskis University.

Opponent: **Researcher Vladimir Hönig**, PhD
Faculty og Agrobiology, Food and Natural Resources, Department of Chemistry, Czech University of Life Sciences Prague.

Supervisor: **Professor Jüri Olt**, DSc (Eng)
Institute of Technology
Estonian University of Life Sciences

Defence of the thesis:
Estonian University of Life Sciences, room B136, Kreutzwaldi 56, Tartu
on 3 October, 2014, at 12.15.

Publication of this thesis is supported by the
Estonian University of Life Sciences.

© Risto Ilves, 2014
ISBN 978-9949-536-58-0 (trükis)
ISBN 978-9949-536-59-7 (pdf)

CONTENTS

LIST OF ORIGINAL PUBLICATIONS 7
INTELLECTUAL PROPERTY 8
ABBREVIATIONS AND SYMBOLS 9
INTRODUCTION 14
1. THEORETICAL BACKGROUND 16
   1.1. Study of Prior Art of fuel supply systems 16
      1.1.1. General background 16
      1.1.2. The types of fuel supply systems of a spark ignition engine 16
      1.1.3. The fuel supply system of a compression ignition engine 18
   1.2. The impact of bioethanol on the combustion process of a piston engine 20
   1.3. Discussion 30
2. THE AIM AND TASKS OF THE STUDY 31
3. THE DEVELOPMENT OF A FUEL SUPPLY SYSTEM OF AN ENGINE RUNNING ON BIOFUELS 35
   3.1. The requirements for a fuel supply system of an engine running on biofuels 35
   3.2. The solutions of the developed fuel supply systems 35
      3.2.1. The method for the formation of air-fuel mixture in a piston engine and a complex fuel supply system 35
      3.2.2. An additional fuel supply system for dosing liquid biofuels into an piston engine 37
   3.3. The advantages and disadvantages of the developed fuel supply systems 39
   3.4. The construction and operating parameters of a prototype device of the pulveriser fuel supply system 39
   3.5. The quality of the air-fuel mixture formed by the pulveriser fuel supply system and its suitability for dosing into an engine 49
   3.6. The development phases and solutions of the developed fuel supply system 55
   3.7. A model for selecting operating parameters of a pulveriser fuel supply system 61
   3.8. Conclusion 68

4. PRELIMINARY TESTS OF THE PULVERISER FUEL SUPPLY SYSTEM ON COMPRESSION AND SPARK IGNITION ENGINES 69
4.1. Methods of engine testing 69
4.2. The pulveriser fuel supply system on a compression ignition engine 77
4.3. Conclusions 85
4.4. The pulveriser fuel supply system for dosing bioethanol in a spark ignition engine 86
4.5. Conclusions 92
5. THE CALCULATION AND ANALYSIS OF MEASUREMENT UNCERTAINTY 93
5.1. The calculation of measurement uncertainty 93
5.2. The uncertainty of test measurement results 94
SUMMARY AND CONCLUSIONS 101
REFERENCES 106
KOKKUVÕTE 111
ACKNOWLEDGEMENTS 115
CURRICULUM VITAE 116
ELULOOKIRJELDUS 118
ETTEKANDED 120

LIST OF ORIGINAL PUBLICATIONS

I Olt, J.; Mikita, V.; **Ilves, R.**; Küüt, A. 2011. Motor method evaluation of fuel-air mixtures created by using qualitative and quantitative methods. In: Efficient and safe production processes in sustainable agriculture and forestry: XXXIV CIOCTA-CIGR V Conference Vienna - Austria.

II Küüt, A.; **Ilves, R.**; Mikita, V.; Olt, J. 2012. The characteristics of bioethanol fuel in internal combustion engines with compression-ignition. 40th International symposium "Actual Tasks on Agricultural Engineering, Opatija, Kosutic, S., 2012, 117–125.

III **Ilves, R.**; Küüt, A.; Mikita, V.; Olt, J. 2012. The development of an additional fuel supply system to an internal combustion engine. In: Proceedings of the 8th International Conf. of DAAAM Baltic Industrial, 19–21 April 2012, Tallinn, 146–151.

IV **Ilves, R.**; Olt, J. 2012. Study of prior art of spark ignition engine fuel supply system. Agronomy Research, 10(1), 55–74.

V **Ilves, R.**; Küüt, A.; Kikas, T.; Olt, J. 2014. The Influence of Bioethanol Small Fuel Drops Size Air-Fuel Mixture on Spark Ignition Engine's Combustion Process. Agronomy Research, 12(2), 341–350.

The contribution of the author to the papers:

Paper	Study design	Data collection	Data processing	Manuscript preparation
I	JO, VM, **RI**, AK,	JO, VM, **RI**, AK,	JO, VM, **RI**, AK,	JO, VM, **RI**, AK
II	JO, AK **RI,** VM, ,	VM, AK**, RI**	AK	AK, JO, **RI**, VM
III	**RI**, AK, JO, VM	AK, JO, **RI**	**RI**, AK	**RI**, AK, JO, VM
IV	**RI,** JO	**RI,** JO	**RI,** JO	**RI,** JO
V	**RI,** AK, JO	**RI,** AK	**RI,** AK, TK, JO	**RI,** TK, AK, JO

RI – Risto Ilves, AK – Arne Küüt, JO – Jüri Olt, TK – Timo Kikas, VM – Villu Mikita.

INTELLECTUAL PROPERTY

I Title: The formation method of air-fuel mixture of reciprocating engine and flexible fuel system

Patent number:	EE 05665 B1
Filing date of the application:	17.03.2011
Priority date:	17.03.2011
Publication date:	17.06.2013
Inventor name:	Olt, J., Küüt, A., **Ilves, R.**

II Title: An additional fuel supply system for dosing liquid biofuels into an piston engine

Patent number:	EE 05693B1
Filing date of the application:	29.12.2011
Priority date:	29.12.2011
Publication date:	16.12.2013
Inventor name:	**Ilves, R.**, Küüt, A., Mikita, V., Olt, J.

Patent application:

III Title: An additional fuel supply system for dosing liquid biofuels into an piston engine

Patent application:	P201200024
Filing date of the application:	28.11.2012
Priority date:	28.11.2012
Publication date:	15.08.2014
Inventor name:	**Ilves, R.**, Põri, T., Olt, J.

The contribution of the author to the patents:

Document	Study design	Preparation and elaboration activities	Study of prior art	Application preparation
I	**RI**, JO, AK	AK, **RI**, JO	AK, JO, **RI**	JO, **RI**, AK
II	**RI**, AK, VM, JO	**RI**, AK, VM, JO	**RI**, AK, JO	**RI**, AK, JO
III	**RI**, TP, JO	TP, **RI**, JO	**RI**, TP, JO	**RI**, TP, JO

RI – Risto Ilves, AK – Arne Küüt, JO – Jüri Olt, VM – Villu Mikita, TP – Taavi Põri.

ABBREVIATIONS AND SYMBOLS

Abbreviations

ATDC	after top dead center
BBDC	before bottom dead center
BE	bioethanol
BTDC	before top dead center
CAD	crank angle degree
DF	diesel fuel
DSA	diesel supply apparatus
EC	exhaust valve closed
EO	exhaust valve open
FSS	fuel supply system
HCCI	homogeneous charge compression ignition
IC	intake valve closed
IO	intake valve open

Symbols

Latin

A	combustion chamber surface area
A_5	sectional area of the fuel line
A_a	sectional area of the pipe between the fuel supply system corps and the air filter
A_b	sectional area of the intake manifold
A_n	nozzle minimum area
A_{pul}	the sectional area of the fuel supply system corps
a	constant of intensity of charge motion
B_f	fuel consumption
B_{f1}, B_{f2} and B_{f3}	amount of pilot injection
b	constant of intensity of charge motion (b = 0.7 with normal combustion)
b_e	specific fuel consumption
b_i	indicated specific fuel consumption
C_d	discharge coefficient
c_p	specific heat at constant pressure
c_v	specific heat at constant volume
D_{32}	Sauter's mean diameter
D_{43}	Herdan mean diameter
D_{50}	mass median diameter

D_{90}	fuel droplet diameter of which 90% of droplets are smaller
D_{10}	arithmetic mean diameter
d	mean diameter of fuel droplets
d^2	relation between the mean diameter of fuel droplets and the area
d^3	ratio between the mean diameter of fuel droplets and volume
d_{cb}	cylinder bore
d_d	nozzle diameter
d_{fop}	diameter of the fuel flow passage of pulveriser injector
d_{len}	lens diameter
F	force affecting the sensor
h_c	sensible enthalpy of injected fuel
h_{cor}	heat-transfer coefficient
i	test number
i_c	cylinder number
k_j	coverage factor
k	thermal conductivity
l	connecting rod length
l_{tb}	length of test stand force arm
m	gas mass in cylinder
m_c	mass of the air-fuel mixture that is directed to the cylinder in one work cycle
m_f	the amount of fuel consumed during the test
m_{fr}	fuel flow rate
m_n	measurement number
m_{spy}	measure range of fuel droplets measurement device
m_{spyd50}	the measure range of the measurement device of fuel droplets during the measurement of parameter D_{50}
N	number of fuel droplets
N_c	number of work cycles
N_i	number of droplets in the size range
N_k	the number of fuel droplets per unit volume
n_d	range of test stand rotational speed
n_e	engine crankshaft rotational speed
P_e	engine power
P_i	Indicated power
P_{fr}	friction power
p	combustion pressure
$p_{1\text{-}5}$	pressure in different sections of the pulveriser injector
p_3	pressure in the pulveriser injector nozzle

p_4	pressure in the injection orifice
p_{ac}	the pressure in the pipe between the fuel supply system corps and the air filter
p_a	compressed air pressure
p_{an}	underpressure
p_b	pressure in the intake manifold
p_{co}	compression
p_e	mean effective pressure
p_{env}	environmental pressure
p_f	fuel pressure
p_{fr}	friction mean effective pressure
p_i	indicated pressure
p_{pul}	pressure in the pulveriser fuel supply corps
p_z	maximum value of the combustion pressure
r_{cr}	crank radius
r_{fd}	droplet radius in the air-fuel mixture
Q_1	compressor capacity
Q_n	net heat release
$Q_{n.\phi-1}$	heat release
Q_{pul}, Q_a, Q_b	the amount of air sucked into the engine in different parts of the fuel supply system
$Q_{f.teor}$	calorific value
$Q_{n.teor}$	gross heat released
q	injection capacity or fuel amount
s_a	distance from the pulveriser injectors to the intake manifold
s_{aop}	length of injection orifices
s_d	nozzle length
s_p	distance between the pulveriser injectors
T	temperature in cylinder
T_{com}	combustion temperature
T_g	mean combustion gas temperature
T_{wall}	mean cylinder wall temperature
T_e	torque
T_{env}	air temperature
t	time for rotating the crank
t_{mix}	time of mixing of the air-fuel mixture in the system corps
t_o	opening time
t_t	measurement time
t_v	evaporation time
t_{Qn}	heat release intensity

U	expanded uncertainty
U_A	standard deviation of the measurement results
U_B	uncertainty of the measurement device
U_c	combined standard uncertainty
U_{BBE}	B-type uncertainty in case of bioethanol droplet measurements
U_{BD}	B-type uncertainty at tests of dosers' capacity
U_{BE}	expanded uncertainty at measurement of bioethanol droplet diameter
U_{Bp}	B-type uncertainty of combustion pressure measurement results
U_{CBE}	combined standard uncertainty at measurement of bioethanol fuel droplet diameter
U_{ABE}	standard deviation during measurement of bioethanol fuel droplets D_{50}
u	specific internal energy
V_c	cylinder volume
V_{cp}	combustion chamber volume
V_f	fuel quantity directed into the cylinder in one work cycle
$v_{1\text{-}5}$	air flow velocity
v_a	air flow velocity in the pipe between the fuel supply system corps and the air filter
v_{afm}	air-fuel mixture combustion velocity
v_b	air flow velocity in the intake manifold
v_p	piston speed
v_{pul}	air flow velocity in the pulveriser fuel supply system corps
W_n	net indicated work per cycle
x_i	measurement result i
$\bar{x}$	the average of the measurement results
$\frac{\mathrm{d}Q_n}{\mathrm{d}\varphi}$	heat release rate
$\frac{\mathrm{d}(mu)}{\mathrm{d}t}$	fuel mass burning rate
$\frac{\mathrm{d}Q_{ht}}{\mathrm{d}t}$	heat transfer
$\frac{\mathrm{d}m}{\mathrm{d}t}$	mass flow rate
$\frac{\mathrm{d}U}{\mathrm{d}t}$	maximum internal energy of system materials

Greek

α	flow coefficient
α_{com}	combustion constant
α_{maxW}	absolute error of the weighing machine CAS CI-2001A
α_i	ignition angle
α_{max}	absolute error of the measurement device
β	the ratio of opening diameters
γ_{hr}	ratio of specific heats
γ_{hrbe}	ratio of specific heats of bioethanol
γ_{hrd}	ratio of specific heats of diesel fuel
Δp	pressure difference
Δp_a	compressed air transfer step
Δp_f	injection pressure
Δs_p	transfer step of distance between injectors
ΔV	cylinder volume variation
λ	thermal conductivity
λ_{afr}	stoichiometric fuel-gas ratio
η_e	engine efficiency
η_f	fuel conversion efficiency
η_{gb}	gear ration
η_i	indicator efficiency
η_t	thermal efficiency
η_v	volumetric efficiency
ν_i	viscosity
ρ_{air}	air density
ρ_{fuel}	fuel density
ρ_{afm}	density of air-fuel mixture
σ_{be}	bioethanol proportion in air-fuel mixture
σ_d	diesel fuel proportion in air-fuel mixture
τ_e	engine stroke cycle
τ_f	time of fuel consumption measurement
τ_d	ignition delay
φ	crank angle
φ_b and φ_{end}	the rotational angles of the crankshaft signifying the beginning and end of the combustion process
μ	dynamic viscosity

INTRODUCTION

Biofuels have progressively been started to use as engine fuels worldwide. This is conditioned by both increasingly strict environmental regulations so as to decrease the impact of exhaust gas emission on the ozone layer as well as the decrease in oil resources. For that reason, directives effective in the European Union establish the wider use of biofuels and reduction in the exhaust gas emissions. In Estonia, the directive 2009/28/EC states that by 2020, 10% of fuel used in transportation must be produced from renewable raw material.

Several alternative engine fuels have been taken into use, such as biomethanol, bioethanol, vegetable oils, biodiesel, and hydrogen. One of the most successful countries in using biofuels as engine fuels is Brazil where mostly first generation biofuels are used (Harndorf et al., 2008). Nevertheless, the use of biofuels as engine fuels has remained modest. This could be due to the complexity and costliness of producing biofuels as well as the issues which may arise when using biofuels in an engine.

Different biofuels may bring about various issues in engines. These issues could be divided into 1) technical, e.g. the wearing of the fuel supply system; 2) technological, e.g. excessive soot in the engine, the flowability of fuel in the fuel supply system; 3) environmental, e.g. the increase in the exhaust gas emission. The problems most commonly concern the fuel supply system, which functions include forming the air-fuel mixture and directing it into the engine cylinder. The wearing of the precise work surfaces of fuel supply apparatuses intensifies when biofuels are used, which can cause these surfaces to stick. This results in the formation of a poor quality air-fuel mixture which cannot be ignited in the engine cylinder without additional energy and which does not burn up completely. As a result, there is an increase in the exhaust gas emission, which is a severe issue with respect to environmental concerns.

Most commonly used piston engines can be divided into compression and spark ignition engines. In these engines, diesel fuel and gasoline are used. The quality of both of these fuels has to meet certain requirements. The properties of a fuel determined by standard are viscosity, density, lubricate properties, etc (EVS-EN 590:2009, EVS-EN 228:2012). The fuel supply systems of compression and spark ignition engines have been

developed to run on the abovementioned standard fuels, thus, they are sensitive to water, acids, and solid components in the fuel. In addition, the viscosity and density affect the sprayability and evaporation of the fuel. Therefore, different fuel supply systems need to be used for different fuels in order to guarantee the formation of a good quality air-fuel mixture and the durability of the fuel supply system.

Biofuels can be divided into standard biofuels, e.g. E85 and biodiesel, and substandard biofuels, e.g. bioethanol with water content and rapeseed oil. The production of these fuels requires less energy and is less complex than the one of standard fuels; however, using these as engine fuels is more sophisticated. Therefore, it is necessary to seek for technical possibilities for using a fuel which production is more competitive.

The aim of the current thesis is to describe the process of developing a novel fuel supply system. The novelty of this particular fuel supply system lies in its ability to dose different fuels into different engines (spark and compression ignition engine). The fuel supply system could be used either as the main fuel supply system or as an additional fuel supply system. This new system would enable agricultural companies to use self-made biofuels as engine fuels, which would in turn lessen the reliance on the system of distribution of oil products.

1. THEORETICAL BACKGROUND

1.1. Study of Prior Art of fuel supply systems

1.1.1. General background

Nowadays, the fuel supply systems of compression and spark ignition engines have been developed in a similar manner, i.e. the fuel is injected directly into the cylinder at a high pressure. In most cases, common rail fuel supply systems and unit injectors are used in compression ignition engines. The differences between compression and spark ignition engines lie in the pressure used in the fuel supply system, the compression ratio, and the method of igniting the air-fuel mixture (Robert Bosch GmbH (1); Robert Bosch GmbH (2)). The fuel supply systems have been designed to run on standard fuels mainly produced from oil. In addition, biofuels which properties have to meet set standards are used (e.g. CEN/TS 15293:2011, EVS-EN 14214:2004). In case of biofuels, the control system of an engine needs to be upgraded to ensure the given output parameters of an engine. For instance, in case of bioethanol fuel E85, it is imperative to increase the fuel supply in order for the output parameters of the engine not to go down. This is conditioned by the smaller calorific value of bioethanol as compared to gasoline (Merker et al., 2012). Therefore, a fuel supply system must enable almost twice as big a fuel supply into the engine. It could be deduced that using biofuels in standard fuel supply systems is feasible; however, it would be necessary to improve their control systems. The fuel supply systems of compression and spark ignition engines have always been substantially different, thus, these cannot be regarded as one (Robert Bosch GmbH (1); Robert Bosch GmbH (2)). Next, the condensed descriptions of fuel supply systems of compression and spark ignition engines are provided.

1.1.2. The types of fuel supply systems of a spark ignition engine

The first fuel supply system of a spark ignition engine included a carburettor. The operating principle of the carburettor lay in sucking the fuel through the nozzle into the cylinder by the underpressure forming in the intake manifold. Nowadays, carburettors are in use on smaller engines (e.g. on the engines of lawn mowers, chainsaws, etc). On passenger car engines, injection systems are being used, which were widely introduced

Table 1.1. The development stages of spark ignition engine injection systems (Robert Bosch GmbH (1); Paper IV)

Year	System	Features
1967	D-Jetronic	Analogue-technology; multipoint injection system Intermittent fuel injection; Intake-manifold-controlled
1973	K-Jetronic	Mechanical-hydraulic multipoint injection system; Continuous fuel injection
1973	L-Jetronic	Electronic multipoint injection system, initially analogue, later digital technology; Intermittent fuel injection; Air-flow sensing
1981	LH-Jetronic	Electronic multipoint injection system; Intermittent fuel injection; Air-mass sensing
1982	KE-Jetronic	K-Jetronic with electronically controlled additional functions
1987	Mono-Jetronic	Single-point injection system; Intermittent fuel injection; Air-flow calculation via throttle-valve angle and engine speed
	Motronic	
	M-Motronic	Mechanically regulated throttle valve; The positioning sensor of the throttle valve
	ME-Motronic	Electronically regulated throttle valve; Potentiometer-type of gas pedal
	DI-motronic	Direct injection
	Bifuel-Motronic	Dual fuel system

by Robert Bosch GmbH in 1967. Injection systems had previously been used in aviation and motorsport (Robert Bosch GmbH (1)). The development stages and types of injection systems are given in Table 1.

As can be seen in Table 1, different types of injection systems have different features that contribute to their specific name. For example, in case of an L-Jetronic type of fuel supply system, one of its features is measuring the airflow directed into the engine (L refers to the German word "Luft"). The newest type of a fuel supply system is Bifuel-motronic that enables to use two different fuels in an engine. The most common fuel types used are gasoline and liquefied natural gas or compressed natural gas (Robert Bosch GmbH (1)). As a general rule, two fuels are not used simultaneously in a spark ignition engine. The reason lies in the fact that the fuel used can be ignited in the engine cylinder without another fuel (unlike compression ignition engines where, e.g. diesel fuel is used to ignite bioethanol) in addition to the fact that using two fuels in the air-fuel mixture can increase the concentration of harmful components in the exhaust gas (Paper I).

The newest development in fuel supply systems nowadays is HCCI (Homogeneous Charge Compression Ignition). Basically, the aim is to ignite the air-fuel mixture in the engine cylinder using pressure. Modern direct injection systems enable to carry out the abovementioned process; nevertheless, the problem of gasoline's high autoignition temperature remains. The autoignition temperature could be decreased by fuel improvers; however, this would also result in an increase in the engine fuel cost (Starck et al., 2010; Wang et al., 2006). A common method of using biofuels in a spark ignition engine is complementing either the multipoint injection or mono injection system with electronic control units that increase the fuel supply into the engine. Such a solution is generally used with bio-methanol and ethanol. Regardless, the given solution is not suitable for dosing substandard fuels as the water in fuel and poor lubricate properties cause corrosion and the wearing of injectors (Ma et al., 2004; Govindarajan, 2008; Paper IV).

1.1.3. The fuel supply system of a compression ignition engine

Direct injection systems have invariably been used in compression ignition engines as they enable the timely injection of the fuel into the cylinder. In order to inject the fuel directly into the cylinder, high pressure is needed in the fuel supply system. This is created by a plunger. The first fuel supply system of a mass production compression ignition engine was a mechanical in-line injection pump. In case of an in-line injection pump, the fuel is dosed by a plunger whereas the amount of fuel injected is regulated by the inversion of the plunger helix in relation to the spill port. The operating of a mechanical in-line injection pump is regulated by a mechanical regulator, which regulates the amount of fuel injected based on the rotational speed of the fuel pump shaft and the position of the accelerator (Heisler et al., 1995; Кривенко & Федосов, 1980). These types of injection pumps have been developed into electronic ones whereas the principle of dosing the fuel has remained the same, but the mechanical regulator has been replaced with an electronic one (Robert Bosch GmbH (2)). Alongside mechanical in-line injection pumps, mechanical distributor-type fuel injection pumps were also developed, which operating principle was based on dosing the fuel into all cylinders by a rotating plunger. In this case, the fuel supply is not dependent on the rotational angle of the plunger but the position of the controlling collar on the plunger. The function of the controlling collar is regulating the fuel flow directed back from the plunger. The more fuel directed back, the smaller the amount of

injected fuel (Heisler et al., 1995; Robert Bosch GmbH (2); Robert Bosch GmbH (3)). Mechanical distributor injection pumps were developed to be electronic. Electronic distributor injection pumps fall into the categories of axial plunger and radial plunger pumps (Robert Bosch GmbH (2)).

In addition to different fuel supply systems of compression ignition engines, unit injectors and unit pump systems have been developed. Nowadays, unit injectors are in use on the engines of trucks and passenger cars. Basically, an injector and an injection pump have been merged whereas the fuel is dosed into the engine by an electro-magnetic valve system (Heisler et al., 1995; Robert Bosch GmbH (2)). In case of unit pump systems, there is one injection pump for each engine cylinder, which is used to dose fuel into the cylinder by a mechanical injector (Robert Bosch GmbH (2)).

Nowadays, common rail fuel supply systems are most prevalent. The operating principle of the particular system lies in the injection pump, which supplies the system with fuel and provides the common rail with pressure. The common rail is connected to electronically controlled injectors. Fuel supply is regulated by opening and closing the backflow valve. This particular fuel supply system enables to break down the injection of fuel into the cylinder into up to five phases, thus, it enables to control the combustion process in the cylinder (Robert Bosch GmbH (2)).

Biofuels are not commonly used in the abovementioned fuel supply systems of compression ignition engines. Some manufacturer companies of fuel apparatuses certify the use of biodiesel in the fuel supply system; however, this is not a widespread tendency as biodiesel can make the seals (mostly rubber) in the fuel supply system brittle. In fact, mechanical fuel supply systems in which vegetable oils are also used are more durable to biodiesel. Fuels that are non-inflammable in a compression ignition engine (e.g. bioethanol, gaseous fuels) can be used as additional fuels. An example of this would be directing bioethanol and diesel fuel into the engine cylinder. Generally, bioethanol is injected into the intake manifold (Masahiro, 2003; Cipo & Bhana., 2009). For injecting bioethanol, injectors of mainly the fuel supply systems of spark ignition engines are used as these contain less precise and water-sensitive units. When bioethanol is injected directly into the cylinder, the injectors and the injection pump are commonly upgraded by using Teflon or nano-composite material work surfaces on work pieces (Courtoy et al., 2009; Ma et al., 2004).

1.2. The impact of bioethanol on the combustion process of a piston engine

Using bioethanol in a spark ignition engine is commonly not problematic if standardized biofuels are used. The main issues concerning the use of substandard bioethanol are corrosion as well as the wearing and sticking of the precise work surfaces of the fuel supply system. In order to sustain the output parameters of an engine, the bioethanol supply should be increased one and a half times compared to the supply of gasoline. Nowadays, several blends of gasoline and bioethanol as well as of diesel fuel and bioethanol are used; nevertheless, mixing these without special improvers hinders the combustion process and increases the concentration of harmful components in the exhaust gas. What is more, starting spark ignition engines at temperatures below 5 °C is rendered difficult. This is conditioned by the high heat of vaporization of bioethanol (Demirbas, 2006; Labeckas et al., 2014). For the purposes of overcoming this issue, it would be necessary to either add improvers to bioethanol, which would ease the cold start of the engine, or warm bioethanol so as to decrease ethanol's heat of vaporization (Situ et al., 2008). Furthermore, the compression ratio of the engine could also be increased as it would ensure higher compression p_{co} and temperature T in the cylinder; however, the combustion pressure p would also increase simultaneously which might result in the breakdown of the crank gear of the engine. Moreover, rebuilding an engine is a complex and time-consuming process.

In conventional compression ignition engines where diesel fuel is used, it is possible to use bioethanol only as an additional fuel due to the high autoignition temperature of bioethanol. In most cases, bioethanol is injected as an additional fuel into the intake manifold from where it is sucked into the cylinder with air. Bioethanol is ignited by diesel fuel which is injected into the cylinder as the main fuel with a regular fuel supply apparatus. Depending on the fuel supply apparatus, bioethanol impacts the combustion process of the engine and the exhaust gas emission differently. For example, the use of bioethanol conditions the increase in the concentration of hydrocarbons (HC) in the exhaust gas. In general, there is a relation according to which the more bioethanol there is in the air-fuel mixture, the more substantial the concentration of hydrocarbons in the exhaust gas. At the same time, the concentration of hydrocarbons decreases as the engine load increases (Kowalewicz & Pajączek, 2003; Abu-Qudais et al., 2000). The abovementioned proc-

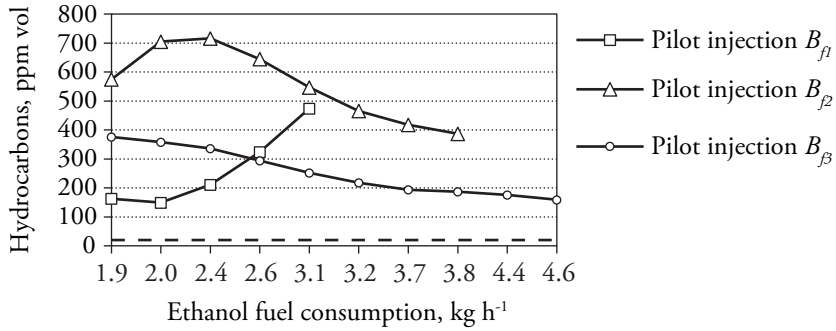

Figure 1.1. The impact of ethanol fuel consumption on the values of hydrocarbons in case of different pilot injections, where B_{f1} = 1.35 kg h^{-1}; B_{f2} = 2.33 kg h^{-1}and B_{f3} = 3.05 kg h^{-1} (Paper I).

ess is more clearly illustrated on Figure 1.1, which reflects the test data of an engine D120 equipped with a mechanical injection pump. The tests were carried out on three pilot injection engine modes whereas the rotational speed of the crankshaft was n_e=1300 rpm. During testing, the proportion of bioethanol in the air-fuel mixture was gradually increased. Load characteristic of the engine was carried out (n_e = const) whereas the engine load increased as bioethanol was added. Exhaust gas emission was measured during tests according to the standard ISO8178. The method of these particular tests is more elaborately described in subchapter 4.1. It can be seen on Figure 1.1 that in case of a short pilot injection B_{f1}, the concentration of HC in the exhaust gas increased simultaneously with the increase in bioethanol amount. This is caused by the decrease in the combustion temperature in the cylinder. In case of a longer pilot injection B_{f3}, the concentration of hydrocarbons decreased as bioethanol was added. This is conditioned by the high engine load and high combustion temperature in the cylinder. The main issue that remains concerns the increase in the concentration of hydrocarbons when bioethanol is added to the air-fuel mixture as compared to using diesel fuel (Paper I).

When using bioethanol, the concentration of carbon monoxide (CO) in the exhaust gas increases in engines equipped with common rail fuel supply apparatuses. This is due to the fact that in such engines, the combustion process is controlled and the fuel combustion efficiency is higher than with bioethanol. In case of engines equipped with mechanical fuel supply apparatuses, the concentration of carbon monoxide – as compared to using diesel fuel – decreases (Abu-Qudais et al., 2000; Kowalewicz &

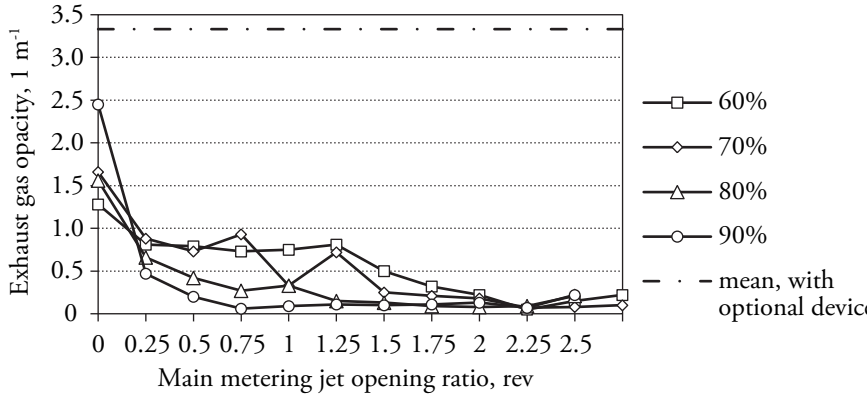

Figure 1.2. The impact of ethanol fuel consumption on the opacities of exhaust gases depending on its concentration (Paper I).

Pajączek, 2003; Paper I). When using bioethanol in engines equipped with a mechanical injection pump and a common rail fuel supply apparatus, the concentration of carbon dioxide (CO_2) decreases (Chauhan et al., 2001; Kowalewicz & Pajączek, 2003; Paper I). In case of mechanical injection pumps, the concentration of nitrogen (NO_x) in the exhaust gas decreases. Similarly, the concentration of nitrogen decreases on low modes of engines equipped with a common rail fuel supply apparatus. At high engine loads, the concentration remains of the same magnitude as when diesel fuel is used (Kowalewicz & Pajączek, 2003).

The opacity of engine exhaust gas decreases when bioethanol is used in the air-fuel mixture, regardless of the fuel supply apparatus type (Abu-Qudais et al., 2000; Kowalewicz & Pajączek, 2003; Paper I). This is caused by cleaner combustion of bioethanol and smaller amount of diesel fuel in the air-fuel mixture as compared to using only diesel fuel at the same engine load. The impact of bioethanol fuel of different concentrations on the exhaust gas opacity of a compression ignition engine is given on Figure 1.2. The tests were carried out on the engine D120, the rotational speed of the crankshaft being n_e=1800 rpm.

Based on the abovementioned examples of exhaust gas components, it could be deduced that using bioethanol in a compression ignition engine is reasonable when the combustion process of diesel fuel and bioethanol is effective enough to ensure engine performance and the accordance of exhaust gas emission with fixed standards. Figure 1.3 illustrates the combustion process in the cylinder of a compression ignition engine when

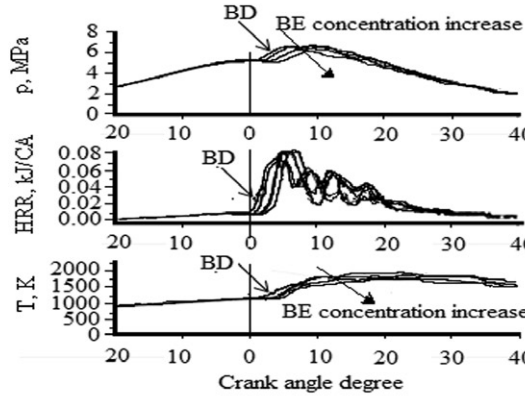

Figure 1.3. The impact of bioethanol on the combustion process of a diesel engine; BD – biodiesel; BE – bioethanol (Lu. et al., 2008).

biodiesel fuel and bioethanol are used jointly. It can be seen that increasing the amount of bioethanol in the air-fuel mixture decreases combustion pressure, combustion temperature in the cylinder, and combustion gas temperature (Paper II). Ignition delay as well as the amount of energy released during fuel combustion increase.

The decrease in the combustion temperature T_{com} and the lengthening of the ignition delay τ_d increase the proportion of hydrocarbons in the exhaust gas, lengthen the combustion time of the air-fuel mixture and decrease the combustion pressure p. The combustion time of the air-fuel mixture can be reduced by altering the timing of the angle of diesel fuel injection. Kowalewicz & Pajączek, 2003, recommends the injection angle to be 25–35 deg BTDC, depending on engine load. However, this solution does not increase the combustion temperature T_{com} and pressure p in the cylinder as the evaporation of bioethanol requires a great deal of energy. Namely, the energy acquired from the air-fuel mixture directed into the cylinder is not released promptly enough to ensure an increase in the combustion temperature T_{com} and pressure p. This is caused by the lengthening of evaporation time (whereas evaporation is conditioned by the size of bioethanol and diesel fuel droplets in the air-fuel mixture), the lengthening of flame diffusion time as well as the combustion time of unvaporized fuel droplets. The evaporation of injected liquids' drops is described in several sources, e.g: Abramzon & Sirignano, 1989; Norvaišiene, 2013; Johnson, 1982; Elwardany et al., 2013, Sazhin et al., 2014. The abovementioned issues could be solved by reducing the size of fuel droplets. Smaller fuel droplets enable fuel to vaporize more quickly

and to accelerate flame diffusion in the cylinder for which reason more energy is released at a time. The drawback of the solution, however, lies in the too quick combustion of the air-fuel mixture, which may cause engine power loss. In addition, in case of direct fuel injection supply systems, the mixing of too small fuel droplets with air is rendered difficult and the amount of energy acquired from the combustion is minor, thus, it is necessary for the entire combustion chamber to be filled with air-fuel mixture (Jankowski et al., 2002). When bioethanol that is injected into the intake manifold is used as an additional fuel in a compression ignition engine, it is recommended to form the bioethanol air-fuel mixture so that the fuel droplets in it would be as small as possible. Reducing the size of fuel droplets enhances the more effective combustion of air-fuel mixture in the engine cylinder. Since the air-fuel mixture is divided into two parts in the combustion chamber when two fuels are used – firstly, diesel fuel and bioethanol air-fuel mixture, and secondly, bioethanol air-fuel mixture – the regular combustion of diesel fuel ensures the ignition and duration of the air-fuel mixture in the cylinder. The quick combustion of bioethanol fuel ensures the increase in the combustion pressure p and temperature T_{com} in the cylinder. The average diameter of fuel droplets in the fuel spray is described by Sauter's mean diameter D_{32} which is expressed by the equation (Filippa et al., 2012; Sescu et al., 2011; Pacek et al., 1998):

$$D_{32}=\frac{\sum N_i d^3}{\sum N_i d^2}, \tag{1.1}$$

where N_i – the number of droplets in the size range ($N_i = d_{max} \ldots d_{min}$); d^3 – the relation between the mean diameter of fuel droplets and volume; and d^2 – the relation between the mean diameter of fuel droplets and the area.

The size of a fuel droplet influences the heat release rate $\frac{\mathrm{d}Q_n}{\mathrm{d}t}$ and the heat release time t_{Qn} during combustion (Marchenko et al., 2012; Kuleshov et al., 2005). The decrease in the heat release time t_{Qn} is conditioned by an increase in the combustion velocity v_{bv} of the air-fuel mixture (Farouk & Dryer, 2011), thus, more energy is released during combustion. Heat release rate is expressed in the equation (Heywood, 1988):

$$\frac{\mathrm{d}Q_n}{\mathrm{d}t}=\frac{\gamma_{br}}{\gamma_{br}\text{-}1}p\frac{\mathrm{d}V_c}{\mathrm{d}t}+\frac{1}{\gamma_{br}\text{-}1}V_c\frac{\mathrm{d}p}{\mathrm{d}t}, \tag{1.2}$$

where Q_n –the heat amount that is released as the fuel burns in the cylinder;

t – time for rotating the crank;
γ_{hr} – ratio of specific heats, which in case of ethanol fuel use is γ_{hr} = 1.26 (Kamboj & Kairimi, 2012);
p – combustion pressure;
V_c – cylinder volume.

Based on the equation (1.2), in order to increase the heat release rate, combustion pressure p must also increase (which occurs due to a decrease in the diameter of fuel droplets D_{32}) as the cylinder volume V_c and its variation ΔV are dependent on the mechanical parts of the engine and the ratio of specific heats γ_{hr} is in case of this particular process constant γ_{hr} = const. To characterize the impact of the size of fuel droplets, combustion pressure is expressed from the equation of fuel mass burning rate (Heywood, 1988; Paper V):

$$\frac{\mathrm{d}(mu)}{\mathrm{d}t} = -p\frac{\mathrm{d}V_c}{\mathrm{d}t} + \frac{\mathrm{d}Q_{ht}}{\mathrm{d}t} + h_c\frac{\mathrm{d}m}{\mathrm{d}t} \rightarrow p = \frac{-\frac{\mathrm{d}(mu)}{\mathrm{d}t} + \frac{\mathrm{d}Q_{ht}}{\mathrm{d}t} + h_c\frac{\mathrm{d}m}{\mathrm{d}t}}{\frac{\mathrm{d}V_c}{\mathrm{d}t}}, \quad (1.3)$$

where m – gas mass in the cylinder;
u – specific internal energy;
h_c – sensible enthalpy of injected fuel.

From the previous equation, we can express the fuel mass combustion rate $\frac{\mathrm{d}(mu)}{\mathrm{d}t}$, heat transfer $\frac{\mathrm{d}Q_{ht}}{\mathrm{d}t}$ and mass flow rate $\frac{\mathrm{d}m}{\mathrm{d}t}$ as follows (Heywood, 1988).

Heat transfer $\frac{\mathrm{d}Q_{ht}}{\mathrm{d}t}$ is expressed by:

$$\frac{\mathrm{d}Q_{ht}}{\mathrm{d}t} = Ah_{cor}\left(T_g - T_{wall}\right), \quad (1.4)$$

where A – combustion chamber surface area;
T_g – mean combustion gas temperature;
h_{cor} – heat-transfer coefficient;
T_{wall} – mean cylinder wall temperature.

Heat-transfer coefficient h_{cor} can be expressed with the combustion rate of the heat flux emitted from the cylinder head as follows:

$$\frac{h_{cor}d_{cb}}{k} = a\left(\frac{\varrho_{afm}v_p d_{cb}}{\mu}\right)^b \rightarrow h_{cor} = \frac{ak\left(\frac{d_{cb}v_p\varrho_{afm}}{\mu}\right)^b}{d_{cb}}, \quad (1.5)$$

where a – constant of intensity of charge motion $0.35 \le a \le 0.8$;

b – constant of intensity of charge motion (b = 0.7 with normal combustion);

k – thermal conductivity;

d_{cb} – cylinder bore;

ρ_{afm} – air-fuel mixture density;

μ – dynamic viscosity;

v_p – piston speed.

The equation (1.2) is expressed from the first law of thermodynamics in case of an open system (Heywood, 1988):

$$\frac{\mathrm{d}U}{\mathrm{d}t} = \frac{\mathrm{d}Q_{ht}}{\mathrm{d}t} - p\frac{\mathrm{d}V_c}{\mathrm{d}t} + \sum_i h_c m_{fr} , \tag{1.6}$$

where $\frac{\mathrm{d}U}{\mathrm{d}t}$ – the maximum internal energy of system materials whereas this relation is valid $\frac{\mathrm{d}U}{\mathrm{d}t} \approx \frac{\mathrm{d}(mu)}{\mathrm{d}t}$;

m_{fr} – fuel flow rate and in this case $\frac{\mathrm{d}m}{\mathrm{d}t} = m_{fr}$, which is expressed as follows:

$$m_{fr} = -\frac{m_c \cdot V_{cp}}{V_c^2}\frac{\mathrm{d}V_c}{\mathrm{d}t} , \tag{1.7}$$

where V_{cp} – combustion chamber volume;

m_c – the mass of the air-fuel mixture that is directed into the cylinder in one work cycle, expressed as follows:

$$m_c = V_c \varrho_{afm} , \tag{1.8}$$

where ρ_{afm} – density of air-fuel mixture.

The combustion rate of one fuel droplet $\frac{\mathrm{d}(mu)}{\mathrm{d}t}$ is expressed according to F.A. Williams by:

$$\frac{\mathrm{d}(mu)}{\mathrm{d}t} = -4\pi r_{fd}^2 \varrho_f \frac{\mathrm{d}r_{fd}}{\mathrm{d}t} , \tag{1.9}$$

where r_{fd} – droplet radius in the air-fuel mixture where $r_{fd} = \frac{D_{32}}{2}$;

D_{32} – Sauter mean diameter.

To evaluate the mass combustion rate of the entire air-fuel mixture, the equation (1.9) has to be modified to determine the mass combustion rate of fuel droplets found in the entire air-fuel mixture. For this, one fuel droplet mass combustion rate $\frac{\mathrm{d}(mu)}{\mathrm{d}t}$ has to be multiplied with the number of all fuel droplets, *N,* in the air-fuel mixture; and to get the heat emitted per unit of time during combustion, it must be multiplied with

the fuel calorific value $Q_{f.teor}$

$$\frac{\mathrm{d}(mu)}{\mathrm{d}t} = -4\pi\left(\frac{D_{32}}{2}\right)^2 \varrho_f \frac{\mathrm{d}(\frac{D_{32}}{2})}{\mathrm{d}t} Q_{f.teor} N\,, \tag{1.10}$$

where $Q_{f.teor}$ – fuel calorific value;

N – the number of fuel droplets in the air-fuel mixture, which is expressed as the relation between fuel quantity directed into the cylinder V_f and fuel droplet volume:

$$N = \frac{V_f}{\frac{4}{3}\pi(\frac{D_{32}}{2})^3}\,, \tag{1.11}$$

where V_f – the fuel quantity directed into the cylinder in one work cycle.

Taking into account equations (1.4), (1.5), (1.7), (1.8) and (1.10) and replacing them into equation (1.3), we get an equation for calculating combustion pressure p; with the help of this, the variation in combustion pressure p can be evaluated based on the diameter D_{32} of fuel droplets in the air-fuel mixture. Based on equations (1.3), (1.7) and (1.10), it is a differential equation, which entails two types of derivatives, $\frac{\mathrm{d}(\frac{D_{32}}{2})}{\mathrm{d}t}$ and $\frac{\mathrm{d}V_c}{\mathrm{d}t}$. The intensity of variation in the size of fuel droplets $\frac{\mathrm{d}(\frac{D_{32}}{2})}{\mathrm{d}t}$ can be deduced from the air-fuel mixture's combustion velocity v_{afm} equation. Therefore, the relation $\frac{\mathrm{d}(\frac{D_{32}}{2})}{\mathrm{d}t} \approx v_{afm}$ is valid and air-fuel mixture combustion velocity is expressed by this equation (Williams et al., 1985):

$$v_{afm} = \frac{\lambda}{\varrho_{afm} c_p}\sqrt{4\pi\left(1+\frac{1}{\lambda_{afr}}\right) N_k \frac{D_{32}}{2} \ln(1+a_{com})}\,, \tag{1.12}$$

where λ – thermal conductivity;

c_p – specific heat at constant pressure;

λ_{afr} – stoichiometric fuel-gas ratio;

N_k – the number of fuel droplets per unit volume;

a_{com} – combustion constant.

The change of cylinder volume at different crankshaft angles of rotation can be expressed as a ratio of cylinder volume change and time (Williams et al., 1985; Heywood, 1988):

$$\frac{\mathrm{d}V_c}{\mathrm{d}t}=\frac{V_c+\frac{\pi\cdot d_{cb}^{\,2}}{4}\left(l+r_{cr}-(r_{cr}\cos\varphi+\sqrt{l^2-r_{cr}^{\,2}\cdot\sin^2\varphi})\right)}{t}, \qquad (1.13)$$

where r_{cr} – crank radius;
l – connecting rod length;

Following from the above, combustion pressure p calculation model (1.3) is expressed as follows (Paper V)

$$p=\frac{4\pi\left(\frac{D_{32}}{2}\right)^2\varrho_f\frac{\lambda}{\varrho_{afm}c_p}\sqrt{4\pi\left(1+\frac{1}{\lambda_{afr}}\right)N_k\frac{D_{32}}{2}\ln(1+a_{com})\,Q_{f.teor}N}}{\frac{V_c+\frac{\pi r_{cb}^{\,2}}{4}\left(1+r_{cr}-\left(r_{cr}\cos\varphi+\sqrt{l^2-r_{cr}^{\,2}\sin^2\varphi}\right)\right)}{t}}+$$

$$\frac{A\cdot\frac{ak\cdot\left(\frac{d_{cb}v_p\varrho_{afm}}{\mu}\right)^b}{d_{cb}}\left(T_g-T_{wall}\right)}{\frac{V_c+\frac{\pi r_{cb}^{\,2}}{4}\left(l+r_{cr}-\left(r_{cr}\cos\varphi+\sqrt{l^2-r_{cr}^{\,2}\sin^2\varphi}\right)\right)}{t}}+h_c\left(-\frac{\left(V_c\varrho_{afm}\right)V_{cp}}{V_c^{\,2}}\right) \qquad (1.14)$$

This equation enables calculating combustion pressure on different working modes of the engine, depending on the size of fuel droplets in the air-fuel mixture. The evaporation of the air-fuel mixture has not been considered since in case of the given solution, it is not exactly known how the evaporation in the intake manifold and cylinder of the engine take place. In addition, further research is needed is needed on the homogeneity of the air-fuel mixture in the engine cylinder.

To simplify equation (1.14), a sample graphic has been compiled based on this (Figure 1.4), which characterizes the change in combustion pressure depending on the size of fuel droplets. The calculation has used the data of a spark ignition engine of a regular passenger car. The calculation results have been transferred to percentages, where p_z = 100% and p_{min} = 0. The size range of fuel droplets D_{32} has been chosen to be D_{32} = 5…500 µm.

According to the chart, the increase D_{32} = 200...500 µm in the diameter of fuel droplets causes the increase in the combustion pressure to slow down. The reduction of the diameter of fuel droplets of up to 20 µm makes the combustion pressure increase rapidly. For example, in this

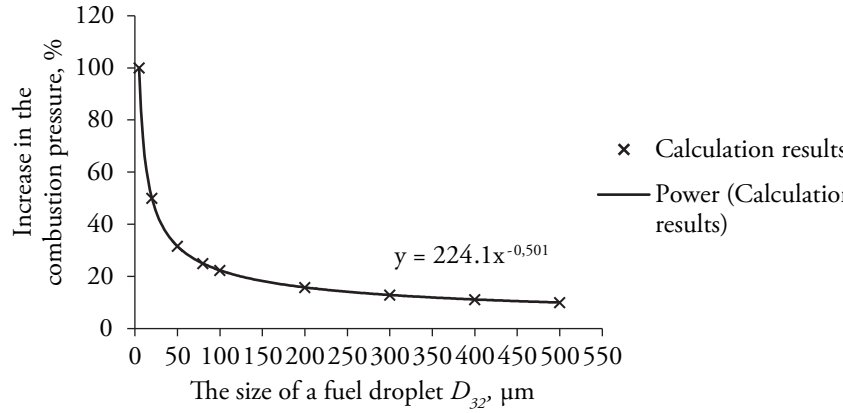

Figure 1.4. Variation in combustion pressure depending on the size of fuel droplets in the air-fuel mixture (Ilves et al., 2014).

particular case, the combustion pressure is roughly doubled as the size of fuel droplets is reduced from 80 µm to 20 µm. When the size of fuel droplets is reduced to be less than 20 µm, there is a rapid increase in the combustion pressure which might cause a detonating combustion in the engine cylinder. Therefore, it is important to form the air-fuel mixture so that the combustion in the engine cylinder would remain controllable. In case of Figure 1.14, it is relevant that according to different technical data of the engine, at the droplet diameters of 20…80 µm, the variation in the combustion pressure was 7–60%. Since not all parameters and their changes can be accurately determined in the combustion pressure, reducing the droplet diameter D_{32} = 80...20 µm increases the combustion pressure on different conditions by an average of 20%. The relation between the size of fuel droplets and variations in pressure calculated by equation 1.14 can be simplified by using the equation given on Figure 1.4. The equation on Figure 1.4

$$y=224.1x^{-0.501} \longrightarrow p=224.1D_{32}^{-0.501} \quad (1.15)$$

enables to assess the variation in the combustion pressure depending on the diameter of fuel droplets in the air-fuel mixture (Paper V).

Based on the abovementioned, it can be said that the size of fuel droplets in the air-fuel mixture impacts the combustion pressure p in the cylinder. In general, the combustion pressure p increases in the cylinder as the diameter of fuel droplets D_{32} reduces. This is conditioned by the increase in the amount of energy released at a time. The size of fuel droplets D_{32} influences the evaporation time t_v and the combustion velocity v_{afm} of the air-fuel mixture. As the diameter of fuel droplets D_{32} reduces, both

the evaporation time t_v and the combustion velocity v_{afm} of the air-fuel mixture increase. The advantage of reducing the size of fuel droplets D_{32} lies in, for example, using bioethanol and diesel fuel in a compression ignition engine. To be more exact, the quicker combustion of bioethanol air-fuel mixture enables to compensate for the increase in the combustion time of the air-fuel mixture conditioned by the ignition delay. In addition, the quicker combustion of fuel droplets that have not evaporated in the cylinder is ensured.

1.3. Discussion

Based on the data presented in this chapter, it can be deduced that there are several methods of using biofuels in a spark or a compression ignition engine. Biofuels can be dosed into the engine as either the main fuel or an additional fuel. The fuel supply systems have either been modified to ensure the resistance of the fuel supply system to the properties of biofuels, or an additional fuel supply system has been added to an engine. The modifications of a fuel supply system or the use of an additional fuel supply system are necessary as biofuels may cause the untimely wearing of the work units, corrosion and sticking of fuel supply systems. This results in poor quality air-fuel mixture that hinders the combustion process and increases exhaust gas emission. What is more, biofuels may impact the rubber details and seals in the fuel supply systems, making these brittle.

Another problem of using biofuels and engine fuels arises concerning the exhaust gas emission as the combustion of biofuels in the cylinder is not as effective as with standard fuels. Due to this, the exhaust gas emission of the engine increases.

The solution would lie in a fuel supply system that can ensure the formation of a high-quality air-fuel mixture from several biofuels and which work units would not be significantly impacted by the different physicochemical properties of different fuels. Furthermore, it is recommended to form biofuel air-fuel mixture where the size of fuel droplets is smaller or equal to the ones in a standard fuel air-fuel mixture. This would ensure the quick combustion of the air-fuel mixture with minimal residues. In addition, the quick and effective combustion of biofuels enables to replace the proportion of standard fuel in the air-fuel mixture to a greater extent since the combustion process is less hindered.

2. THE AIM AND TASKS OF THE STUDY

The use of biofuels in spark and compression ignition engines brings about several issues which are conditioned by the impact of physicochemical properties of biofuels on both the fuel supply system of the engine as well as on the combustion process. The aim of this study was to develop a fuel supply system which would enable to dose different biofuels into the cylinder of spark and compression ignition engines whereas the formation of small fuel droplets in the air-fuel mixture and the resistance of the fuel supply system to the physicochemical properties of biofuels would be ensured.

In order to complete the aim, the following tasks were set:

1. To analyze the existing fuel supply systems and their aptitude for using biofuels in spark and compression ignition engines.
2. To provide an overview of the combustion process in the cylinder of a compression ignition engine and the exhaust gas emission when biofuels are used as additional fuel. This particular overview was constructed based on one particular biofuel.
3. To develop a fuel supply system prototype that would enable to dose different biofuels into the engine cylinder.
4. To study the size of fuel droplets in the air-fuel mixture formed by the developed fuel supply system.
5. To modify the developed fuel supply system so that it could be used on spark and compression ignition engines.
6. By using the developed fuel supply system, run engine tests on spark and compression ignition engines.
7. To analyze the data obtained at engine tests and draw conclusions as to the suitability of the fuel supply system for dosing biofuels into the engine.

TIPS (the theory of inventive problem solving) methodology has been used to develop the fuel supply system. In order to examine the efficiency of the developed fuel supply system, the size of fuel droplets in the air-fuel mixture formed was measured. For doing so, laser diffraction-based method was used. At engine tests, the methods of determining partial load characteristic and idle characteristic were resorted to in case of spark and compression ignition engines accordingly.

To solve the tasks set for completing the aim, an action program was drawn based on which the following activities were carried out:

1. To analyze the construction and working principles of existing fuel supply systems, the technical literature of several databases (the databases of Thomson Reuters, ScienceDirect, Scopus, Espacenet and PatBase as well as Google search engine) were studied. The fuel supply systems of spark and compression ignition engines were studied separately. Next, the fuel supply systems which allow to dose biofuels into the engine cylinder were chosen and their construction and aptitude for use on spark and compression ignition engines were analyzed. Based on these fuel supply systems, innovative fuel supply system solutions or modifications to existent systems were proposed.
2. To describe the combustion process and the exhaust gas of the engine, the data in the literature was studied and the most essential nuances that described the use of bioethanol and diesel fuel together were outlined. According to the analyzed data, an engine testing plan was designed. During the tests, it was studied how the use of bioethanol impacted both the exhaust gas of an engine equipped with a mechanical injection pump and the combustion process when a carburettor was used as the fuel supply system for dosing bioethanol. The objective of the particular test was to study how the type of the main and additional fuel supply system affected the exhaust gas emission and air-fuel mixture combustion. The tests were carried out at both engine nominal and maximum load. The concentrations of carbon dioxide, carbon monoxide, hydrocarbons, nitro compounds, and soot were measured in the exhaust gas.
3. Based on the novel fuel supply system solutions proposed in the literature, the most suitable regarding the objective was chosen and first prototypes were constructed. The formation of air-fuel mixture from different liquid biofuels was researched as well as charting the working parameters of the fuel supply systems and evaluating their suitability for different engines. During the process of building and testing the prototypes, different issues arose, based on which one solution was chosen for further development according to the requirements set for a fuel supply system. Tests were run on the particular fuel supply system during which the impact of working parameters on the fuel supply system productivity was researched.
4. The reason for examining the quality of the air-fuel mixture was to determine the suitability of the fuel supply system for working on an engine. For this purpose, the air-fuel mixture formed by the

developed fuel supply system was compared with the air-fuel mixture formed by an existing fuel supply system, to be more exact, that of a mechanical fuel supply system of a compression ignition engine. The quality of the air-fuel mixture was evaluated based on determining the size of fuel droplets in it. In order to do so, a special-purpose device using laser diffraction-based measurement method was used. The parameters of the air-fuel mixture formed by the existing fuel supply system were used as a basis for evaluating the quality of the air-fuel mixture. Based on that, the quality of the air-fuel mixture formed by the novel fuel supply system was considered to be suitable if its parameters (the size of fuel droplets in the air-fuel mixture) were equivalent to or smaller than the ones of the existing fuel supply system. Test results were analyzed according to comparative analysis method.

5. The development of the fuel supply system for use on spark and compression ignition engines results in the use of the fuel supply system being more flexible, however, it is also expected that the fuel supply system can be controlled on either engine. This complicates the control system of the fuel supply system significantly. To run the fuel supply system, the control parameters of spark and compression ignition engines were charted and a solution for using these in the control unit of the fuel supply system was found. An essential difference in spark and compression ignition engines is that the developed solution can be used as the main fuel supply system on spark ignition engines but as an additional fuel supply system on compression ignition engines. Therefore, in case of a compression ignition engine, the control unit must run jointly with the main fuel supply system.
6. By using the developed fuel supply system, the purpose of engine tests was to research the impact of the fuel supply system on the combustion process, output parameters and exhaust gas emission. Furthermore, idle mode tests were run on a compression ignition engine during which the combustion pressure in the cylinder as well as the exhaust gas emission were measured. The fuel supply system was used as an additional fuel supply system and bioethanol was used as the test fuel. The test results were compared to the data provided in the literature and the impact of the fuel supply system on the combustion process and exhaust gas emission was outlined. On a spark ignition engine, the developed fuel supply system was used as the main fuel supply system with the test fuels being bioethanol and gasoline E95. Partial load characteristic was carried out on engine

tests during which the output parameters of the engine, combustion pressure and fuel consumption were measured. The test results were compared to the data obtained during the use of the original fuel supply system of the test engine at same loads and control settings.

7. Based on the data acquired during engine tests, the impact of the fuel supply system on the functioning of the engine was analyzed and its efficiency and usability on an engine were evaluated.

3. THE DEVELOPMENT OF A FUEL SUPPLY SYSTEM OF AN ENGINE RUNNING ON BIOFUELS

3.1. The requirements for a fuel supply system of an engine running on biofuels

According to previous discussion, the following requirements can be set for a fuel supply system in which different biofuels are used:

1. Resistance to the physicochemical properties of the fuel, i.e. the work units of the fuel supply system need to be resistant to water, acids and ensure the functioning of the system with fuels of poor lubricating properties.
2. Ensuring the formation of a high quality air-fuel mixture when fuels of different physicochemical properties are used.
3. Suitability for use on both spark and compression ignition engines.
4. Possibility to control the fuel supply system precisely and fast to ensure the formation of a suitable air-fuel mixture at different engine modes.
5. Such construction of the fuel supply system which enables its swift mounting onto an engine.
6. Straightforward serviceability.
7. Easily adjustable with regard to different engines.

3.2. The solutions of the developed fuel supply systems

3.2.1. The method for the formation of air-fuel mixture in a piston engine and a complex fuel supply system

For the purpose of generating technical solutions of the developed fuel supply systems, the analogues of the fuel supply systems covered in the literature (e.g. patent documents CN201486652, US2005217642, US2009114196, WO2009106647) were analyzed and technically upgraded to solve the abovementioned issues. Two of these ideas will be covered in detail.

The main wearing parts in the fuel supply system are the details with precise work surfaces (Ma et al., 2004; Govindarajan, 2008). The technical solution of the developed fuel supply system is also based around that.

The conception lies in the lack of precise work surfaces in the fuel supply system. Precise work surfaces ensure that the exact amount of fuel is dosed into the engine and that the working parameters of the fuel supply system meet the requirements. In addition, volatile fuels that evaporate easily, e.g. gasoline, can be dosed into the engine in bigger droplets than fuels that need more energy for evaporation, e.g. diesel fuel. Based on that, pulveriser injectors have been taken into use in the developed fuel supply system (patent EE05665B1). Figure 3.1 depicts the scheme of the working principle of the fuel supply system. The operating principle of pulveriser injectors lies in generating underpressure in the fuel flow line 423 and 424 that is positioned on the side of the pulveriser injector whereas the generation of underpressure is caused by the compressed air being directed through the injector. Due to underpressure, the fuel is directed into the pulveriser injector 433 where it mixes with air 425 and 426 after which it is directed from the injector into the intake manifold of the engine. The pulveriser injectors 433 are positioned opposite of each other so that the fuel sprays directed out of the pulveriser injectors 425 and 426 clash. Fuel droplets in the fuel spray clash wherefore they complementary fall into smaller drops 427 and once more mix with air in the intake manifold. Compressed air is directed into the pulveriser injector along the compressed air line 64. Compressed air is generated by a com-

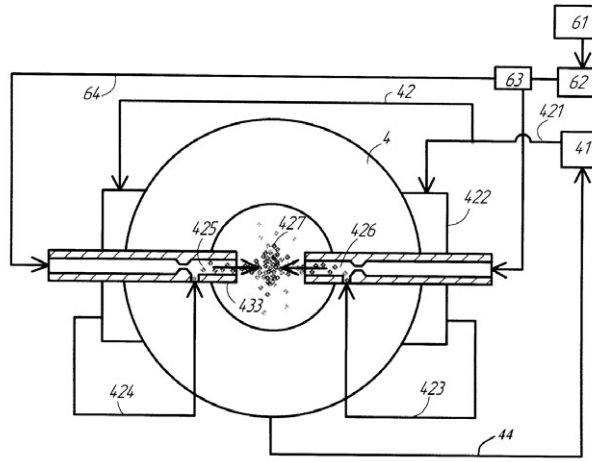

Figure 3.1. The principle scheme of air-fuel mixture formation in a pulveriser fuel supply system (Patent I). 4 – corps; 61 – compressor; 62 – pressure vessel; 63 – air-pressure regulator; 64 – air line; 41 – fuel tank; 44 – return line; 421 – fuel line to fuel-flow regulator; 422 – fuel-flow regulator; 423 and 424 – fuel line to pulveriser; 433 – pulveriser injector; 425 and 426 – first-step carburetion; 427 – second-step carburetion.

pressor 61 from where the air moves on to the pressure vessel 62 and from there to the pressure regulator 63. The fuel is directed from the fuel tank 41 to fuel-flow regulators 422. From there, due to underpressure, the fuel is directed into the pulveriser injectors 433. When fuel is injected, some of it condenses on the corps of the device 4 and flows back to the fuel tank 41 along the return line 44. This method ensures the formation of high quality air-fuel mixture with different fuels (Paper III).

An important nuance in the particular method of air-fuel mixture formation is the two-step carburetion whereas the first carburetion occurs in the pulveriser injector with the fuel being directed into the air flow and the second-step carburetion occurs when the fuel drops clash within the corps of the device. The work of the fuel supply system is controlled by regulation of the air flow and pressure. The pulveriser injectors are positioned opposite of each other on the same axis. Depending on engine power, a sufficient number of pulveriser injector pairs are added to the fuel supply system in order to guarantee the engine being supplied with fuel (Patent I).

3.2.2. An additional fuel supply system for dosing liquid biofuels into an piston engine

The operating principle of the developed fuel supply system is based on the working principle of a KE-jetronic type of a fuel supply system (Robert Bosch GmbH (1)). The fuel is injected simultaneously from all injectors into the intake manifold, behind the intake valve from where it is directed during intake stroke into all cylinders. The concept of the developed fuel supply system is based on the working principle of the abovementioned fuel supply system, however, system control has been upgraded and the device for dosing fuel has been replaced (Patent II). In addition, the system can only be used as an additional fuel supply system which implies that the engine should also have a main fuel supply system in use. The construction of the device is given on Figure 3.2. (patent EE05693B1). The fuel is directed from the fuel tank 41 by means of the fuel pump 42 through the fuel filter 43 into the fuel pressure regulator 44. The function of the pressure regulator 44 is ensuring a steady fuel pressure in the fuel supply system. From the pressure regulator 44, the fuel is directed along the fuel flow line 45 into the inlet passage 33 of the doser 30. Superfluous fuel is directed along the return line 46 back into the fuel tank 41. The fuel flows into the outlet passage 34 through

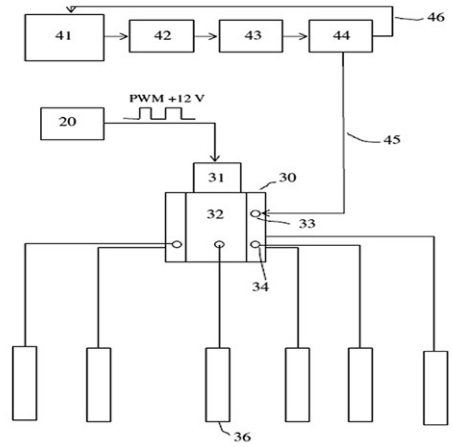

Figure 3.2. The principle scheme of an additional fuel supply system (Patent II): 41 – fuel tank; 42 – fuel pump; 43 – fuel filter; 44 – fuel pressure regulator; 45 – fuel line; 46 – backflow line; 30 – doser; 31 –electro-magnetic valve; 32 – fuel distributor; 33 – inlet passage; 34 – outlet passage; 36 – injector; 20 – control unit.

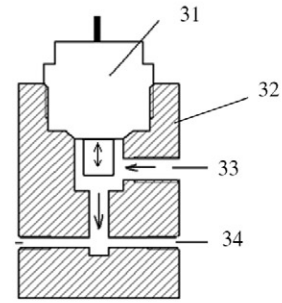

Figure 3.3. The doser of an additional fuel supply system (Patent II): 31 – electro-magnetic valve; 32 – fuel distributor; 33 – inlet passage; 34 – outlet passage.

the doser 30 and from there on into the injectors 36. The engine has one injector for each cylinder. Fuel pressure in the fuel supply system is p_f = 1…5 bar, depending on engine power and the amount of fuel injected. The doser consists of an electro-magnetic valve 31 and a distributor 32 (see Figure 3.3). The electro-magnetic valve 31 opens or closes the fuel flow passage with a valve. If the valve is open, the fuel flows into the injectors and injection occurs whereas in case the valve is closed, no injection occurs. The electro-magnetic valve is controlled by a pulse-width modulation according to which the working frequency of the valve is 10 Hz and by increasing the opening time t_o of the valve the amount of fuel injected q_c also increases. The electro-magnetic valve is controlled by

a control unit 20 which is made up of a signal generator and a transistor-controlled system (Patent II). The novelty of the fuel supply system lies in the doser which consists of one electro-magnetic valve and a fuel distributor. The fuel distributor has one fuel flow passage and a separate outlet passage for each injector.

3.3. The advantages and disadvantages of the developed fuel supply systems

The main advantage of the complex fuel supply system, hereinafter pulveriser fuel supply system, is the formation of high quality air-fuel mixture of fuels of different viscosities without altering the operating parameters of the fuel supply system. A disadvantage would be controlling the fuel supply for which reason a lot of fuel condensates on the walls of the corps of the fuel supply system. In addition, the precise positioning of the pulveriser injectors in relation to each other is of utmost importance; however, this makes the construction of the fuel supply system more complicated than that of an addition fuel supply system. The advantage of the additional fuel supply system lies in the simplicity of its construction and the possibility to use it jointly with a main fuel supply system on different engines. The main issue in using the additional fuel supply system is the formation of the air-fuel mixture of fuels of higher viscosity than ~3 $mm^2 s^{-1}$ (40 °C). This is due to both the low pressure of the fuel supply system and injectors with large injection orifices. As a result, the injection quality and the evaporation of fuel decrease. This issue could be solved by modifying the injection orifices; nevertheless, this would also imply a need to increase the fuel pressure which in turn causes the too slow opening of the valve. All in all, the fuel supply of the injected fuel would be imprecise. Regarding the given solutions, the main selection criteria is the quality of air-fuel mixture formation for which reason this particular research is focused on developing a pulveriser fuel supply system.

3.4. The construction and operating parameters of a prototype device of the pulveriser fuel supply system

The first steps in developing a novel fuel supply system are working out and building its construction. The construction of the fuel supply system

depends on the operating principle of the device, operating parameters, and the fuel used in it. The impact that the operating parameters of fuel supply system pulveriser injectors have on the capacity of injection has been researched in conjunction with PhD Arne Küüt and MS Rivo Sepping. The test data obtained during the process of co-supervision is also provided in the MA thesis of Rivo Sepping. The construction of the fuel supply system was begun by researching its operating parameters. The pulveriser injector of the fuel supply system works on the principle of a Venturi pipe (see Figure 3.4). Compressed air is directed along the canal 1 through the nozzle 2 into the injection orifice 4. The movement of air through the nozzle 2 into the injection orifice 4 slows down the air flow which causes an increase in the pressure which in turn conditions the creation of underpressure in the fuel line 3.

The air-fuel mixture is formed as the fuel drops in the air-fuel mixtures injected mutually are flung against each other for which reason the pulveriser injectors need to be positioned on the same axis in the fuel supply system corps, mutually to each other (Figure 3.5) (Patent I).

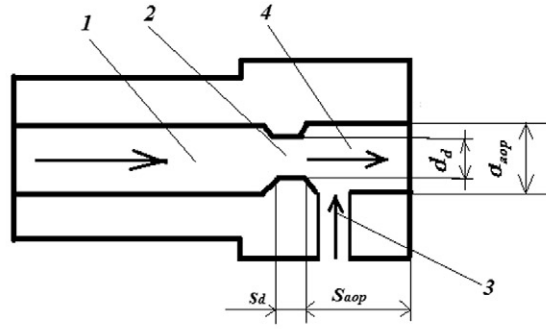

Figure 3.4. Pulveriser injector construction: 1 – compressed air canal; 2 – nozzle; 3 – fuel inlet passage; 4 –injection orifice (Injection orifice length s_{aop}, injection orifice diameter d_{aop}, nozzle length s_d, nozzle diameter d_d).

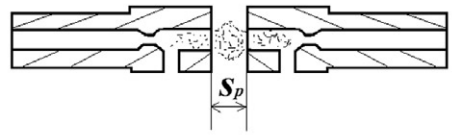

Figure 3.5. The positioning of the pulveriser injectors in the fuel supply system corps (s_p - distance between injectors).

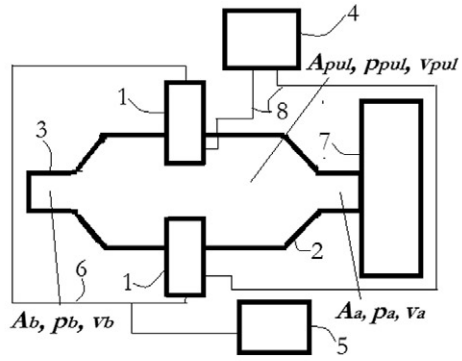

Figure 3.6. The principle scheme of the pulveriser fuel supply system test device: 1 – pulveriser injector; 2 – corps; 3 – intake manifold; 4 – fuel tank; 5 – compressor; 6 – compressed air line; 7 – air filter; 8 – fuel line (Patent I).

Pulveriser injectors are situated in the corps of the fuel supply system, which in turn is positioned in front of the intake manifold (Figure 3.6).

The diameter of the fuel supply system corps is bigger than that of the intake manifold. This slows down the air flow into the engine and lengthens the time during which the air and fuel droplets mix in the system corps. This particular process can be described by Bernoulli equation.

$$\frac{p_a}{\varrho_{air}} + \frac{v_a^2}{2} = \frac{p_{pul}}{\varrho_{air}} + \frac{v_{pul}^2}{2} = \frac{p_b}{\varrho_{air}} + \frac{v_b^2}{2}, \tag{3.1}$$

where p_a – the pressure in the pipe between the fuel supply system corps and the air filter;

p_b –pressure in the intake manifold;

p_{pul} –pressure in the pulveriser fuel supply corps;

v_a –air flow velocity in the pipe between the fuel supply system corps and the air filter;

v_b –air flow velocity in the intake manifold;

v_{pul} –air flow velocity in the pulveriser fuel supply system corps;

ρ_{air} – air density.

In case of a pulveriser fuel supply system, the diameter of the system corps is bigger than the diameter of the pipe between the intake manifold, air filter and the fuel supply system corps. In addition, the same amount of air passes through the whole system, thus, in the given solution, the following

relations are valid: $A_{pul} > A_a$, $A_{pul} > A_b$, $A_a \leq A_b$ and $Q_{pul} = Q_a = Q_b$, where A_{pul} – the sectional area of the fuel supply system corps; A_a – the sectional area of the pipe between the fuel supply system corps and the air filter; A_b – the sectional area of the intake manifold; Q_a, Q_b – the amount of air sucked into the engine in different parts of the system (Figure 3.6).

Based on the abovementioned, the following relation between the air flow velocities exists: $v_a > v_{pul}$, $v_b > v_{pul}$, $v_a \leq v_b$.
The air flow velocity can be expressed from the equation of air flow Q_{pul}:

$$Q_{pul}=A_{pul}v_{pul}=A_a v_a=A_b v_b \tag{3.2}$$

In this particular case, it has been considered that fuel droplets move in the fuel supply system corps with the same velocity as air. The air flow velocities v_{pul}, v_a and v_b are expressed by:

$$v_{pul}=\frac{Q_{pul}}{A_{pul}},\quad v_a=\frac{Q_a}{A_a},\quad v_b=\frac{Q_b}{A_b}. \tag{3.3}$$

The parameters for determining the amount of air Q_{pul} flowing through the fuel supply system are engine displacement and volumetric efficiency. In case of a cylinder of a four-stroke engine, the amount of air flowing through the fuel supply system can be expressed as follows:

$$Q_{pul}=V_c\eta_v\frac{n_e}{2}, \tag{3.4}$$

where V_c – the displacement of one cylinder, dm^3;
η_v – volumetric efficiency;
n_e –the rotational speed of the engine crankshaft, rpm.

The time t_{mix} for mixing the air-fuel mixture in the system corps is expressed by:

$$t_{mix}=\frac{s_a}{v_{pul}}, \tag{3.5}$$

where s_a – the distance between pulveriser injectors and the intake manifold;

v_{pul} – air flow velocity in the fuel supply system corps.

The time spent on mixing the air-fuel mixture is dependent on the length s_a between the pulveriser injectors and the intake manifold. The parameter s_a is dependent on the construction of the fuel supply system, engine displacement and the volumetric efficiency of the engine.

The initial prototype of the device, which has been used to study the formation of air-fuel mixture, was constructed based on the principle scheme of the above-given fuel supply system. The following was taken into account in constructing the device. The operating parameters of a pulveriser fuel supply system are the compressed air pressure p_a in the pulveriser injector and the amount of fuel q injected. Operating parameters are dependent on the diameters of the pulveriser injector nozzle d_d and the injection orifice d_{aop}. In order to select a pulveriser injector with a suitable diameter of the nozzle and injection orifice, tests to study the operating parameters of injectors were carried out on injectors with different nozzles and injection orifices. To be more exact, the impact of compressed air pressure p_a of pulveriser injectors and the distance s_p between the injectors on fuel injection capacity q ($q = f(p_a, s_p)$) was studied. Furthermore, air flow velocity in the pulveriser injector was monitored. Theoretically, the work process of a pulveriser injector can be described by equations derived from Bernoulli's equations for flow and flow velocity. Figure 3.7 describes the work of a pulveriser injector.

On Figure 3.7, the parameters p_1, Q_1 and v_1 signify compressed air pressure regulated by a regulator, compressor capacity and air flow velocity accordingly. The parameter indexes 1, 2…5 signify the abovementioned parameters in different sections of the pulveriser injector. Parameter A signifies the sectional area of the opening. The air flow velocity and pressures in different sections of the injector can be derived from the Bernoulli equation (Parr, 1998).

$$\frac{p_1}{\varrho_{air}} + \frac{v_1^2}{2} = \frac{p_2}{\varrho_{air}} + \frac{v_2^2}{2} \rightarrow \frac{p_2}{\varrho_{air}} + \frac{v_2^2}{2} = \frac{p_3}{\varrho_{air}} + \frac{v_3^2}{2} \rightarrow \text{etc} \tag{3.6}$$

where $p_{1\text{-}5}$ – pressure in different sections of the pulveriser injector;
$v_{1\text{-}5}$ – airflow velocity;
ρ_{air} – air density.

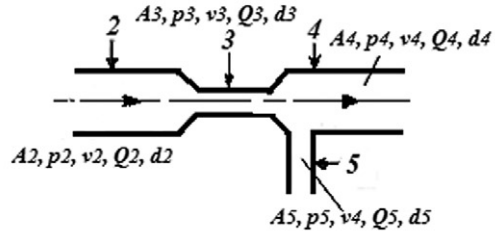

Figure 3.7. The principle operating scheme of a pulveriser injector.

To express fuel flow, the value of underpressure p_5 created in the fuel flow passage is calculated and it is seen as the pressure difference between the pulveriser injector nozzle and the injection orifice:

$$p_5=p_{env}-(p_3-p_4)\,, \tag{3.7}$$

where p_{env} – environmental pressure;
p_3 – pressure in the pulveriser injector nozzle;
p_4 – pressure in the injection orifice.

Fuel flow into the injector can be calculated according to flow equation given in standard ISO 5167:

$$q=aA_5\sqrt{\frac{2(\Delta p)}{\varrho(1-\beta^4)}}\rightarrow q=aA_5\sqrt{\frac{2(p_{env}-p_5)}{\varrho_{fuel}(1-\beta^4)}}\,, \tag{3.8}$$

where A_5 – the sectional area of the fuel line;
Δp –pressure difference;
ρ_{fuel} – fuel density;
β – the ratio of opening diameters ($\beta=\frac{d_4}{d_3}$);
a – flow coefficient dependent on the type of obstruction (0.6… 0.9).

Based on the abovementioned, SolidWorks 2010 program enables to simulate air travel in a pipe of variable geometry. In this particular study, SolidWorks program was used to research air travel in pulveriser injectors of different injection orifice diameters d_{aop}, lengths of injection orifices s_{aop}, diameters d_d and lengths s_d of the nozzle. When running experimental tests, such parameters characterizing the opening of pulveriser injectors which alteration hinders fuel flow into the injector were chosen. Based on that, the diameter of the pulveriser injector nozzle is d_d = 1 mm, and the diameter of the fuel flow passage is d_{fop} = 2.5 mm. The length s_{aop} and diameter d_{aop} of the injection orifice influence the value of injection spray (the diameter of the injection spray when emerging from the injector) as well as fuel flow into the pulveriser injector. Based on this, Table 3.1 provides the parameters of the pulveriser injector which alteration impacts the size and quality of the injection spray.

SolidWorks 2010 program was used to create simulations that characterize air travel in pulveriser injectors of different geometry. These are given on Figure 3.8.

Table 3.1. The parameters of an injection orifice and the fuel flow passage of a pulveriser injector (Sepping, 2011)

Injector no.	Injection orifice		Nozzle	
	Length s_{aop}, mm	Diameter d_{aop}, mm	Length s_d, mm	Diameter d_d, mm
1	5	2	1.1	1
2	10	3	1.1	1
3	10	2	1.1	1
4	5	2	6.1	1
5	5	3	1.1	1

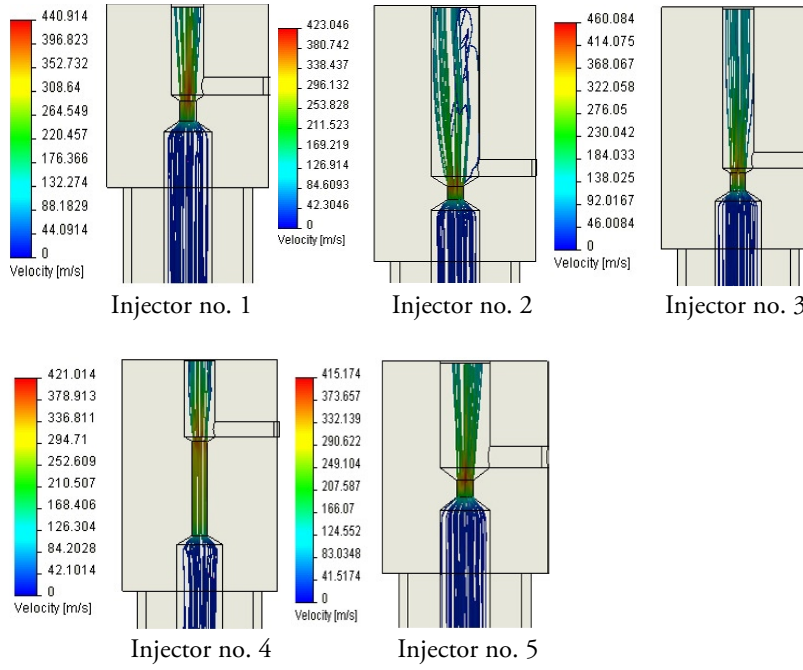

Figure 3.8. A simulation characterizing air travel in a pulveriser injector under pressure p_a = 2.5 bar (Sepping, 2011).

Similarly to illustrations on Figure 3.8, analogous simulations were carried out under compressed air pressure of p_a = 2…3.5 bar with a transfer step of Δp_a = 0.5 bar. The simulations let assume that the air flow velocity in the nozzle reaches about v_3=350 m s^{-1} whereas the same figure at the end of the injection orifice of the injector is v_4=100 m s^{-1}. The same velocity is achieved by fuel droplets in the air flow. Based on the simulation, it

can also be said that in case of a big diameter and long injection orifice, air vortexes, which may cause the misdistribution of fuel droplets in the fuel spray, are created in the orifice (see Figure 3.8, injector no. 2).

In addition, a big diameter $d_{aop} > 2$ of the injection orifice does not impact the diameter of the fuel spray (Figure 3.8, injector no. 5). The diameter of fuel spray is determined by the diameter d_d of the nozzle. Nozzle length does not impact air flow velocity v_4 in the injection orifice of the pulveriser injector (injector no. 4). Tests with pulveriser injectors of different geometries to study the impact of injection pressure p_a and fuel viscosity v_i on the injection capacity q ($q = f(v_i, p_a)$) of one injector were carried out. What is more, the impact of firstly, the distance between injectors, and secondly, liquids of different viscosity on the injector injection capacity $q = f(v_i, s_p, p_a)$ was studied. A test plan was compiled to carry out the tests:

1. To construct nozzles of different geometries which parameter variations are given in Table 3.1.
2. To measure the injection capacity of the pulveriser injector in case of different fuels and injection pressures. For doing so, it is necessary to weigh the fuel tank before and after the test and calculate the injector injection capacity. During each test, the amount of fuel flowing through the injector within 60 seconds has to be measured.
3. To use water, rapeseed oil and diesel fuel as test fuels to study the impact of different viscosities v_i on the injection capacity q of the pulveriser injector. The objective is to determine the equation $q = f(v_i)$.
4. To study the impact of injection pressure and fuel viscosity on the injection capacity q ($q = f(v_i, p_a)$) of one pulveriser injector. The comparison of the test data of this particular test with the data obtained during tests with injector pairs illustrates the impact of mutually positioned injectors on injection capacity q.
5. To study the mutual impact of the injectors whereas the distance between them is chosen to be $s_p = 5\ldots13$ mm with a transfer step of $\Delta s_p = 2$ mm. The amount of fuel q flowing through the injectors of different geometries is measured on different distances of the injectors given in Table 3.1. The tests are carried out under injection pressures $p_a = 2\ldots4.5$ bar with the transfer step being $\Delta p_a = 0.5$ bar. On tests, the maximum value of the injection pressure p_a is dependent on achieving the maximum fuel supply of different fuels.
6. To analyze the data obtained during tests and choose the most suitable injector to be used in the construction of the fuel supply system.

During tests, the injection capacity of an injector pair was measured per time. The example depicts the injection capacity of the injector pair no. 3 running on water and rapeseed oil under different injection pressures (Figures 3.9 and 3.10).

When comparing Figures 3.9 and 3.10, it becomes evident that as the fuel viscosity increases (water has significantly lower viscosity than rapeseed oil), the injection capacity of injectors decreases substantially (almost

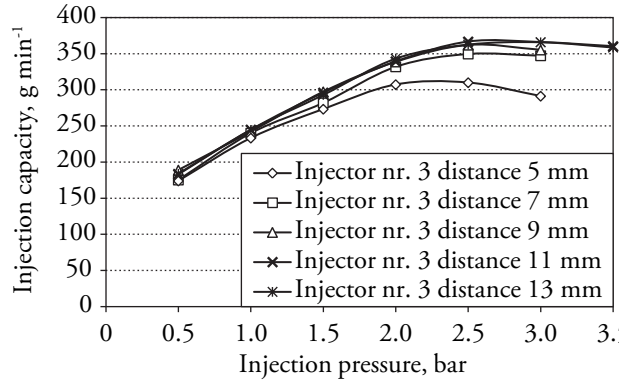

Figure 3.9. The injection capacity of the injector no. 3 depending on injection pressure and distance between injectors (Sepping, 2011). The fuel injected is water. Measurements were carried out under the following environmental parameters: air temperature T_{env} = 21.4 °C, air humidity ϕ_{env} = 26%, atmospheric pressure p_{env} = 764 1018.58 hPa.

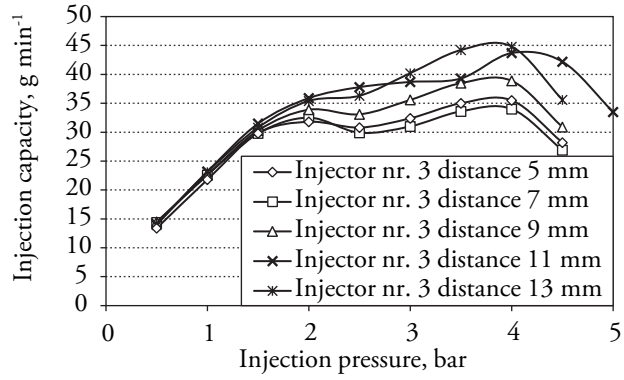

Figure 3.10. The injection capacity of the injector no. 3 depending on injection pressure and distance between injectors (Sepping, 2011). The fuel injected is rapeseed oil. The measurements were carried out under the following environmental parameters: air temperature T_{env} = 22.1 °C, air humidity ϕ_{env} = 23%, atmospheric pressure p_{env} = 1014.58 hPa.

eight times in this particular case of an injector pair). When fuel of a low viscosity is used, the increase in the injection pressure brings about an increase in the injection capacity q of up to p_a = 2.5 bar (Figure 3.9). In case of liquids that have high viscosity (e.g. rapeseed oil), the injection capacity q of injectors increases up to p_a = 4 bar. What is more, the injection capacity is impacted by the distance s_p between the injectors. Based on the given tests, it can be said that the bigger the distance s_p between injectors, the higher the injection capacity q. At the same time, it must be taken into account that the longer the distance between the injectors, the lower the velocity of fuel drops in clashing with each other. Figure 3.10 illustrates that the highest injection capacity is achieved on the injector distance of s_p = 11…13 mm. Similar tests were carried out using each test liquid and injectors of different geometries. Based on the tests, it can be implied that the injector geometry did not substantially impact variations in the abovementioned influencing factors. Based on the test data, an injector for the pulveriser fuel supply system was chosen which most relevant parameters are given in Table 3.2.

Table 3.2. The parameters of the injector chosen according to the test data (Sepping, 2011).

	Nozzle diameter d_d, mm	Nozzle length s_d, mm	Injection orifice diameter d_{aop}, mm	Injection orifice length s_{aop}, mm	Injection pressure p_a, bar
Injector no. 3	1	1.1	2	10	2.5

The injector of the parameters given in Table 3.2 enabled the highest possible injector injection capacity q. The injection pressure of p_a = 2.5 bar ensures the smallest possible pressure produced by the compressor chosen for the system. A general rule states that the higher the pressure p_a produced by the compressor and the capacity Q_l of the compressor, the bigger its construction and cost. The injectors were installed into a cylindrical system corps, which was complemented with rigs for regulating the injector position. The material of the system corps was chosen to be Plexiglas to enable the visual observation of the work process of the fuel supply system working on an engine. When running the tests with pulveriser injectors, it became evident that a small error in the work process of one injector impacts the entire process of the air-fuel mixture formation significantly. In addition, in the particular system, the precise positioning of injectors' axes is essential so that the injected fuel sprays

would clash. With regard to this, the manufacturing quality of the injectors must also be precise to reduce the impact of air vortexes created in the injector on the fuel spray.

3.5. The quality of the air-fuel mixture formed by the pulveriser fuel supply system and its suitability for dosing into an engine

The quality of the air-fuel mixture can be determined by the size of fuel droplets in the air-fuel mixture. One possibility for examining the quality of the air-fuel mixture would be using either the laser diffraction-based method or the two-wavelength laser absorption-scattering method (Li et al., 2011). For the purposes of this particular thesis, the metering device Malvern Spraytec STP5911, which is based on measuring the size of fuel droplets using a laser diffraction-based method, was used (Malvren, 2007). The idea of a laser diffraction-based method lies in measuring the intensity of the angle of the laser beam light at the moment the laser beam permeates the fuel spray. Large fuel droplets bring about a small difference in the angle of the laser beam on the detector of the metering device whereas small droplets cause a more significant difference in the angle. The size of fuel droplets is calculated according to the pattern on the detector reflecting the variation in the angle of the laser beam light for which the Mie light theory is used (Malvren, 2012). The measuring range of the metering device in case of a d_{len} = 300 mm lens is m_{spy} = 0.1… 900 µm and the measure accuracy is +/- 1% D_{50} of the NIST standard (in case of a D_{50} parameter, the measure range is m_{spyd50} = 0.5…600 µm). The device is controlled with Spraytec software (Malvren, 2007). The software enables to calculate the most essential parameters for measuring the fuel droplets and reflects these either in a table or as graphs. The most relevant parameters measured are the laser beam transmission (Trans, %) and the arithmetic mean diameter D_{10} of the droplet, expressed by (Sescu et al., 2011):

$$D_{10} = \frac{\sum N_i d}{\sum N_i}, \tag{3.9}$$

where d – the mean diameter of fuel droplets;
N_i – the number of droplets in the size range i ($N_i = d_{max} \ldots d_{min}$).

Another parameter measured is the droplet diameter D_{50} based on which 50% of the droplets are smaller and 50% larger than D_{50} in the volume

(D_{50}, Mass Median Diameter). In addition, the fuel droplet diameter D_{90} of which 90% of droplets are smaller (Malvern, 2012), the Sauter mean diameter D_{32} (equation (1.1)), and the Herdan mean diameter D_{43} that characterizes the size of fuel droplets most common in the injected fuel spray are measured. The Herdan mean diameter is expressed by the equation (Sescu et al., 2011 and Malvern, 2012):

$$D_{43}=\frac{\sum N_i d^4}{\sum N_i d^3}, \tag{3.10}$$

When measuring the size of fuel droplets, the fuel supply system was placed so that the formed air-fuel mixture would at some point be in the measure range of the laser beam. The test scheme is given on Figure 3.12. The laser beam was positioned above the pulveriser injectors of the fuel supply system to ensure the two-step carburetted air-fuel mixture falling in the laser beam. The distance of the laser beam from the injectors was not relevant for the purposes of this particular test as the fuel supply system forms the air-fuel mixture in the system corps where the air sucked into the engine mixes with it. The metering device Malvern Sprytec STP2911 (see Figure 3.11) enables the constant measurement of the size of fuel droplets for which reason the graph (see Figure 3.13) provides the size of fuel droplets measured throughout the entire injection process. During the process of running the tests, the environmental parameters were the following: air temperature: 21 °C, atmospheric pressure: 1015.92 hPa and air humidity: 60%.

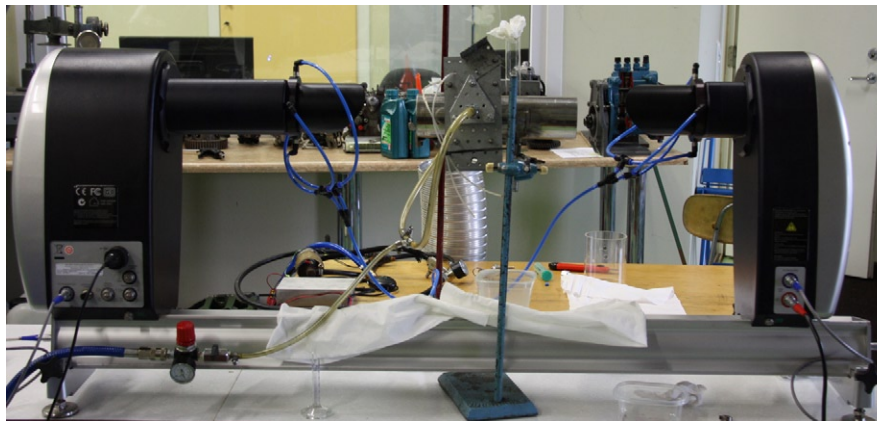

Figure 3.11. The placement of the pulveriser fuel supply system in the metering device Malvern Sprytec STP2911.

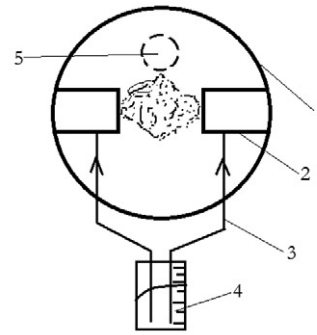

Figure 3.12. The scheme of measuring the size of fuel droplets: 1 – corps; 2 – pulveriser injector; 3 – fuel line; 4 – measuring glass; 5 – laser beam position.

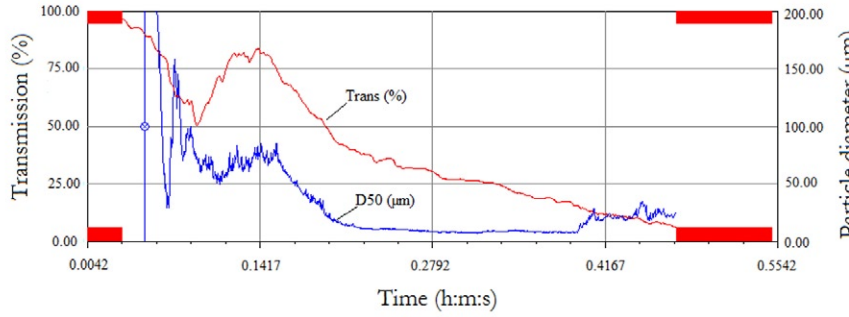

Figure 3.13. The distribution of the size of diesel fuel droplets throughout the injection process where a – beginning, b – end.

To measure the size of fuel droplets, the air-fuel mixture was formed of four fuels, namely, of 96.4% ethanol, diesel fuel, rapeseed oil, and water. The test fuel was injected $q = 3$ cm^3 during one session. The characteristic of the distribution of diesel fuel droplets is given on Figure 3.13.

The line "Trans" characterizes laser beam transmission throughout the process. If the laser beam transmission is 100%, then there are no fuel droplets in the laser beam.

Based on Figure 3.13, it can be said that by reducing the diameter D_{50} of the droplets, the laser beam transmission decreases simultaneously. Depending on the precision of fuel supply in the initial prototype of the fuel supply system, the measure range on the graph was chosen to be $a \rightarrow b$. The zone before point a has come about due to the imprecision of the starting of the fuel supply system injection process as one of

the injectors started injecting fuel before the other. Conditioned by this, there was no clashing of fuel droplets, thus, the fuel droplets did not fall into additionally smaller droplets. This issue can be resolved by increasing the precision of both the fuel supply as well as the work of injectors. The zone after point *b* characterizes the ending of fuel in the system where the injection of fuel sprays against each other is not complete as the air sucked into the system does not ensure the clashing of fuel droplets against each other. Therefore, the data of the measure range $a \rightarrow b$ was chosen for the calculation data. Three measurements were performed with all test fuels and their averaged measurement data was calculated (Table 3.3…3.5)

The injection quality of the pulveriser fuel supply system was compared to the quality of the air-fuel mixture formed by the injector (Stanadyne 781649) of the fuel supply apparatus of the engine Valmet 320 DS. In this particular study, determining the quality of air-fuel mixture was based on the parameters characterizing the air-fuel mixture formed by the fuel supply apparatus of the abovementioned diesel engine. If the size of fuel droplets in the air-fuel mixture was of the same magnitude or smaller than the size of fuel droplets in the air-fuel mixture formed by the diesel engine fuel supply system, then the air-fuel mixture would be of high quality. Stanadyne 781649 injector has five injection orifices of which one injected the fuel into the laser beam. The distance between the injector and the laser beam of the metering device was 10 mm and the amount of fuel injected per one injection orifice was 20 mm^3. The measurement data is given in Table 3.3. The laser beam transmission was greater in case of a pulveriser fuel supply system since a greater amount of fuel was injected during one test. The results indicate that the Sauter mean diameter D_{32} and the arithmetic mean diameter D_{10} of the droplets were smaller in case of a pulveriser fuel supply system. The Mass Median Diameter D_{50} was of the same magnitude (around ~30 µm) in both fuel supply systems. In case of parameter $D_{90,}$ the fuel droplets in the air-fuel mixture formed by the pulveriser fuel supply system were significantly smaller. Similarly, the Herdan mean diameter D_{43} that characterizes the diameter of fuel droplets most common in the air-fuel mixture was smaller in case of a pulveriser fuel supply system. Based on the abovementioned, it can be claimed that the diameter of fuel droplets in the air-fuel mixture formed by the pulveriser fuel supply system is smaller. During tests, several issues regarding the use of the primary prototype of the pulveriser fuel supply system arose, e.g. the uneven distribution of fuel between injectors, which impacted the formation of the air-fuel mixture.

Table 3.3. The parameters of the diesel fuel air-fuel mixture formed with the pulveriser fuel supply system and DSA.

Parameter	Diesel fuel	
	Pulveriser fuel supply system (Injection pressure p_a = 2 bar)	DSA injector (200 bar)
Trans (%)	39.2	53.8
D_{10} (µm)	4.1	9.8
D_{50} (µm)	30.6	31.7
D_{90} (µm)	132.6	176.6
D_{32} (µm)	9.6	19.8
D_{43} (µm)	56.20	65.3

Table 3.4. The impact of the pressure of compressed air in the pulveriser fuel supply system on the quality of the air-fuel mixture.

Parameter	Injection pressure p_a		
	1 bar	2 bar	2.5 bar
Trans (%)	43.9	76.1	47.5
D_{10} (µm)	32.4	12.2	17.7
D_{50} (µm)	65.1	57.5	35.6
D_{90} (µm)	135.0	164.5	72.6
D_{32} (µm)	49.7	22.5	28.2
D_{43} (µm)	77.0	75.8	44.4

Table 3.5. The size of fuel droplets in the air-fuel mixtures of rapeseed oil and water formed by a pulveriser fuel supply system.

Parameter	Fuel	
	Rapeseed oil (p_a = 2 bar)	Water (p_a = 2 bar)
Trans (%)	58.8	46.4
D_{10} (µm)	2.3	15.4
D_{50} (µm)	14.2	49.1
D_{90} (µm)	79.7	150.2
D_{32} (µm)	5.2	23.6
D_{43} (µm)	30.1	69.0

In a pulveriser fuel supply system, compressed air is directed through the pulveriser injector for which reason underpressure p_{an} is created in the fuel flow passage. The pressure of compressed air is regulated in the interval p_a = 1…2.5 bar. The impact of pressure on the quality of the air-fuel mixture is given in Table 3.4.

The tests were carried out using bioethanol with a concentration of 96.4%. Test results with regard to different injection pressures reveal that as the pressure increases, generally, the diameter of fuel droplets in the air-fuel mixture reduces. This does not apply to parameters D_{32} and D_{90}. In case of parameter D_{32}, the smallest diameter of fuel droplets has been achieved under the injection pressure p_a = 2 bar. What is more, the indicator characterizing D_{90} is the largest when the injection pressure is p_a = 2 bar. Under the pressure p_a = 2 bar, the mean diameter of bioethanol fuel droplets is generally of the same value as in case of diesel air-fuel mixture formed by a diesel supply system. It should be stated, however, that the parameters most commonly affecting injectability, namely, density ρ_{fuel} and viscosity v_i, are different in diesel fuel and bioethanol. The positive effect lies in the fact that the fuel droplets in the air-fuel mixture formed with bioethanol are generally of the same size or smaller than the diesel fuel droplets formed by a diesel fuel supply system (according to the comparison of the parameter D_{90} in Table 3.3 and Table 3.4). Depending on the Sauter mean diameter $D_{32,}$ a sufficient injection pressure for the formation of a high quality air-fuel mixture in a pulveriser fuel supply system is p_a = 2 bar. Table 3.5 provides an overview of air-fuel mixtures formed by a pulveriser fuel supply system with both cold-pressed rapeseed oil and water.

The test results in Table 3.5 bring forth the fact that the air-fuel mixture formed with rapeseed oil has a significantly smaller concentration of fuel droplets than the fuels formed with water, bioethanol, or diesel fuel. Based on that, it can be deduced that as the viscosity v_i of fuel increases, the quality of the air-fuel mixture also increases. This claim contrasts with common knowledge according to which the quality of air-fuel mixture decreases as the viscosity of fuel increases. When commonly known injection methods are used, the injection spray is broken down due to air-resistance for which reason fuels of lower viscosities are easier to break down than fuels of higher viscosities. In case of the injection method developed in the framework of this thesis, the fuel droplets are additionally broken down as they clash with other fuel droplets. However, it is not exactly known what happens as the fuel droplets clash. This outcome requires further research. In case of the pulveriser fuel supply system, the quality tests of the air-fuel mixture revealed that the device is suitable for dosing fuels of different viscosity. When compared to the diesel fuel supply system, the size of droplets in the air-fuel mixture is generally of the same magnitude. Therefore, it might be said that for the combustion of bioethanol air-fuel mixture in the cylinder, the same amount of time

is consumed as for the combustion of diesel fuel (equation 1.7). The compressed air pressure on tests was p_a = 2 bar (Table 3.4).

3.6. The development phases and solutions of the developed fuel supply system

When developing the pulveriser fuel supply system, the renown TIPS methodology was used, which in the given case consisted of the following basic stages (Fowlkes, 2010; Ulrich, 1995; Paper III):

1) identifying and phrasing the problem;
2) finding a typical problem similar to the phrased problem;
3) analyzing the known solutions;
4) finding the most suitable solution for the problem at hand.

Next, the development phases and examples of technical solutions developed throughout these phases are given. The description consists of firstly, Table 3.6 where the development phases of the fuel supply system and the activities performed during these are given, and secondly, following the table, the description of phases, i.e. the description of arisen issues and their solutions (Paper III).

Next, comments on the development phases in Table 3.6 are provided (Paper III).

Feasibility study. To apply the concept of the air-fuel mixture formation, it is necessary to develop a suitable fuel supply system construction that would guarantee the engine being supplied with high quality air-fuel mixture and being resistant to the vibration as well as to the physico-chemical properties of the fuel. In order to achieve this, the impact that the operating parameters of the fuel supply system injectors have on the fuel supply and the quality of the air-fuel mixture was studied. This particular process is more closely described in subchapters 3.4 and 3.5. During tests, it became evident that the injected fuel condenses on the walls of the fuel supply system corps, which is conditioned by the inaccurate regulation of the fuel amount. Therefore, an airflow regulator was added to the compressed air line of the fuel supply system.

Applied research, stage I. During engine tests with the initial fuel supply system, it became evident that the underpressure created in the intake manifold impacts the fuel flow into the pulveriser injector. To be more

Table 3.6. The development phases of a pulveriser fuel supply system (Paper III).

Stage	Activities	Description
Feasibility study Concept realization and construction of the test device	1. Carrying out preliminary study. 1.1. Selecting the injectors. 1.2. Checking the injection methods, process modelling. 1.3. Elaborating the principle of system construction. 2. CAD modelling. 3. Preparing for 3D drawings. 4. Preparing control programmes for CNC benches. 5. Technological mapping. 6. Processing the details in CNC.	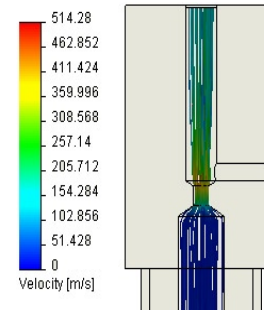
Applied research **I** Study of the processes in the fuel supply system	1. Preparation of simplified test device. 2. Monitoring of processes and making conclusions. 3. Elaboration of enhanced test device	
II Study of the operation of the improved fuel supply system	1. Improving the construction of the test device. 2. Monitoring the operation process of the test device and making conclusions. 3. Elaborating the enhanced construction of prototype devices	
Product development **I** Designing the prototype device	1. Preparation of the improved prototype devices. 2. Testing and solving any problems that might arise.	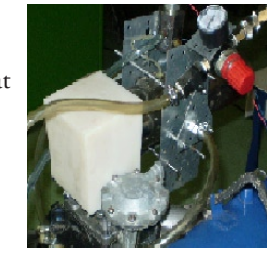
II Designing the improved prototype device	1. The preparation of an improved fuel supply system, which solves the issues that came about when the previous prototype device was used. 2. Running complementary tests on the engine and solving any emerging issues. 3. Determining the efficiency of the prototype device.	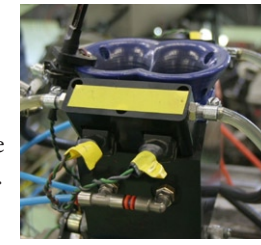

exact, the underpressure in the intake manifold caused the fuel being sucked into the engine through the pulveriser injector, which resulted in an uncontrollably running engine. To solve this issue and better regulate the fuel flow into the injector, a doser was added to the fuel supply system. The doser consists of an electro-magnetic valve and a distributor. In the closed position of the electro-magnetic valve, the fuel flow into the pulveriser injector is paused. The doser is controlled with a pulse-width modulation on a certain frequency by changing the fill factor of the signal. As the fill factor increases, the valve is open for a longer period of time, thus, more fuel is directed into the pulveriser injector. The doser should be positioned as close to the pulveriser injector as possible to reduce the effect the fuel in the fuel line has on the engine operating mode. The given solution enables to use a fuel supply system without an airflow regulator.

Applied research, stage II. When testing the fuel supply system, it became evident that the formed air-fuel mixture is condensed on the fuel supply system corps, which causes the liquid fuel to flow into the engine cylinder. To remove the superfluous fuel from the system, a return line was added to the device. For doing so, the position of the fuel supply system corps was altered so that the condensed fuel would flow into the return line without causing failures in the work of the engine.

Product development, stage I. During the design of the prototype device, the fact that the fuel must flow from the fuel supply system corps into the return line on different positions of the engine was taken into account. During tests, problems arose when the fuel supply system was tested on a spark ignition engine. As the cylinder is filled with a rich air-fuel mixture, the combustion process lasts for a substantial amount of time for which reason the opening of the intake valve may bring about backfires into the intake manifold. Due to the effect of the backfires, the fuel condensed in the fuel supply system corps ignites. To solve this issue, it was necessary to add a lambda sensor to the fuel supply system so that the proper concentration of air-fuel mixture in the engine would be ensured. For the safe use of the device, it was necessary to work out a new construction, which would ensure the formation of a high-quality air-fuel mixture and lack a place for the condensed fuel to accumulate.

Product development, stage II. For the construction of the improved fuel supply system prototype, the issues having emerged during previ-

ous development phases were analyzed and their solutions improved. As a result of the analysis, a construction of a new fuel supply system was designed, which is controlled by an electronic control unit. The following paragraphs describe the fuel supply system with the novel construction more precisely.

In order to guarantee safety when operating the pulveriser fuel supply system, there can be no condensed fuel in the system as it could ignite when the engine backfires. Therefore, the fuel supply must be precise enough to ensure fuel supply into the engine on the air-fuel ratio of 1/14.7 on each engine mode. The construction of the fuel supply system must be designed so as not to enable the accumulation of condensed fuel. To achieve the abovementioned requirements, a construction of a pulveriser fuel supply system dosing apparatus was developed, given on Figure 3.14. The following solution and model of the fuel supply system was developed during the supervision process of Taavi Põri's Master's thesis. The patent application P201200024 which was compiled based on that thesis will be published 15th August 2014 before the defence of the doctoral thesis.

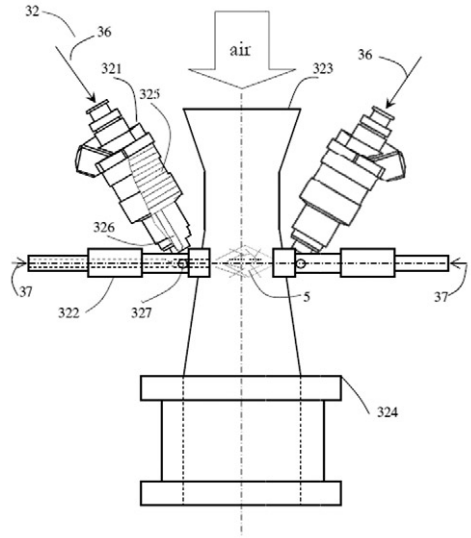

Figure 3.14. The principle scheme of an improved prototype of the pulveriser fuel supply system dosing apparatus (Patent III): 32 – pulveriser fuel supply system dosing apparatus; 36 – fuel line; 37 – air line; 321 – doser; 322 – pulveriser injector; 323 – mixture flue; 325 – coil ; 326 – closing needle; 327 – fuel flow passage into the pulveriser injector; 324 – corps; 5 – air-fuel mixture.

The most substantial difference in the novel solution as compared to the previous one is the fuel supply principle. Whereas in the previous systems, the fuel was sucked into the pulveriser injector, the singularity of the given solution lies in the fuel being directed into the pulveriser injector under pressure. This enables to precisely regulate the amount of fuel dosed. In addition, the fuel supply can be increased by increasing the fuel pressure in the line (in case of high viscosity fuels, the fuel supply reduced substantially (subchapter 3.4, Figures 3.9 and 3.10)). The fuel supply system corps is positioned upright on the engine. The corps has been designed so that the fuel would be injected into the airflow which is sucked into the engine. This solution enables for the air-fuel mixture to move directly into the intake manifold without condensing (Patent III).

Similarly to previous prototypes, the compressed air is directed along the air line 37 into the pulveriser injector 322 and from there into the mixture flue. The fuel is directed along the fuel line into the doser 321. From the doser 321, the fuel is directed to the closing needle 326. By applying a voltage to the coil 325, the closing needle 326 moves into the coil, thus, opening the fuel flow passage 327 into the pulveriser injector 322. The fuel mixes with air in the pulveriser injector and is then directed into the mixture flue 232 where the air-fuel mixture 5 is formed as the fuel sprays clash. From the mixture flue 323, the air-fuel mixture moves through the intake manifold into the engine cylinder. The pulveriser injectors are positioned in a special corps 324 to ensure their exact mutual positioning. In order to avoid the condensation of the air-fuel mixture in the intake manifold, it is necessary to use a close-loop fuel supply regulation. This means that the air-fuel ratio in the engine is determined by a lambda sensor. Based on the signal from the lambda sensor, the amount of fuel injected is either reduced or increased. The fuel dosers are controlled according to the rotational speed and load of the crankshaft. For this purpose, a control unit MegaSquirt II developed to control the work of spark ignition engines is used. The fuel supply system can be used on spark ignition engine as the main fuel supply system and on compression ignition engine as an additional fuel supply system. The main difference in the system lies in the sensors based on which the work of the engine is controlled. As an example, Figure 3.15 depicts the principle scheme of a pulveriser fuel supply system for use on a compression ignition engine (Patent III).

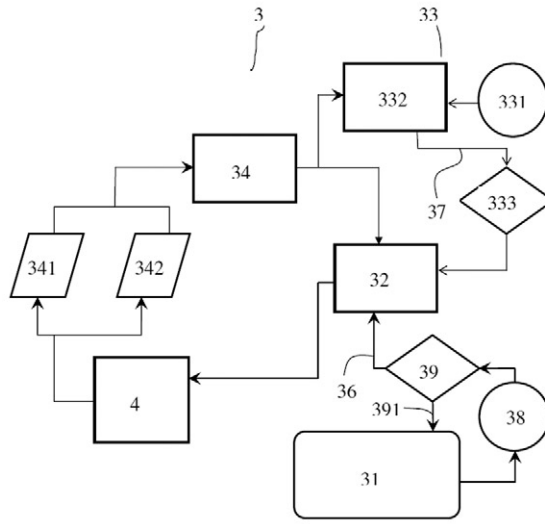

Figure 3.15. The principle scheme of a pulveriser fuel supply system (Patent III).

The fuel is directed from the fuel tank 31 by a fuel pump 38 into the fuel pressure regulator 39. From the pressure regulator 39, the fuel is then directed into the dosing apparatus. Superfluous fuel is directed along the return line 391 back into the fuel tank 31. The compressed air system 33 consists of a compressor 331, an electronic valve 332, an air pressure regulator 333, and an compressed air line 37. From the compressor 331, the compressed air is directed through the electronic valve 332 into the air pressure regulator 333 and from there on along the air line 37 into the dosing apparatus 32. From the dosing apparatus 32, the air-fuel mixture formed is directed into the engine 4. A control unit 34 controls the work of the dosing apparatus 32. The control unit runs the dosing apparatus 32 based on the signals obtained from the position sensor of the accelerator 341 and the crankshaft rotational speed sensor 342.

The developed pulveriser fuel supply system can be applied as the fuel supply system on both spark and compression ignition engines. In case of spark ignition engines, it can be used as the main fuel supply system, e.g. when using bioethanol as the engine fuel. In case of compression ignition engines, the system can be used as an additional fuel supply system to ensure the proper ignition timing of the air-fuel mixture. On compression ignition engines, the system is controlled by the crankshaft rotational speed sensor, the intake manifold pressure sensor, pressure sen-

sor and accelerator position sensor whereas on spark ignition engines, the system is controlled by the crankshaft position sensor, crankshaft rotational speed sensor, intake manifold sensor and the lambda sensor (Patent III).

When testing the novel pulveriser fuel supply system on engines, the abovementioned issues did not emerge. Next, a model for adjusting the operating parameters of the fuel supply system is given. The model simplifies the choice of fuel supply system operating parameters when different fuels are used.

3.7. A model for selecting operating parameters of a pulveriser fuel supply system

The amount of fuel dosed into the pulveriser fuel supply system depends on the operating parameters, i.e. fuel pressure in the system and the pressure of compressed air. In addition, the amount of fuel dosed is significantly impacted by the viscosity of fuel and the distance between injectors. Based on the abovementioned, a model for calculating the amount of fuel with regard to operating parameters and the viscosity of fuel was drawn. Based on this calculation model, a theoretical amount of fuel for different engines to ensure a sufficient number of injection pairs in a fuel supply system can be determined.

For the purposes of drawing up the calculation model, the pressures effective in the fuel line of the fuel supply system affecting the fuel flow into the injector have been treated separately. Based on the abovementioned operating principle of the fuel supply system, the calculation model includes the pressure p_f in the fuel line and underpressure p_0 created by the compressed air p_a directed through the pulveriser injector. The value of underpressure p_0 in the fuel line is affected by the pressure of compressed air directed into the pulveriser injector. During tests, the underpressure was measured depending on the pressure of compressed air $p_0 = f(p_a)$. Test data makes it evident that the as the pressure of compressed air increases, the underpressure in the fuel line also increases. The variation in the underpressure p_0 can be characterized by the variation in the pressure in the system, i.e. $p_0 = p_{env} - \Delta p_0$. To describe the variation in the pressure Δp_0 in the fuel line depending on the pressure of compressed air p_a, the test data can be used as a basis for constructing a polynomial, which is

characterized by the following equation:

$$\Delta p_0(p_a)=c_1p_a^2+c_2p_a+c_3\ , \tag{3.11}$$

where Δp_0 – the variation in the pressure in the fuel line;

p_a – the pressure in the air line;

c_1, c_2, c_3 – constants that are dependent on the compressed air size range in the system $p_{a.i} = p_{amax}\ldots p_{amin}$, the diameters of the pulveriser injection nozzle d_d and the injection orifice d_{aop} as well as the precision of manufactured surfaces.

The abovementioned constants are calculated experimentally. To calculate the constants, a test was carried out during which the variation in pressure Δp_0 was measured in the fuel line heading for the pulveriser injector depending on the value of compressed air pressure p_a directed through the pulveriser injector. In this particular case, the value of compressed air pressure was varied in the range p_a = 0.5…2.2 bar. During tests, pulveriser injectors which parameters were described in the subchapter 3.4 were used. The values of constants $c_1\ldots c_3$ obtained during tests are given in the equation on Figure 3.16. More precisely, Figure 3.16 characterizes the variation in the pressure in the fuel line.

The amount of fuel q directed into the injector is proportional to the amount of fuel flowing through the doser q_d ($q = q_d$) since the underpressure p_0 also impacts the fuel flow in the doser. Therefore, the pressure p affecting the fuel is expressed as the sum of fuel pressure p_f regulated by

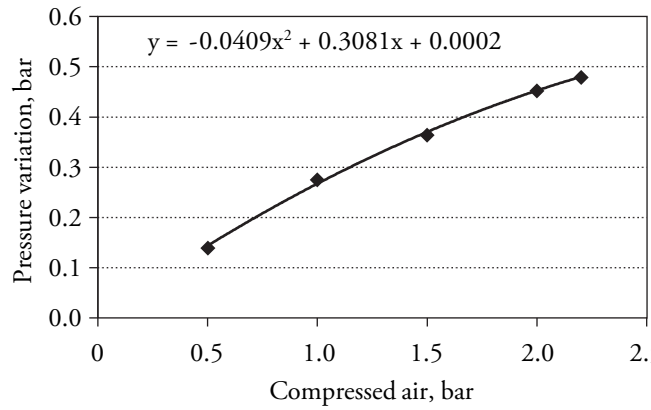

Figure 3.16. Pressure variation in the fuel line depending on the value of the pressure of compressed air.

the fuel pressure regulator in the system and the variation of underpressure Δp_0 in the fuel line:

$$p(p_f,p_a)=p_f+\Delta p_0(p_a)\,, \tag{3.12}$$

where p – the pressure impacting the fuel in the system;

p_f – the fuel pressure regulated by a pressure regulator in the system.

The amount of fuel directed into the injector depends on the pressure p for which reason, the following relation is valid: as the pressure p affecting the fuel increases, the amount of fuel q directed into the injector also increases.

The capacity q of dosers, which takes into account the concurrence of the fuel pressure p_f and the pressure variation $\Delta p_{0,}$ can be expressed by the equation:

$$q(p_f,p_a) = k_1 p\left(p_f,p_a\right)^3 + k_2 p\left(p_f,p_a\right)^2 + k_3 p\left(p_f,p_a\right) + k_4\,, \tag{3.13}$$

where k_1, k_2, k_3, k_4 – constants, which are determined experimentally and are dependent on the size range of the compressed air pressure and fuel pressure used in the fuel supply system. To determine the constants, tests were carried out during which the amount of fuel flowing through the dosers under different fuel pressures p_f was measured. The fuel pressure p_f was varied in the range of p_f = 1…5 bar with the measurement time being t_t = 15 s. Figure 3.17 characterizes the test data.

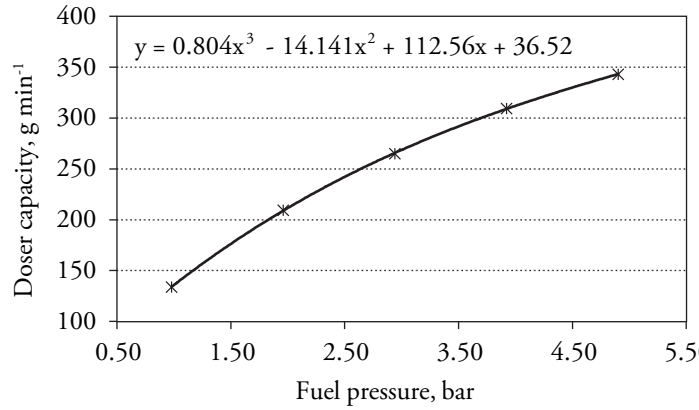

Figure 3.17. The amount of fuel flowing through the dosers in one minute depending on the fuel pressure in the fuel line.

Based on the abovementioned, it can be claimed that the fuel pressure p_f given on Figure 3.17 is equal to the pressure p affecting fuel in the pulveriser fuel supply system. The main difference concerning the fuel supply system lies in the fact that the entire pressure affecting fuel is expressed as an equation (3.12). Therefore, if the regulated fuel pressure in the pulveriser fuel supply system is p_f = 2 bar and the compressed air pressure equals p_a = 2 bar, the pressure affecting fuel is p = 2.45 bar. According to Figure 3.17, the amount of fuel directed into the pulveriser injector during one minute under the given pressure is $q \approx 240$ g min^{-1}.

The abovementioned equation characterizes the amount of fuel dosed by one doser and a pulveriser injector. The amount of fuel dosed by the entire fuel supply system is expressed as the sum of the amount of fuel dosed by each injector.

Based on the discussion in subchapter 3.4, the amount of fuel injected is affected by the distance s_p of mutually positioned pulveriser injectors. To calculate the exact impact the distance between pulveriser injectors has, a characteristic was drawn, which qualifies the decrease in the amount of fuel injected in percentages in case of different distances between pulveriser injectors. To be more exact, the amount of fuel q flowing through the mutually positioned injectors depending on the distance s_p between the pulveriser injectors was measured experimentally, i.e. $q = f(s_p)$. To work out the equation to describe the variation in the amount of fuel injected in percentage terms, the maximum amount of fuel measured during tests was valued to be q_{max} = 100%. Other measurement results were valued according to the decrease (%) in the variation of the fuel amount of the maximum fuel amount. For instance, if in the distance of s_p = 13 mm between pulveriser injectors, the largest amount of fuel injected is q_{max} = 343.3 g min^{-1} = 100% (using gasoline), then consequently, in the distance of s_p = 7 mm, the amount of fuel is q = 332 g min^{-1}, which constitutes q_{max} 96.7% of the maximum amount of fuel injected. Therefore, in the injector distance of s_p = 7 mm, the value characterizing the variation in the amount of fuel injected is 96.7%. The impact of the distance between pulveriser injectors on the amount of fuel injected is characterized by the equation:

$$a_{sp}(s_p) = \frac{s_1 s_p^3 + s_2 s_p^2 + s_3 s_p + s_4}{100} \ , \tag{3.14}$$

where s_p – the distance between pulveriser injectors;

s_1, s_2, s_3 and s_4 – constants, which characterize the variation in the amount of fuel in percentage terms in case of different distances between the injectors and are measured experimentally. To qualify the values of constants, tests were carried out where the amount of injected fuel q was measured depending on the pulveriser injector distance s_p, i.e. $q = f(s_p)$. During tests, the distance between the injectors was chosen to be s_p = 5…13 mm. Figure 3.18 characterizes the amount of fuel injected depending on the distance s_p between the injectors.

The equation on Figure 3.18 illustrates the values of constants s_1 and s_2. The equation can be used to determine the decrease in the amount of fuel in percentage terms if the distance between the injectors is reduced from, e.g. s_p = 13 mm to 7 mm. By substituting the distance between injectors s_p in the equation, it is found that in case of 7 mm distance between the injectors, the amount of fuel injected is 94.3% as compared to the amount of fuel when the distance between injectors is s_p = 13 mm.

The impact of viscosity on the amount of fuel injected can be characterized by a logarithm equation where the variation in the amount of fuel depending on the viscosity v_i of the fuel is expressed similarly to the equation characterizing the impact of the distance between injectors.

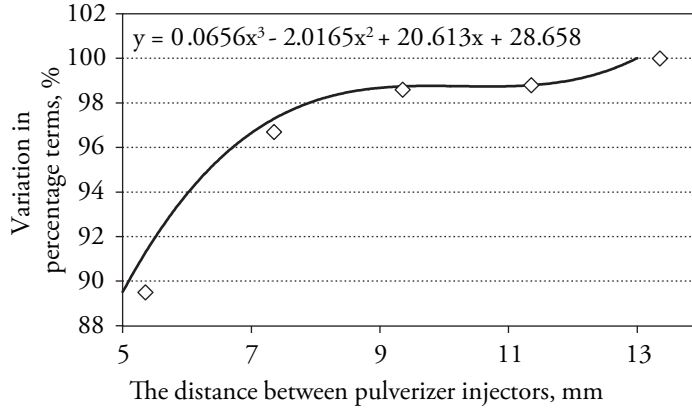

Figure 3.18. The variation in the amount of fuel injected depending on the distance between pulveriser injectors.

The following equation characterizes the impact that the variation in the viscosity v_i has on the amount of fuel:

$$a_{qv}(v_i)=\frac{v_1 \ln(v_i)+v_2}{100}, \tag{3.15}$$

where v_i – fuel viscosity;

v_1 and v_2 – constants, which characterize the variation in the amount of fuel depending on viscosity and are measured experimentally. To qualify the constants v_1 and v_2, tests were carried out during which the variation in the amount of fuel q depending on the viscosity of the fuel v_i has been studied, i.e. $q=f(v_i)$. The tests were carried out using a fuel which viscosity was v_i = 1…31 mm^2 s^{-1}. The test results are presented on Figure 3.19.

The values of constants v_1 and v_2 are given in the equation on Figure 3.19.

The values calculated in the equations (3.14) and (3.15) are ratios, which characterize the variation in the corresponding parameters. Therefore, the equations (3.14) and (3.15) are expressed in the equation (3.13) as follows:

$$q(p_f,p_a,s_p,v_i)=a_{sp}(s_p)a_{qv}(v_i)\left(k_1 p\left(p_f,p_a\right)^3+k_2 p\left(p_f,p_a\right)^2+k_3 p\left(p_f,p_a\right)+k_4\right) \tag{3.16}$$

By substituting the equations and constants obtained during abovementioned tests in the equation (3.16), a model is created which characterizes the impact that the operating parameters of the dosers and pulveriser injectors of the designed fuel supply system as well as the viscosity of fuel have on the amount of fuel injected.

$$q(p_f,p_a,s_p,v_i)=\frac{0.067s_p^3-2.017s_p^2+20.613s_p+28.658}{100}\cdot$$

$$\frac{-25.33\ln(v_i)+95.233}{100}\cdot(0.804\left(p_f-0.0409p_a^2+0.3081p_a+0.0069\right)^3-$$

$$14.141\left(p_f-0.0409p_a^2+0.3081p_a+0.0069\right)^2+$$

$$112.56\left(p_f-0.0409p_a^2+0.3081p_a+0.0069\right)-36.52) \tag{3.17}$$

Based on the model, a three-dimensional graph was constructed (Figure

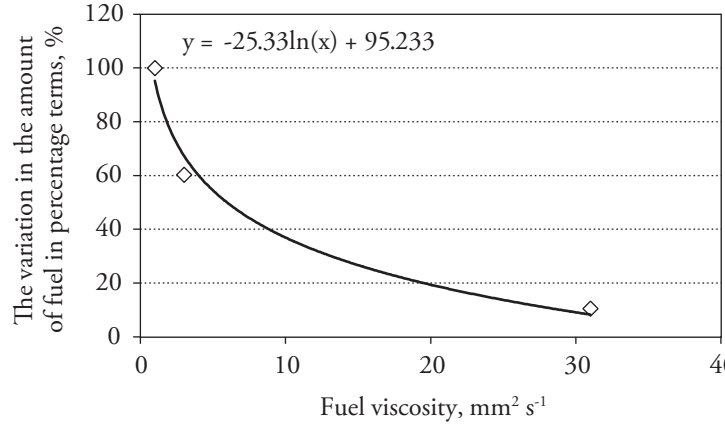

Figure 3.19. The variation in the amount of fuel depending on fuel viscosity.

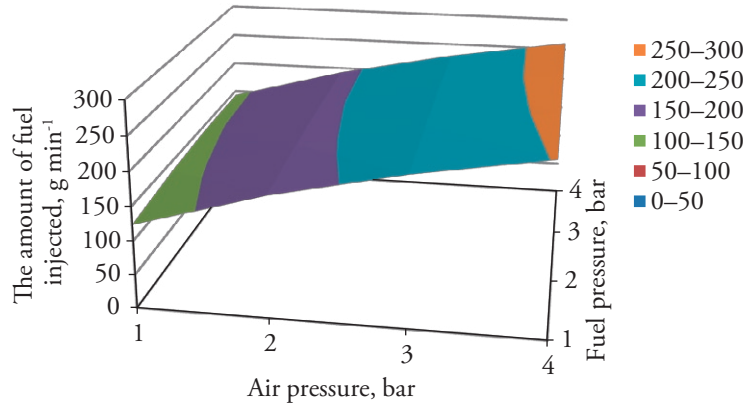

Figure 3.20. The relation between the amount of fuel injected and the pressures of compressed air and fuel.

3.20), which characterizes the amount of fuel injected in the fuel supply system whereas the fuel viscosity equals v_i = 2 mm^2 s^{-1} and the distance between pulveriser injectors equals s_p =11 mm.

What is important in the given model is that the calculation of the amount of fuel would be carried out in the range of given values. The variation ranges of different parameters are as follows: p_f = 1…4 bar; p_a = 0.5…4 bar; v_i = 1…31 mm^2 s^{-1}; s_p = 5…13 mm.

3.8. Conclusion

The development of the fuel supply system results in an electronically controlled fuel supply system which can either be used as the main or an additional fuel supply system. The main difference when using it as the main or additional fuel supply system lies in the electronic adjustment of the system. Fuels of different viscosities can be used in the fuel supply system. The viscosity impacts mostly the amount of fuel injected, which can be increased or decreased by varying the operating parameters of the system, the fuel pressure and compressed air pressure. The operating parameters of the fuel supply system can be selected with the help of a model that calculates the amount of fuel at different operating parameters. When using the fuel supply system on an engine, it is essential to ensure its sufficient supply with fuel on different engine loads. This is dependent on the operating parameters of the fuel supply system and the number of injector pairs used. Researching the quality of the air-fuel mixture of the fuel supply system made it evident that the size of fuel droplets in the air-fuel mixture formed was of the same magnitude or smaller in case of bioethanol than the size of fuel droplets in the air-fuel mixture formed by a fuel supply system of a compression ignition engine equipped with a common mechanical fuel supply apparatus in case of diesel fuel. To test the efficiency of the particular fuel supply system, preliminary tests were carried out during which the developed fuel supply system was used on spark and compression ignition engines. These particular tests will be described and analyzed in the following chapter.

4. PRELIMINARY TESTS OF THE PULVERISER FUEL SUPPLY SYSTEM ON COMPRESSION AND SPARK IGNITION ENGINES

4.1. Methods of engine testing

For the purposes of the current thesis, engine tests were carried out on spark and compression ignition engines. Compression ignition engine testing was in turn divided into two parts: 1) researching the impact of bioethanol on the output parameters and combustion process of a compression ignition engine; 2) researching the impact of bioethanol on the output parameters and combustion process of a compression ignition engine when using the developed fuel supply system. In case of spark ignition engine testing, the output parameters and combustion process of the test engine were studied when using 1) the developed fuel supply system; 2) the original fuel supply system of the test engine, and the results obtained were analyzed and compared. More precise engine testing methods are provided next.

The impact of bioethanol on the output parameters and combustion process of a compression ignition engine. The aim of the test was to determine how the 96.4% bioethanol impacts the output parameters and combustion process of an engine. In addition, it was studied what the maximum proportion of bioethanol in the air-fuel mixture should be to ensure the stable running of an engine. A condensed overview of these particular test results and their comparison with similar tests carried out by other authors has been provided in the subsection 1.2. The test engine used was a Russian compression ignition engine D120. The engine is equipped with a mechanical in-line injection pump. Bioethanol was dosed into the intake manifold of the test engine. The amount of bioethanol directed into the engine was regulated by changing the main metering jet opening ratio of the carburettor. In the closed position of the main metering jet at the engine maximum torque mode $T_{e.max}$ (n_e = 1300 rpm), the flow of bioethanol into the engine was ~1.9 kg h^{-1}. This is conditioned by the constructional speciality of the carburettor for which reason some of the fuel is directed into the carburettor flue from the opening next to the main metering jet. In case of a closed position of the main metering jet, the amount of bioethanol directed into the cylinder depends on the engine speed mode.

Diesel fuel and bioethanol were used jointly in an engine as diesel fuel ignited bioethanol in the cylinder. In case of the given test, the injection of diesel fuel was called a pilot injection. Three amounts of pilot injection were used during tests: B_{f1} = 1.35 kg h^{-1}; B_{f2} = 2.33 kg h^{-1} and B_{f3} = 3.05 kg h^{-1}. Engine load characteristic was carried out at tests whereas the pilot injection amount during the test was constant. The engine load characteristic was carried out on two speed modes of the engine: n_e = 1300 rpm and n_e = 1800 rpm. When bioethanol was added to the air-fuel mixture, engine load increased. Bioethanol was added to the air-fuel mixture as long as the engine was running stable. During tests, the engine crankshaft rotational speed, torque, combustion pressure, exhaust gas emission, and the amounts of bioethanol and diesel fuel dosed into the engine were measured. The technical data of the test engine and measurement devices are given in Table 4.1 (Fuel consumption measurement system and exhaust gas analyzer specification in Table 5.6).

The results of the tests carried out are more precisely given in Paper I.

Table 4.1. The technical data of the engine D120 (Küüt, 2013).

Description	Value
Number of cylinders	2
Cylinder diameter, mm	105
Piston stroke, mm	120
Engine displacement, dm^3	2.08
Power, kW	18.4
Compression ratio	16.5
Cooling system	air-cooled
Nominal rotational speed, rpm	1800
Maximum torque achieved between, rpm	1260 – 1400
Maximum rotational speed, rpm	1950
Minimal rotational speed, rpm	800 – 1050
Injection pressure, MPa	17±0.7
Specific fuel consumption, g kWh^{-1}	241+7
Injection angle, BTDC	α_{pn}=22…24°
Valve timing	IO = 16° BTDC IC = 40° BBDC EO = 40° BBDC EC = 16° ATDC
The measurement devices used at tests	
Engine test stand	Schenck Dynad 3 LI250
Combustion pressure measurement system	AVL IndiModul 621
Fuel consumption measurement system	weighing machine CAS CI-2001A
Exhaust gas analyzer	Bosch BEA 350 (CO, CO_2, HC, NO_x, O_2, opacity)

The impact of bioethanol on the output parameters and combustion process of a compression ignition engine when using the developed fuel supply system. During tests, bioethanol was dosed into a compression ignition engine by the pulveriser fuel supply system. The particular pulveriser fuel supply system is an untested prototype, thus, tests were run on the idle mode of the engine. Based on preliminary tests (subchapter 1.2), it can be said that when the developed fuel supply system is used on full load, the combustion process becomes more effective. Therefore, the amount of bioethanol dosed into the engine also decreases. The aim of the tests was to study the impact of the fuel supply system on the output parameters and combustion process of the engine, test the stability of the operating of the fuel supply system, and detect possible defects in construction. The pulveriser fuel supply system was mounted on the engine according to Figure 3.15 where bioethanol is injected into the intake manifold of the engine. The system was complemented with an underpressure sensor which allows for the control unit to regulate the fuel supply more precisely. A test engine was not used to operate the compressor that was in use in the system. Therefore, when analyzing the data, it must be taken into account that engine power has not been used to operate the compressor, which could affect the combustion pressure of the engine. The test engine used was a compression ignition engine D120 equipped with a mechanical injection pump.

Tests were run at the rotational speeds of 900, 1320, 1600 and 1800 rpm on the idle mode of the engine crankshaft. The environmental parameters during tests were as follows: T_{env} = 25.5 °C, p_{env} = 1018.58 hPa, φ_{env} = 28%. As the amount of bioethanol injected was increased, the amount of diesel fuel injected decreased, according to the operating principle of a mechanical injection pump. This particular solution enabled to maintain a stable rotational speed n_e = const of the engine crankshaft. The test fuels used were bioethanol of 96.4% and standard diesel fuel. The amount of bioethanol in the air-fuel mixture was gradually increased until the soot content in the engine exhaust gas started to increase. The increase in the soot content of the exhaust gas indicates that the combustion process of the engine was not effective enough to ensure the combustion of soot particles. At each test, the proportion of bioethanol was gradually reduced (~3% at every test). In addition, the concentrations of CO, CO_2, HC and NO_x in the exhaust gas were measured. The amount of bioethanol injected was regulated by the software of the pulveriser fuel supply system control unit (MegaSquirt II). The concentration of exhaust

gas was measured with the analyzer Bosch BEA 350 and the combustion pressure with a device AVL IndiModul 621.
The heat release rate in relation to the rotational angle of the crankshaft is expressed as follows (Heywood, 1988):

$$\frac{\mathrm{d}Q_n}{\mathrm{d}\varphi} = \frac{\gamma_{hr}}{\gamma_{hr}\text{-}1} p \frac{\mathrm{d}V_c}{\mathrm{d}\varphi} + \frac{1}{\gamma_{hr}\text{-}1} V_c \frac{\mathrm{d}p}{\mathrm{d}\varphi}, \tag{4.1}$$

where φ – crank angle;
γ_{hr} – the ratio of specific heats;
p – pressure in the cylinder;
V_c – cylinder volume.
The ratio of specific heats γ_{hr} depends on the specific heat of the fuel and is expressed by (Heywood, 1988):

$$\gamma_{hr} = \frac{c_p}{c_v}, \tag{4.2}$$

where c_p – specific heat at constant pressure;
c_v – specific heat at constant volume.
When diesel fuel is used, the ratio of specific heats remains in the range of 1.3...1.4, depending on engine load and combustion temperature. The given tests were carried out without any load, thus, the ratio of specific heats was chosen to be $\gamma_{hr} = 1.3$. In case of bioethanol, specific heat at constant pressure and specific heat at constant volume is $c_p = 1.49$ kJ (kg·K)$^{-1}$ and $c_v = 1.19$ kJ (kg·K)$^{-1}$ accordingly (Kamboj & Kairimi, 2012), thus, according to the equation (4.2), when bioethanol is used, the ratio of specific heats in an engine is approximately $\gamma_{hr} = 1.26$. When diesel fuel and bioethanol are jointly used in the engine cylinder, two fuels impact the heat release. To calculate the impact of fuels during the combustion of the air-fuel mixture, the ratio of specific heats was calculated in relation to the proportion of fuels in the air-fuel mixture. However, this was done on the assumption that the variation in the impact of fuels in relation to the proportion (%) of fuels in the air-fuel mixture is linear.
The ratio of specific heats is expressed as follows:

$$\gamma_{hr} = \gamma_{hrd}\,\sigma_d + \gamma_{hrbe}\,\sigma_{be}, \tag{4.3}$$

where γ_{hrd} – the ratio of specific heats of diesel;
σ_d – diesel fuel proportion in air-fuel mixture;
γ_{hrbe} – ratio of specific heats of bioethanol;
σ_{be} – bioethanol proportion in air-fuel mixture.
According to the equation (4.3), at 1800 rpm tests, the ratios of specific heats at different proportions of bioethanol in the air-fuel mixture are $\gamma_{hr23} = 1.29$, $\gamma_{hr42} = 1.28$, $\gamma_{hr56} = 1.277$.

The net heat released during the combustion process takes into account heat transfer into the cylinder walls as well as air-fuel mixture and is expressed by (Heywood, 1988):

$$Q_n = \frac{\mathrm{d}Q_n}{\mathrm{d}\varphi} + Q_{n.\varphi\text{-}1}\,, \tag{4.4}$$

where Q_n – net heat release;
$Q_{n.\phi\text{-}1}$ – the energy released in the combustion process per crank angle.

The gross heat released during combustion is expressed by the equation (Heywood, 1988):

$$Q_{n.teor} = \int_{\varphi_b}^{\varphi_{end}} \frac{\mathrm{d}Q_{n.teor}}{\mathrm{d}\varphi}\,\mathrm{d}\varphi = qQ_{f.teor}\,, \tag{4.5}$$

where φ_b and φ_{end} – the rotational angles of the crankshaft signifying the beginning and end of the combustion process;
q – the amount of fuel injected into the cylinder during one work cycle;
$Q_{f.teor}$ – the calorific value of fuel.

The amount of fuel injected during one work cycle ($mm^3\ c^{-1}$) based on fuel consumption is expressed as follows:

$$q = \frac{\frac{B_f}{60 \cdot 0{,}001 \cdot \varrho_{fuel}}}{N_c} \cdot 1000\,, \tag{4.6}$$

where B_f – fuel consumption;
N_c – number of work cycles;
ρ_{fuel} – fuel density.

The work of one engine cylinder per cycle is expressed by the equation (Heywood, 1988):

$$W_n = \int p\,\mathrm{d}V_c\,, \tag{4.7}$$

Fuel conversion efficiency η_f indicates the conversion of energy directed into the cylinder into net indicated work and is expressed as the relation between the net indicated work in the cylinder and the gross heat release (Heywood, 1988):

$$\eta_f = \frac{W_n}{Q_{f.teor} q_c}\,, \tag{4.8}$$

where q_c – the amount of fuel injected into the cylinder per work cycle;

$Q_{f.teor}$ – the calorific value of fuel;
W_n – net indicated work per cycle.

Thermal efficiency η_t is expressed as the relation (Pulkrabek, 1997):

$$\eta_t = \frac{W_n}{Q_{f.teor} q_c \eta_c}, \tag{4.9}$$

where η_c – fuel combustion efficency (0.95 – 0.98).

The pulveriser fuel supply system for dosing bioethanol in a spark ignition engine. To study the impact of the pulveriser fuel supply system on the output parameters of a spark ignition engine, the construction of the fuel supply system as well as on stability of operating, a part-load engine speed characteristic was compiled. The fuel used was standard gasoline E95. In addition, engine part-load characteristic was carried out using 96.4% bioethanol as the test fuel. The test engine was an Audi 1.8 ADR spark ignition engine, which technical data is given in Table 4.2. The tests were carried out using the original fuel supply system of the engine (motronic multipoint injection system) and the pulveriser fuel supply system. The test data obtained during the use of the pulveriser fuel supply system was compared to the data obtained during the use of the original fuel supply system of the test engine. In order to use bioethanol in the engine, the original fuel supply system was complemented with a specific device, Flexi Tune Sequential, which lengthens the opening time of the injectors to compensate for the loss of power in the engine due to smaller calorific value of bioethanol. In case of the pulveriser fuel supply system, a compressor separate from the engine was used, thus, data analy-

Table 4.2. Audi 1.8 ADR engine technical data (Autodata 2005).

Parameter	Value
Fuel supply system	MPI-Bosch Motronic M3.2
Cylinder number	4
Bore, mm	81
Stroke, mm	86.4
Engine displacement, cm^3	1781
Cooling system	liquid cooled
Power, kW	92 (5800 rpm)
Torque, Nm	173 (3960 rpm)
Compression ratio	10.3
Friction torque, Nm	26

sis should be carried out while considering the fact that engine power is not used for operating the compressor. A compressor added to an engine impacts the combustion pressure as well as fuel consumption.

During tests, the test stand KI5543 (specification in Table 5.6) of modified engines, which maximum braking power is 55 kW and the rotational speed of braking falls in the range of n_d = 1500…3000 rpm, was used. Based on this, the test engine was complemented with a gearbox and during tests, the second gear with a gear ration of η_{gb2} = 1.84 was used. Bioethanol and gasoline consumptions were measured with a weighing machine CAS CI-2001A. The environmental parameters during tests with the original fuel supply system were: T_{env} = 18.6 °C, p_{env} = 1015.92 hPa, φ_{env} = 28%; whereas the same parameters during tests with the pulveriser fuel supply system were: T_{env} = 20.8 °C, p_{env} = 1006.58 hPa, φ_{env} = 25%. For more detailed characterization of the test data, the data is generally converted to standard conditions, which calculation specifications are given in standards GOST 18509-88, ISO 1585, DIN 70 020, SAE J 1349 etc. Converting to standard conditions is rational when comparing the data of an engine working on heavy load. For example, based on the standard GOST 18509-88, the output parameters of the engine can be converted to standard conditions when the mean effective pressure of the engine is $p_e \geq 0.50$MPa (GOST 18509-88). When testing the pulveriser fuel supply system on a spark ignition engine, the mean effective pressure did not rise to the abovementioned value. In given conditions, the test data was contrasted and compared without considering the difference in the abovementioned environmental parameters.

The original fuel supply system of the test engine is a multipoint, indirect injection type of a system where the injection of fuel onto each cylinder is controlled separately. The fuel is injected into the intake manifold, behind the intake valve. The pulveriser fuel supply system is a mono-injection system where the air-fuel mixture is formed before the throttle valve and is sucked into the cylinder by underpressure. The fuel supply is controlled by the variation in the underpressure and the signal from the lambda sensor. The Sauter mean diameter of fuel droplets in the injection spray of bioethanol fuel E85 in the original fuel supply system of the test engine is $D_{32} \approx 80$ µm (Gandhi et al., 2008). In case of a pulveriser fuel supply system, the Sauter mean diameter D_{32} of fuel droplets is around 23 µm (Table 3.4), for which reason, according to the equation (1.14), the combustion pressure in the cylinder increases.

During engine tests, the rotational speed n_e of the engine crankshaft, torque T_e, fuel consumption B_f and combustion pressure p were measured. To compare the test data obtained with two fuel supply systems, the engine torque and the engine crankshaft rotational speed were of the same value during tests with either fuel supply system. The following parameters characterizing the work of the engine were calculated based on the test data (Heywood, 1988):

The engine torque T_e is expressed by a relation:

$$T_e = F l_{tb}, \tag{4.10}$$

where F – the force impacting the sensor;
l_{tb} – force arm length.

The engine power P_e is expressed in an equation:

$$P_e = 2\pi n_e T_e, \tag{4.11}$$

where T_e – engine torque;
n_e – engine crankshaft rotational speed.

Fuel consumption B_f is expressed by:

$$B_f = \frac{m_f}{\tau_f}, \tag{4.12}$$

where m_f – the amount of fuel consumed during the test;
τ_f –time of fuel consumption measurement.

The specific fuel consumption b_e is expressed as the relation between fuel consumption B_f and engine power P_e (Heywood, 1988):

$$b_e = \frac{B_f}{P_e}, \tag{4.13}$$

The mean effective pressure p_e is expressed by:

$$p_e = \frac{P_e \tau_e}{V_c i_c n_e}, \tag{4.14}$$

where τ_e – engine stroke cycle;
i_c –the number of cylinders.

The indicated pressure p_i is expressed by:

$$p_i = p_e + p_{fr}, \tag{4.15}$$

where p_{fr} – friction mean effective pressure.

Indicated power P_i is expressed by:

$$P_i = P_e + P_{fr}\,, \tag{4.16}$$

where P_{fr} – friction power.

The indicated specific fuel consumption b_i is expressed by an equation:

$$b_i = \frac{B_f}{P_i}\,, \tag{4.17}$$

The engine efficiency η_c is expressed by:

$$\eta_e = \frac{1}{Q_{f.teor} b_e}\,, \tag{4.18}$$

The indicator efficiency is expressed by the following equation:

$$\eta_i = \frac{1}{Q_{f.teor} b_i}\,, \tag{4.19}$$

4.2. The pulveriser fuel supply system on a compression ignition engine

The method of carrying out the following tests is given in the previous subsection 4.1. The tests demonstrated that as the fuel supply system was used at low rotational speeds of the engine (n_e = 900 and 1320 rpm), there was no substantial impact on the combustion process. This is conditioned by the high heat of vaporization of bioethanol. When taking into consideration that diesel engines run cold on idle mode, the energy directed into the cylinder is not sufficient to combust the air-fuel mixture of bioethanol and diesel fuel. In case of particular tests, test data has been presented where engine runs on air-fuel mixture of high bioethanol proportion. This data complements the data given in subchapter 1.2.

Engine tests made it evident that at low rotational speeds of the engine crankshaft (n_e = 900 and 1320 rpm), the proportion of carbon monoxide (CO) in the exhaust gas increased when bioethanol was used in the air-fuel mixture. In general, the increase in the proportion of carbon monoxide was around 0.15%. When bioethanol was used at low rotational speeds of the engine crankshaft, the proportion of carbon dioxide (CO_2) in the exhaust gas decreased by approximately 0.1%. During tests, the maximum proportion of bioethanol in the air-fuel mixture was 76%. The proportion of hydrocarbons (HC) increased substantially when

bioethanol was used, in accordance with the increase in the proportion of bioethanol in the air-fuel mixture. At the same time, the proportion of nitrogen compounds in the exhaust gas decreased significantly. An example of the concentration of exhaust gas at the rotational speed of n_e = 900 rpm of the engine crankshaft is given on Figures 4.1 and 4.2.

Figures 4.1 and 4.2 indicate that the proportions of CO and HC in the exhaust gas increase. This is conditioned by the great amount of bioethanol in the air-fuel mixture for which reason the proportion of energy needed for the evaporation of fuel in the work process of the engine increases. The reasons for the increase in the components in the exhaust gas at the increased rotational speed of the engine (n_e = 1800 rpm) are further discussed in Results and subchapter 4.3 (Conclusion).

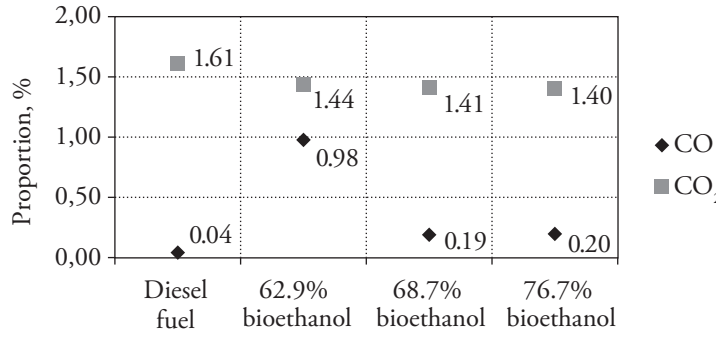

Figure 4.1. The concentration of carbon monoxide and carbon dioxide at crankshaft rotational speed of n_e = 900 rpm of the test engine.

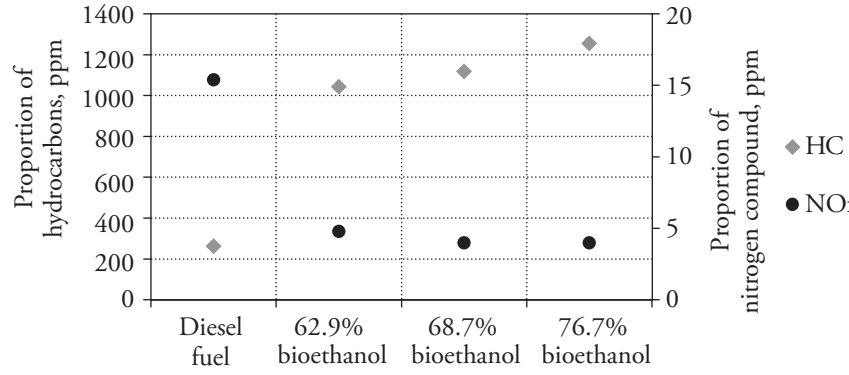

Figure 4.2. The proportion of hydrocarbons and nitrogen compounds in the exhaust gas at crankshaft rotational speed of 900 rpm of the test engine.

At a rotational speed of n_e = 1800 rpm of the engine crankshaft, the variations in the harmful components in the exhaust gas remained virtually the same as at low rotational speed of the engine crankshaft (Table 4.3). The increase in the proportion of bioethanol in the air-fuel mixture to 23% did not increase the proportion of CO in the exhaust gas substantially. Based on the given data, the air-fuel mixture formed by the novel fuel supply system does not affect the exhaust gas of the engine. The impact of the air-fuel mixture formed by the fuel supply system becomes evident during the combustion process. To describe the combustion process, the combustion pressure of an engine running on two fuels was measured. Based on that, heat release, heat release rate and engine work in one work cycle were calculated. The calculations were carried out based on ten work cycles of one cylinder, which data has been averaged.

Based on test data, Figure 4.3 displays the heat release at combustion of air-fuel mixtures of different proportions of diesel fuel as well as diesel fuel and bioethanol, heat release rate and combustion pressures.

Table 4.3. Test results of the engine at crankshaft rotational speed of 1800 rpm.

Rotational speed: 1800 rpm	Diesel fuel	Bioethanol Test 1.	Bioethanol Test 2.	Bioethanol Test 3.
Diesel fuel consumption kg h^{-1}	1.35	1.14	1.15	1.20
Bioethanol consumption kg h^{-1}	0	1.5	0.84	0.36
Total fuel consumption kg h^{-1}	1.35	2.64	1.99	1.56
Proportion of bioethanol %	0,0%	56.8%	42.3%	23.1%
Proportion of diesel fuel %	100.0%	43.2%	57.7%	76.9%
Temperature of diesel fuel °C	24.33	26.21	25.94	26
Density of diesel fuel kg m^{-3}	822.16	821.41	821.59	821.53
Deviation %	0.42	0.77	0.32	0.47
Measurement uncertainty %	1.04	1.91	0.7	1.17
CO %	0.05	0.22	0.11	0.07
CO_2 %	2.19	2.11	2.00	1.99
HC ppm	101.20	985.40	2177.75	844.80
NO_x ppm	17.2	4.6	3	3.2
Opacity m^{-1}	0.04	0.09	0.02	0.04

Figure 4.3 illustrates the fact that as bioethanol was added (~23%), the heat release rate was approximately of the same value as when using only diesel fuel. At the same time, the amount of theoretical energy directed into the cylinder increased (the amount of fuel dosed, according to Table 4.2). Unlike the data on Figure 1.3, in case of air-fuel mixture with the proportion of bioethanol of 23%, the time of heat release was shorter than in using diesel fuel. Therefore, it might be said that the air-fuel mixture formed in the fuel supply system is of sufficient quality to ensure the quick combustion of bioethanol and diesel fuel air-fuel mixture (see Figure 4.3, $dQ/d\phi$ and $dQ/d\phi$ BE23). In this particular instance, it is necessary to specify how the combustion process is affected by the construction of the fuel supply system. By increasing the proportion of bioethanol in the air-fuel mixture of up to 42%, the heat release rate decreased ($dQ/d\phi$ BE42). This is conditioned by the increase in the amount of energy necessary for the evaporation of the air-fuel mixture, which also conditions an increase in the ignition delay for which reason less energy is released per one crank angle degree in the process. As the proportion of bioethanol was increased in the air-fuel mixture, the time of heat release rate also increased (Figure 4.3, $dQ/d\phi$ BE42). This is due to the high heat of vaporization of bioethanol that conditions the drop in the combustion pressure in the cylinder.

As the proportion of bioethanol was increased up to 56.8%, the combustion pressure in the cylinder and the heat release rate decreased. In addition, the time of heat release rate lengthened. It might be deduced that in case of too high concentration of bioethanol in the air-fuel mixture, too much energy is spent on the evaporation of bioethanol. Therefore, when bioethanol is used in a compression ignition engine as additional fuel, it is relevant to determine the optimal proportion of bioethanol in the air-fuel mixture that would ensure as effective combustion process as possible. The control unit of the fuel supply system should regulate the proportion of bioethanol in the air-fuel mixture. Figure 4.3 also depicts the heat release of the combustion process.

To characterize the heat release at the combustion process, it is necessary to compare the heat release at the combustion process with the theoretical, gross heat release of the fuel dosed into the engine. Figure 4.4 illustrates the comparison of heat release at the combustion process with the gross heat release as well as the theoretical energy, which implies that approximately 98% of fuel is burned in the cylinder.

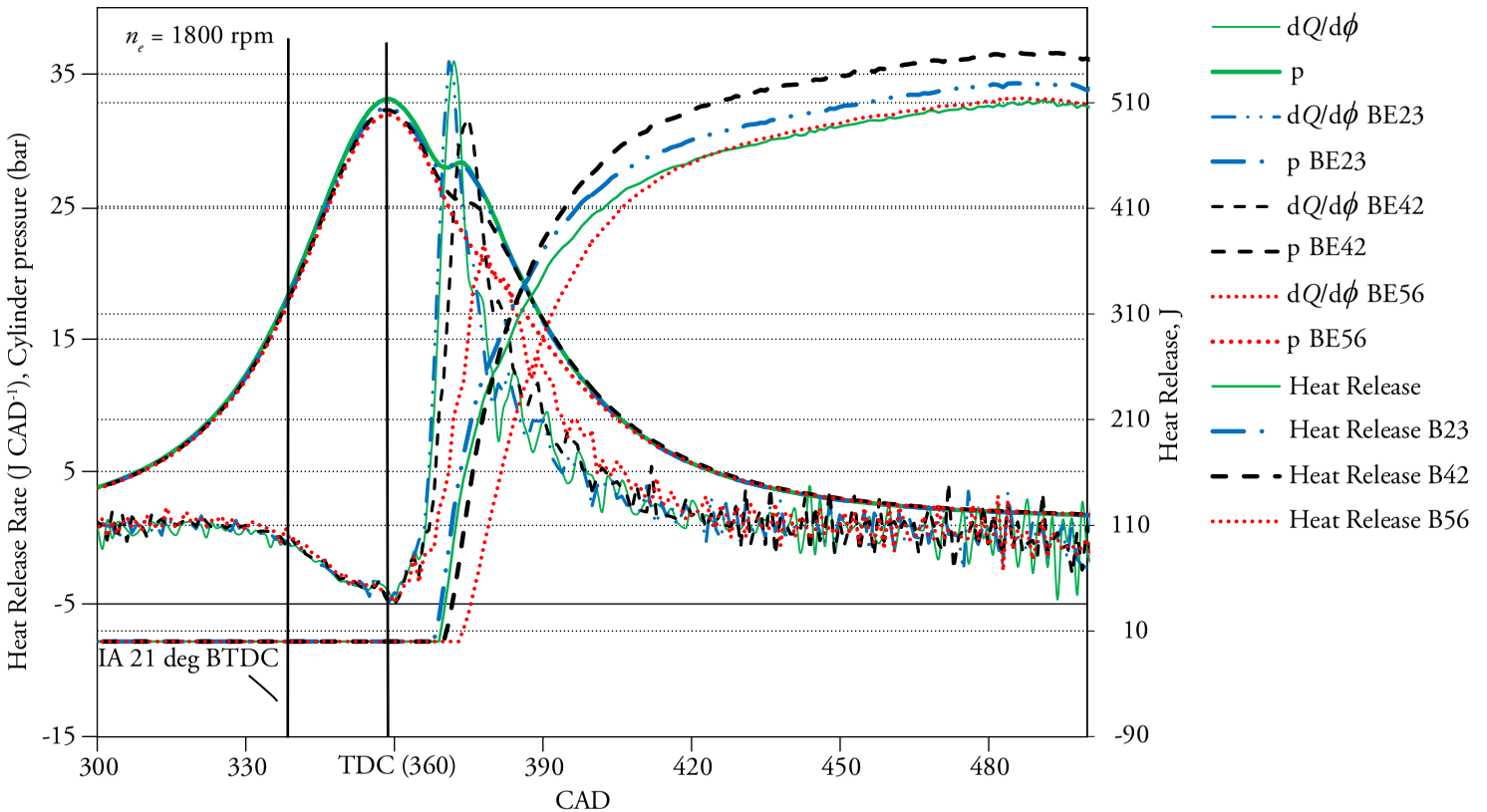

Figure 4.3. Heat release at combustion of different bioethanol proportion air-fuel mixtures in the engine D120 cylinder.

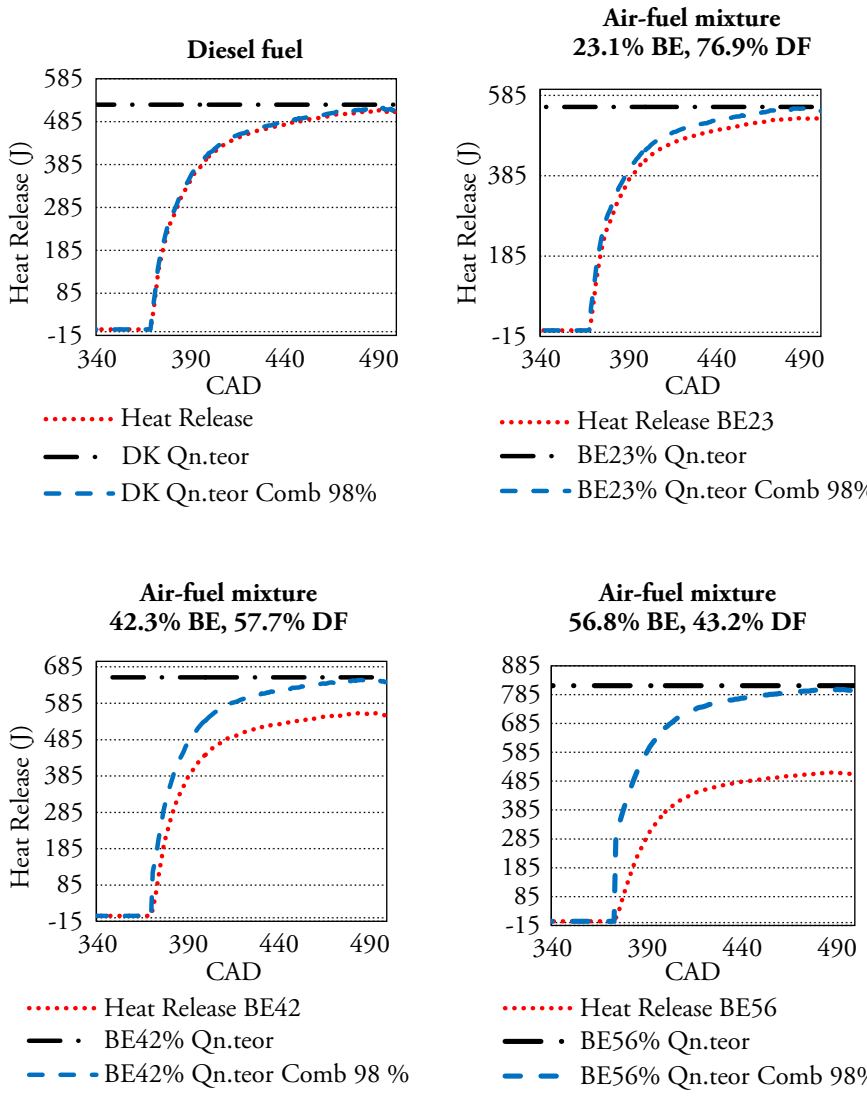

Figure 4.4. The proportion of heat release at the combustion process as compared with gross heat release in the joint use of diesel fuel and bioethanol in a compression ignition engine.

Figure 4.4 indicates that when diesel fuel is used in the air-fuel mixture, the heat release constitutes 97% of the theoretical gross heat release directed into the cylinder. This can be caused by the small amount of fuel directed into the cylinder which combustion consumes most of the

energy to overcome the friction force of the engine. In case of bioethanol air-fuel mixture, it becomes evident that when the proportion of bioethanol in the air-fuel mixture is 23.1%, energy absorption in the combustion process is increased. This is caused by bioethanol's high heat of vaporization. As the proportion of bioethanol in the air-fuel mixture is increased, the proportion of absorbed energy also increases. In addition, the amount of energy (the amount of fuel) directed into the cylinder also increases and the energy obtained from it is used to vaporize bioethanol. The amount of energy necessary for vaporization increases as the proportion of bioethanol is increased in the air-fuel mixture. If the proportion of bioethanol is increased up to 56.8%, the proportion of absorbed energy is approximately 36%, thus, the use of the given air-fuel mixture would not be effective as a great amount of energy directed into the cylinder is spent on fuel evaporation. In case of air-fuel mixtures with bioethanol proportion of 42.3% and 23.1%, the proportions of absorbed energy are ~14% and 4% accordingly. Based on that, it is pertinent to ensure the optimal proportion of diesel fuel and bioethanol in the air-fuel mixture. An optimal proportion in case of an engine equipped with the particular fuel supply system can be considered air-fuel mixture with bioethanol proportion of ~25%. Since the optimal proportion of bioethanol in the air-fuel mixture may change when the engine is working on load, the fuel supply system should be calibrated separately for different engines.

The work graph of one working cycle is depicted on Figure 4.5, which provides the work rendered during the compression stroke and work stroke of the engine. The graph indicates that in case of diesel fuel and air-fuel mixture of bioethanol proportion of up to 42.3%, the net indicated work per cycle remains of a similar magnitude. In case of bioethanol proportion of 56.8%, the net indicated work per cycle in the cylinder decreases. This is caused by a gross drop in temperature in the cylinder, which also conditions a decrease in the combustion pressure. The decrease in the net indicated work in the cylinder can be explained with the bioethanol condensing on cylinder walls as this process reduces the amount of energy consumed by the upward movement of the cylinder. However, this particular issue requires a more thorough study on a single cylinder research engine where the impact of other engine cylinders on the combustion process is eliminated. It is relevant that the use of air-fuel mixture of bioethanol proportion of 56.8% is not rational on the given work mode of the engine.

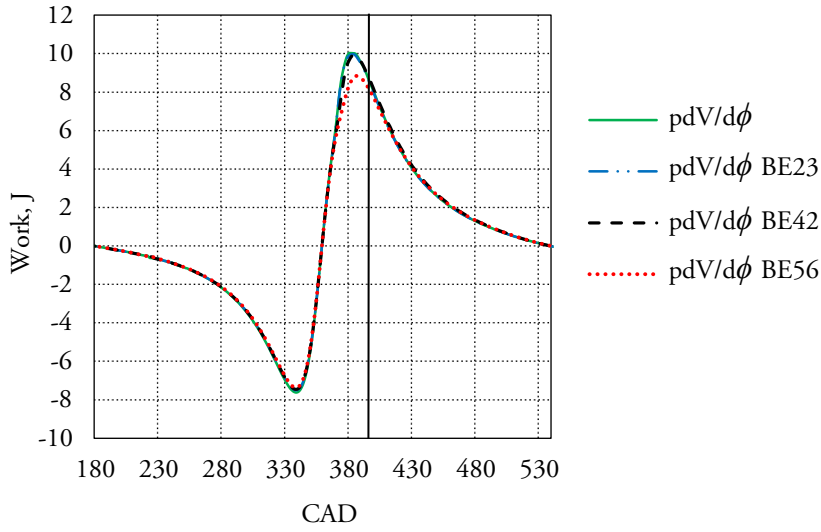

Figure 4.5. The net indicated work per cycle in the cylinder at the rotational speed of 1800 rpm of the crankshaft.

Table 4.4. The parameters characterizing one work cycle of the test engine.

Parameter	DF	BE23.1%	BE 42.3%	BE 56.8%
Fuel amount per work cycle q,	15	18.16	22.7	30
DF $mm^3\ c^{-1}$	15	14	13	13
BE $mm^3\ c^{-1}$	0	4.16	9.7	17
Gross heat release $Q_{n.teor}$ J	525	556	656	816
Net indicated work per cycle W_n J	133	136	145	112
Fuel conversion efficiency η_f	0.253	0.244	0.221	0.137
Thermal efficiency η_t	0.258	0.248	0.225	0.140

Based on the test data, Table 4.4 was drawn which provides the net indicated work W_n of one engine cylinder per cycle, the amount of fuel q injected per work cycle, fuel conversion efficiency η_f and thermal efficiency η_t.

Table 4.4 indicates that the thermal efficiency η_t of the engine decreases proportionally to the increase in bioethanol in the air-fuel mixture. What is more, thermal efficiency η_t is substantially decreased in case of air-fuel

mixture of bioethanol proportion of 56.8%. This is caused by firstly, the increase in the amount of energy directed into cylinder as compared to using diesel fuel, and secondly, the decrease in the net indicated work per cycle W_n. The net indicated work per cycle W_n in case of air-fuel mixture of bioethanol proportion of 42.3% increases. This can be conditioned by the increase in the friction force in the cylinder which is caused by the difference in temperatures. In case of air-fuel mixtures of diesel fuel and bioethanol proportion of 23.1%, the net indicated work per cycle W_n does not differ substantially. Similarly to the variation in thermal efficiency η_t, the fuel conversion efficiency η_f also changes.

4.3. Conclusions

When testing the pulveriser fuel supply system as an additional fuel supply system on a compression ignition engine, it became evident that the proportions of HC and CO in the exhaust gas increased at low rotational speeds on engine idle mode when bioethanol was used. As the engine crankshaft rotational speed grew faster, only the proportion of hydrocarbons in the exhaust gas increased. Considering the heat release rate and its intensity (Figure 4.3, $dQ/d\phi$), it becomes evident that when the proportion of bioethanol in the air-fuel mixture is up to 25%, the time of heat release in the combustion process is short enough to ensure the effective operating of the engine. Based on this, it can be said that at engine idle mode rotational speeds, it is not rational to use more than 25% of bioethanol in the air-fuel mixture. The increase in the proportion of HC is conditioned by the water vapour forming in the cylinder during bioethanol combustion, which hinders the complete combustion of diesel fuel. Based on the parameters characterizing exhaust gas, the use of bioethanol at idle mode rotational speeds of the engine is not rational. To decrease the proportion of HC in the exhaust gas, additional devices, e.g. catalysts, should be used to ensure the permitted proportion of hydrocarbons in the exhaust gas. It is necessary to study the variation in the proportion of HC in the exhaust gas on different engine loads to ascertain the optimal proportion of bioethanol in the air-fuel mixture. In case of engine load, the parameters characterizing the exhaust gas of the engine vary substantially. All in all, the fuel supply system worked stably on the engine and no constructional defects were detected.

4.4. The pulveriser fuel supply system for dosing bioethanol in a spark ignition engine

The test method of spark ignition engines is given in subchapter 4.1. In case of given tests, the pulverizer fuel supply system was used as the main fuel supply system. The data obtained during tests as well as their analysis is provided next. The pulveriser fuel supply system together with the test engine is depicted on Figure 4.6.

Based on the abovementioned equations (in subchapter 4.1), Table 4.5, which provides the results of tests carried out using gasoline, was drawn.

Table 4.5 indicates that the engine torque T_e, crankshaft rotational speed n_e and ignition angle α_i were of the same value when tests were run with either fuel supply systems. Therefore, the work efficiency of a fuel supply system is characterized by the amount of fuel consumed B_f and the combustion pressure p. Table 4.5 also indicates that when a pulveriser fuel

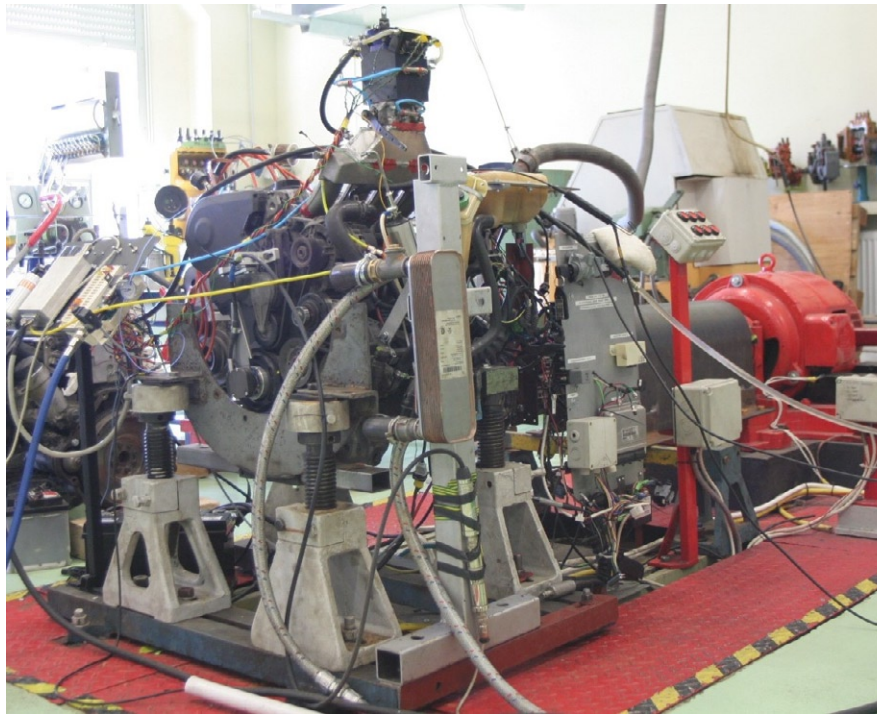

Figure 4.6. The pulveriser fuel supply system on a spark ignition engine.

Table 4.5. The test results of a part-load speed characteristic of a spark ignition engine.

Symb.	Unit	TEST NR.								
		1	2	3	4	5	6	7	8	9
α_i	deg	33	37	38	37.5	37.5	37.5	37.5	37	36
n_e	rpm	5000	4520	4240	4000	3960	3760	3520	3240	3000
T_e	Nm	0	2.7	4.9	7.1	7.1	9.8	11.4	15.8	19.6
P_e	kW	0	1.3	2.2	3.0	2.9	3.9	4.2	5.3	6.1
Pulveriser fuel supply system										
B_f	kg h^{-1}	4.5	4.86	4.62	5.04	4.68	4.62	4.8	4.56	5.4
b_e	g (kW h)$^{-1}$	∞	3778.8	2127.4	1703.1	1597.5	1199.5	1141.0	852.8	878.6
p_e	MPa	0	0.019	0.034	0.049	0.049	0.068	0.080	0.110	0.137
p_i	MPa	0.181	0.200	0.216	0.231	0.231	0.250	0.261	0.291	0.318
P_i	kW	13.6	13.6	13.7	13.8	13.7	14.1	13.8	14.2	14.3
b_i	g (kW h)$^{-1}$	330.7	357.7	337.0	364.0	341.5	328.0	348.2	321.9	377.4
η_e	-	0.014	0.022	0.039	0.049	0.052	0.069	0.073	0.097	0.094
η_i	-	0.250	0.231	0.246	0.227	0.242	0.252	0.238	0.257	0.219
Audi 1.8 ADR original fuel supply system										
B_f	kg h^{-1}	4.92	5.1	5.46	5.28	5.28	5.16	5.28	5.52	5.04
b_e	g (kW h)$^{-1}$	∞	3965.4	2514.2	1784.2	1802.3	1339.7	1255.1	1032.3	820.0
p_e	MPa	0	0.019	0.034	0.049	0.049	0.068	0.080	0.110	0.137
p_i	MPa	0.181	0.200	0.216	0.231	0.231	0.250	0.261	0.291	0.318
P_i	kW	13.6	13.6	13.7	13.8	13.7	14.1	13.8	14.2	14.3
b_i	g (kW h)$^{-1}$	361.6	375.4	398.2	381.4	385.2	366.4	383.0	389.7	352.2
η_e	-	0.014	0.021	0.033	0.046	0.046	0.062	0.066	0.080	0.101
η_i	-	0.229	0.220	0.208	0.217	0.215	0.226	0.216	0.212	0.235

supply system was used, at the crankshaft rotational speed of n_e = 5000… 3240 rpm, fuel consumption was on average ~11% smaller. However, at the crankshaft rotational speed of n_e = 3000 rpm, the gasoline consumption in using a pulveriser fuel supply system increased by ~7%. The variations in gasoline consumption are characterized on Figure 4.7. In case of a pulveriser fuel supply system, the decrease in the gasoline consumption is conditioned by the quicker combustion of air-fuel mixture as compared to the air-fuel mixture formed by the original fuel supply system. The combustion process is more thoroughly characterized in the analysis of bioethanol tests. However, it should be mentioned that the impact of air-fuel mixture on the combustion process was similar in using gasoline and bioethanol. The increase in gasoline consumption at n_e = 3000 rpm is conditioned by the ignition angle and too small diameter of air flues in the developed fuel supply system since these cause the decrease in volumetric efficiency as the engine load increases. To improve volumetric

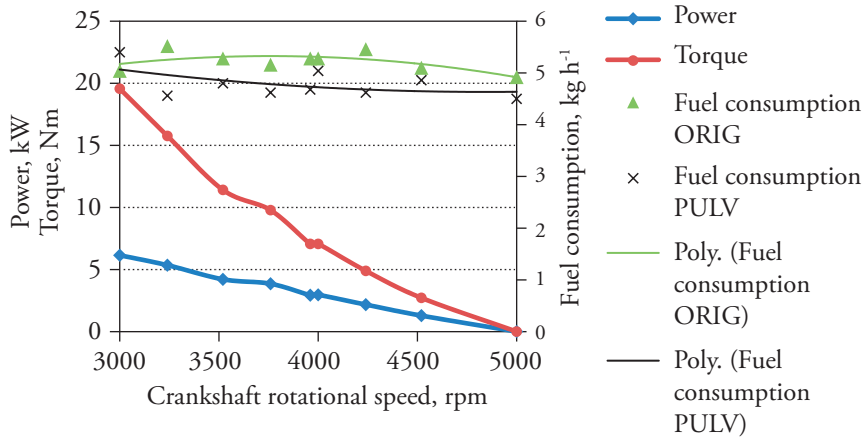

Figure 4.7. The variation in gasoline consumption depending on the fuel supply system used during a test.

efficiency, it is necessary to either enlarge the diameter of air flues or add an additional air valve to the system, which will facilitate the air flow into the engine on certain work modes. To determine the ignition angle α_i, the adjustment of the control unit of the engine running with the original fuel supply system was used, according to which the ignition timing of tests with the pulveriser fuel supply system was adjusted. To increase engine efficiency, it is necessary to draw up a new ignition timing map.

Depending on the rate of gasoline consumption, other parameters b_e, p_e, p_i, P_i,b_i, η_e, η_i (see Table 4.5) characterizing the work of the engine also vary. A part-load characteristic, which test data is provided in Table 4.6, was carried out during tests with bioethanol. The tests were carried out at maximum torque rotational speed of n_e = 3960 rpm on engine loads T_{e1} = 7 Nm, T_{e2} = 30 Nm and T_{e3} = 55 Nm.

Table 4.6 indicates that on engine loads T_{e1} = 7 Nm and T_{e2} = 30 Nm, the consumption of bioethanol decreased by almost 3% when a pulveriser fuel supply system was used as compared to the use of an original fuel supply system. The reason for the decrease in bioethanol consumption may be the high quality of air-fuel mixture and its quick combustion. In addition, the economic parameters of an engine are substantially affected by the ignition timing α_i, which in the given case was adjusted according to the original fuel supply system. Therefore, bioethanol consumption may be reduced when using a pulveriser fuel supply system by adjusting the

Table 4.6. The test data of a part-load characteristic of a spark ignition engine.

Symbol	Unit	ORIG FSS			PULV FSS		
		1	2	3	4	5	6
α_i	deg	37.5	33	23	37.5	33	23
n_e	rpm	3960	3960	3960	3960	3960	3960
T_e	Nm	7	30.0	55.0	7	30.0	55.0
P_e	kW	2.9	12.4	22.5	2.9	12.4	22.5
B_f	kg h^{-1}	**9.1**	**14.9**	**22.1**	**8.9**	**14.58**	**24.0**
b_e	g (kW h) $^{-1}$	3092.5	1200.5	982.4	3031.1	1176.3	1065.0
p_e	MPa	0.049	0.209	0.379	0.049	0.209	0.379
p_i	MPa	0.231	0.390	0.561	0.231	0.390	0.561
P_i	kW	13.7	23.2	33.3	13.7	23.2	33.3
b_i	g (kW h) $^{-1}$	661.0	642.2	664.6	647.9	629.3	720.5
η_e	-	0.043	0.112	0.137	0.044	0.114	0.126
η_i	-	0.203	0.209	0.202	0.207	0.214	0.186

ignition timing to be optimal. If the ignition timing α_i is not optimal, this may bring about an increase in bioethanol consumption and a decrease in the combustion pressure in the cylinder. An optimal ignition angle α_i ensures as high combustion pressure p in the cylinder as possible and as small bioethanol consumption B_f as possible. In different fuel supply systems, the length of the intake manifold differed (the intake manifold of the original fuel supply system was in this case substantially longer); however, the overall tendency indicates that in case of a long intake manifold, the volumetric efficiency of the engine at crankshaft rotational speed of n_e = 1000…5500 rpm is as good or better than in case of a short one (Heisler, 2001). Based on this, it can be said that in case of a pulveriser fuel supply system, the volumetric efficiency of the cylinders on the given work modes should reduce for which reason the engine power P_e and combustion pressure p decrease. In addition, air flow into the cylinder is regulated by the throttle valve position, thus, the decrease in bioethanol consumption could be conditioned by the effective combustion of the air-fuel mixture and the ignition timing of the engine. On engine load T_{e3} = 55 Nm, bioethanol consumption increased by 8% when a pulveriser fuel supply system was used. The increase is conditioned by untimely ignition as well as the too small diameter of pulveriser fuel supply system air flues as this causes the decrease in volumetric efficiency when the engine load increases. Figure 4.8 depicts the combustion pressure, heat release rate and heat release of the test engine when bioethanol was used as engine fuel on engine load T_{e2} = 30 Nm. The data given on Figure 4.8

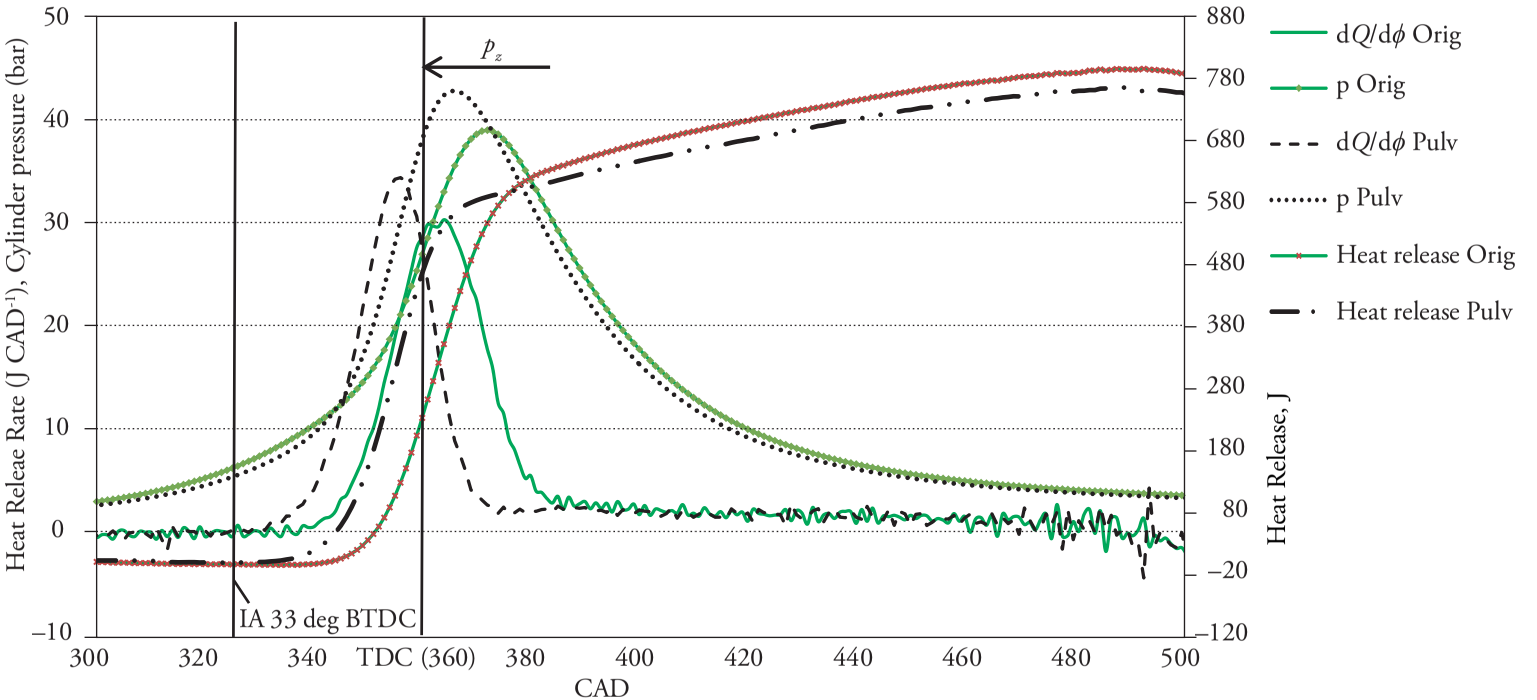

Figure 4.8. The combustion pressure of Audi 1.8 ADR engine in using bioethanol (T_{e2} = 30 Nm, n_e = 3960 rpm) (Paper V).

is based on equations from (4.1) to (4.6). The calculations were carried out while considering the fact that when bioethanol is used as the fuel, the ratio of specific heats in the combustion process is approximately γ_{br} = 1.26, where c_p = 1.49 kJ (kg·K)$^{-1}$ and c_v = 1.19 kJ (kg·K)$^{-1}$ (according to equation (4.2)) (Kamboj & Kairimi, 2012).

During testing, it became evident that the as the pulveriser fuel supply system was used, combustion pressure p in the cylinder increased (see Figure 4.8). The increase in the combustion velocity in case of a pulveriser fuel supply system is quicker at the same ignition timing as compared to the original fuel supply system. This is conditioned by the increase in the heat release rate (see Figure 4.8, dQ/dϕ). In comparison to the original fuel supply system, the heat release rate dQ/dϕ is highest before the top dead centre of the piston, which also conditions the rapid increase in the pressure in the cylinder. In case of the particular adjustment of ignition timing, a situation is created where the maximum combustion pressure is achieved at the top dead centre of the piston, for which reason the increase in the pressure in the cylinder starts hindering the operating of the engine. The average combustion pressure of ten engine work cycles is given on Figure 4.8; however, during tests, the overall tendency indicated that the maximum value of the combustion pressure p_z was achieved at the top dead centre of the piston (TDC = 360 CAD). On this particular work mode, the risk of a detonation in the engine also increases. Based on the given results, it can be implied that the combustion of air-fuel mixture formed with the pulveriser fuel supply system is quicker, which also conditions the quick heat release during the combustion process. For the more effective use of the fuel supply system, it would be necessary to draw an ignition timing map for the engine, based on which the ignition of the air-fuel mixture in the engine would be controlled. If the entire heat release of the combustion process is examined (Figure 4.8), it can be seen that heat release during combustion starts substantially earlier in case of a pulveriser fuel supply system. Taking into account the fact that the theoretical energy directed into a cylinder in one work cycle was $Q_{n.teor.orig}$ = 830 J in case of the original fuel supply system and $Q_{n.teor.pulv}$ = 813 J in case of a pulveriser fuel supply system (according to equation (4.5)), it can be said that ~5% of energy was absorbed in cylinder walls and used for fuel evaporation (Paper V).

4.5. Conclusions

When testing the pulveriser fuel supply system on a spark ignition engine, it became evident that in comparison to the original fuel supply system of the test engine, in general, the bioethanol consumption of the engine decreased. On heavy loads, e.g. on bioethanol fuel tests during which T_{e3} = 55 Nm, the bioethanol consumption increased as the pulveriser fuel supply system was used. This is caused by firstly, the small diameter of air flues in the developed fuel supply system, which conditions the decrease in the volumetric efficiency of the engine, and secondly, untimely ignition due to which the increase in pressure in the cylinder starts hindering the operating of the engine. The proposed solutions would be drawing up an ignition timing map for an engine equipped with a pulveriser fuel supply system, designing an additional air flue pipe for the fuel supply system, or enhancing the diameter of the air flue. During the use of a pulveriser fuel supply system, the combustion pressure in the cylinder increased, conditioned by the heat release rate. Therefore, it might be assumed that the fuel droplets in the air-fuel mixture directed into the cylinder enable the quick evaporation and combustion of the air-fuel mixture in the cylinder as compared to the air-fuel mixture formed by the original fuel supply system. Concerning the particular test, it is necessary to further study the impact of the fuel supply system and the intake manifold on the combustion process. To determine the efficiency of the particular fuel supply system more precisely, it is necessary to improve the air flues of the system and compile an ignition timing map for use of the particular fuel supply system on an engine. Tests indicate that when the pulveriser fuel supply system is used on an engine (with a compressor), presumably, the output parameters of the engine are equal to or better than the ones achieved during the use of the original fuel supply system.

5. THE CALCULATION AND ANALYSIS OF MEASUREMENT UNCERTAINTY

5.1. The calculation of measurement uncertainty

Measurement uncertainty can include many components, some of which can be valued based on the statistical distribution of measurement results and others based on the expected probability theory, experimentally or some other way. Therefore, the abovementioned methods are categorized into type A and B methods of evaluation (Laaneots & Mathiesen., 2002). According to methods of evaluation, the combined standard uncertainty is expressed as follows (Laaneots et al., 2012):

$$U_c=\sqrt{U_A^2+U_B^2}\ , \tag{5.1}$$

where U_A – the standard deviation of the measurement results;
U_B – the uncertainty of the measurement device.

The arithmetic standard deviation of the measurement results is expressed by (Laaneots et al., 2012):

$$U_A=\sqrt{\frac{1}{m_n(m_n\text{-}1)}\sum(x_i\text{-}\bar{x})^2}\ , \tag{5.2}$$

where m_n – measurement number;
x_i – measurement result i;
$\bar{x}$ – the average of the measurement results, expressed according to equation (5.2) as follows:

$$\bar{x}=\frac{1}{m_n}\sum_{i=1}^{m_n}x_i\ , \tag{5.3}$$

To calculate type B uncertainty, the technical parameters of the measurement device are used. The accuracy of the measurement device can be presented as a relative error, conventional error or an absolute error. In case of most digital measurement devices, the measurement error of the device is expressed as an equation. On the assumption that type B uncertainty is of normal distribution, the uncertainty is expressed as the relation between the absolute error of the measurement device and square root of 3 (Laaneots et al., 2012).

$$U_B = \frac{a_{max}}{\sqrt{3}}, \quad (5.4)$$

where α_{max} – the absolute error of the measurement device.

To calculate the expanded uncertainty, which characterizes measurement uncertainty on an extended confidence level, the combined standard uncertainty U_c is multiplied with the coverage factor k_j.

$$U = U_c k_j, \quad (5.5)$$

where k_j – coverage factor.

The coverage factor k_j depends on the recommended confidence level and the distribution of measurement results. For instance, the coverage factor of measurement results (confidence level of 95%) which conform to normal distribution is k_j = 1.96 (Laaneots & Mathiesen., 2002).

5.2. The uncertainty of test measurement results

In measuring the size of fuel droplets in the air-fuel mixture formed by the pulveriser fuel supply system, the combined standard uncertainties are given in Table 5.1. The example given presents the calculation of expanded uncertainty at bioethanol tests. According to equation (5.2), the standard deviation during measurement of bioethanol fuel droplets D_{50} is:

$$U_{ABE} = \sqrt{\frac{1}{3(3-1)} \cdot ((59.27-57.46)^2 + (51.99-57.46)^2 + (61.12-57.46)^2)} = 2.79 \text{ µm}$$

In case of type B uncertainty, the absolute error is expressed as the product of measurement device error (1%) and the graduated scale (Laaneots & Mathiesen., 2002). During given tests, the maximum value of the graduated scale was 600 µm (the exact data of the measurement device STP5911 is given in subchapter 3.5). The type B uncertainty in case of particular measurements is:

$$U_{BBE} = \frac{0.01 \cdot 600}{\sqrt{3}} = 3.46 \text{ µm}$$

The combined standard uncertainty in the given test is:

$$U_{cBE} = \sqrt{2.79^2 + 3.46^2} = 4.45 \text{ µm}$$

The expanded uncertainty conforming to normal distribution with a confidence level of 95% is:

$$U_{BE}=4.45\cdot 1.96=8.68\ \mu m$$

Next, measurement results with the combined standard uncertainty (parameter D_{50}) of the size of fuel droplets is provided (according to Tables 3.3 to 3.5), whereas the calculations follow the examples given above.

Table 5.1 indicates that the combined standard uncertainty is of approximately the same value in all measurements, except in testing water. This could have been conditioned by the variation in the temperature of the test liquid, a human factor, etc. Based on the given table, it can be said that the test data is trustworthy enough and the air-fuel mixture formed by the pulveriser fuel supply system is comparable with the air-fuel mixture formed by the diesel fuel supply apparatus.

To design a model for selecting the work parameters of a pulveriser fuel supply system, doser capacities of the pulveriser fuel supply system depending on fuel pressure were measured and described in **subchapter 3.7**. More precisely, the amount of fuel flowing through the dosers during a certain period of time was measured during tests. The tests were carried out under fuel pressures of p_f = 1…5 bar at a transfer step of Δp = 1 bar. Two tests were carried out under each pressure. The test liquid used was gasoline E95. The time for measuring the amount of fuel flowing through the dosers was t_t = 15 s. The amount of fuel having flown through the dosers was measured with a weighing machine RADWAG WLC 6/A2 whereas the linearity of the measurement device is ± 0.1 g (Radwag). Therefore, type B uncertainty equals to:

$$U_{BD}=\frac{\alpha_{max}}{\sqrt{3}}=\frac{0.1}{\sqrt{3}}=0.058\ \ g$$

Table 5.2 gives an overview of doser capacities measured during the particular tests with combined standard uncertainty.

Based on the calculated uncertainty, it can be said that the measurement data of the particular test is trustworthy. The greatest value of combined standard uncertainty is U_{cD} = 0.702 g.

Subchapter 4.2 studies the impact of the pulveriser fuel supply system on the combustion process of a compression ignition engine. During

Table 5.1. The values of parameter D_{50} characterizing the size of fuel droplets with combined standard uncertainty.

Designation	Results (D_{50})
DFA injector (DF) 200 bar	D_{50} = (30.6 ± 3.58) µm
PULV. FSS (DF) p_a = 2 bar	D_{50} = (31.7 ± 4.36) µm
PULV. FSS (BE) p_a = 2 bar	D_{50} = (57.5 ± 4.45) µm
PULV. FSS (RO) p_a = 2 bar	D_{50} = (14.2 ± 3.78) µm
PULV. FSS (water) p_a = 2 bar	D_{50} = (49.1 ± 8.09) µm
Maximum uncertainty	8.09 µm

Table 5.2. The combined standard uncertainty of doser capacities of the pulveriser fuel supply system.

Fuel pressure p_f, bar	Test 1	Test 2	Average	Standard deviation	Results q
1	34.2 g	32.8 g	33.5 g	0.70 g	q = (33.5±0.702) g
2	53.0 g	51.8 g	52.4 g	0.60 g	q = (52.4±0.603) g
3	66.9 g	65.6 g	66.3 g	0.65 g	q = (66.3±0.655) g
4	77.6 g	77.1 g	77.4 g	0.26 g	q = (77.4±0.262) g
5	86.0 g	85.6 g	85.8 g	0.20 g	q = (85.8±0.208) g
			Maximum uncertainty		0.702 g

Table 5.3. The combined standard uncertainty of the measurement of combustion pressures in a compression ignition engine.

Designation	DF	23.1% BE, 76.9% DF	42.3% BE, 57.7% DF	56.8% BE, 43.2% DF
Standard deviation at crankshaft rotational angle 300 – 420 CAD	0.15 bar	0.15 bar	0.12 bar	0.097 bar
Combined standard uncertainty at crankshaft rotational angle 300 – 420 CAD	± 0.735 bar	± 0.735 bar	± 0.730 bar	± 0.727 bar
Average combustion pressure at crankshaft rotational angle 300 – 420 CAD	16.6 bar	16.38 bar	16.20 bar	15.54 bra

tests, the combustion pressure of the engine was measured during the use of different air-fuel mixtures. The air-fuel mixtures were formed as follows: 1) an air-fuel mixture of 100% diesel fuel; 2) an air-fuel mixture of bioethanol of 23.1% and diesel fuel of 76.9%; 3) an air-fuel mixture of bioethanol of 42.3% and diesel fuel of 57.7%; 4) an air-fuel mixture

of bioethanol of 56.8% and diesel fuel of 43.2%. The results were calculated based on the averaged results of ten work cycles. The combustion pressure was measured with a device manufactured by the company AVL consisting of a pressure sensor, amplifier, control module, and software. The pressure sensor used during the test was Kistler 701A (the linearity being FSO ≤ ±0.5% with a measure range of 0 – 250 bar) (Kistler), whereas the amplifier and the control module used were AVL 2P2E and AVL 621 accordingly. The error of the pressure sensor is determined together with the amplifier and control module, thus, type B uncertainty is expressed as follows:

$$U_{Bp} = \frac{250 \cdot 0.005}{\sqrt{3}} = 0.72 \text{ bar}$$

Table 5.3 presents the measurement uncertainties of the combustion pressure measurements of a compression ignition engine. The standard deviation of measurement data is calculated during ten work cycles, at every rotational angle of the crankshaft. The standard deviation is calculated on averaging all of the pressures measured in relation to the rotational angle of the crankshaft. The greatest variation in pressures takes place at crankshaft rotational angles of 300 – 420 CAD (see Figure 4.3.). To specify the measurement error, the crankshaft rotational angles of 300 – 420 CAD were chosen to determine the standard deviation of the measurement data of combustion pressures.

The combined standard uncertainty of combustion pressures measured during tests is of the same size range in all tests. Based on the given data, it can be said that the measurement data is trustworthy.

When measuring **diesel consumption**, the device AVL 7351 with a measurement frequency of 20 Hz was used to measure diesel fuel consumption. The device calculates the combined standard uncertainty by factoring in the device error and the standard deviation of measurement data. The measurement error of the device is ≤ 0.12 % (AVL). The combined standard uncertainty of diesel fuel consumption during tests with a compression ignition engine at the crankshaft rotational speed of 1800 rpm is given in Table 5.4.

To measure the consumption of bioethanol, the weighing machine CAS CI-2001A was used. The linearity of the measurement device is 0.01% FS while the scale range is 0 – 20 000 g (CI-2001A/B Owner Manual).

Table 5.4. The measurement uncertainty of fuel consumption in a compression ignition engine at the crankshaft rotational speed of 1800 rpm.

Designation	Test 1 DF	Test 2 23.1% BE, 76.9% DF	Test 3 42.3% BE, 57.7% DF	Test 4 56.8% BE, 43.2% DF
Diesel fuel consumption	1.35 kg h^{-1}	1.14 kg h^{-1}	1.15 kg h^{-1}	1.20 kg h^{-1}
Bioethanol consumption	0 kg h^{-1}	1.5 kg h^{-1}	0.84 kg/h	0.36 kg h^{-1}
Combined standard uncertainty DF	1.04%	1.17%	0.7%	1.91%
Uncertainty BE	-	0.001%	0.002%	0.0055%

Bioethanol consumption was measured during 60 s. The given parameters were measured once on each test, thus, the particular measurement error is described using the measurement device error. The absolute error of the measurement device is:

$$a_{maxW}=0.0001\cdot 20000=2 \text{ g}$$

Table 5.4 gives an overview of the measurement data of bioethanol consumption and the measurement uncertainty at the rotational speed of 1800 rpm of the engine crankshaft.

When measuring fuel consumption, the measurement uncertainty of bioethanol considers only the measurement device error. When taking into account that bioethanol consumption was measured during 60 s, the combined standard uncertainty remains in the same range as when measuring diesel fuel consumption (~2%).

The measurement uncertainty in case of a spark ignition engine is determined in three measured parameters, namely, torque, combustion pressure and fuel consumption. In subchapter 4.4, the fuel consumption of the test engine was measured with a weighing machine CAS CI-2001A. The measurement uncertainty of fuel consumption is considered to be the measurement device error, i.e. a_{maxW} = 2 g (formerly given).

To measure the combustion pressure, a device manufactured by AVL consisting of a pressure sensor, an amplifier, a control module and software was used. The averaged measurement results of ten work cycles have been used in the calculations. The pressure sensor used during the test was

Table 5.5. The measurement uncertainty of combustion pressures measured during tests with bioethanol in a spark ignition engine.

Designation	ORIG FSS	PULV FSS
Standard deviation at crankshaft rotational angle 300 – 420 CAD	0.62 bar	0.57 bar
Combined standard uncertainty at crankshaft rotational angle 300 – 420 CAD	± 0.75 bar	± 0.71 bar
Average combustion pressure at crankshaft rotational angle 300 – 420 CAD	16.9 bar	17.54 bar

AVL GH 132-24 (linearity of FSO ≤ ±0.3%, measure range of 0 – 250 bar) (Kistler), the amplifier and control module used were AVL 2P2E and AVL 621 accordingly. The error of the pressure sensor is determined together with the amplifier and control module, thus, type B uncertainty is expressed as follows:

$$U_{Bp}=\frac{250\cdot 0.005}{\sqrt{3}}=0.72 \text{ bar}$$

The measurement uncertainty of combustion pressure during bioethanol tests on engine load T_{e2} = 30 Nm and n_e = 3690 rpm depicted on Figure 4.8 is given in Table 5.5. The measurement uncertainty of combustion pressures is given at rotational angles of 300…420 CAD of the crankshaft.

To measure engine torque, the test stand KI5543 is complemented with a force transducer HBM S2, which deviation from the measurement results is ΔT_e = 0.25% (HBM). In case of the particular force transducer, it is also essential to consider the accuracy of the graduated scale. The smallest unit of the graduated scale of torque is 10 Nm, in which case the maximum reading error of the graduated scale can be considered to be half of the smallest unit, i.e. ΔT_{ms} = 5 Nm. For instance, at engine crankshaft rotational speed of n_e = 3960 rpm and at engine torque of T_{e2} = 30 Nm, the absolute error of the device a_{maxTe} during torque measurement is:

$$a_{maxTe}=T_e\cdot\Delta T_e+\Delta T_{ms}=30\cdot 0.25+5=5.075 \text{ Nm}$$

Type B uncertainty is according to the equation (5.4) expressed as follows:

$$U_{BTe}=\frac{a_{maxTe}}{\sqrt{3}}=\frac{5.075}{\sqrt{3}}=2.93 \text{ Nm}$$

Since one measurement was carried out during the given tests, the value of torque in case of the abovementioned test is T_{e2} = 30 ± 2.93 Nm.

In Table 5.6, the specifications of unfamiliar devices used during tests are given (Кривенко & Федосов, 1980, CI-2001A/B Owner Manual, Bosch BEA 350 manual).

Table 5.6. Measurement systems' specifications.

Engine teststand KI5543	
Rheostat	Liquid type
Braking power	55 kW
Rotational speed at engine regime	400 – 1500 rpm
Rotational speed during braking	3000 – 1500 rpm
Volume of rheostat	300 L
Maximum torque	400 Nm
Weighing machine CAS CI-2001A	
Load cell excitation voltage	DC 5V, up to 4×350Ω load cells
Full scale input range	20 mV, including dead load
Zero adjust range	0.05mV~5mV
Input sensitivity	2 μV/D 0.5 μV/D
System linearity	Within 0.01% of FS
A/D internal resolution	Approximately 200 000 count
A/D external resolution	5 000 dd (NTEP, OIML) 30 000 dd (Non NTEP, OIML)
A/D conversion speed	10 times/sec
Measure range	0.500 – 20.000 kg
Bosch BEA 350	
Dimensions of all BEA variants with trolley (W × H × D)	750 × 1770 × 700 mm
Dimensions of control units and display units (W × H × D)	470 × 260 × 480 mm
Weight of RTM 430	67 kg
Accuracy range	+5 °C – +40 °C
Functional area	+5 °C – +45 °C
Storage temperature	-25 °C – +60 °C
Power supply	230 V
CO measuring range 0.000 – 10.00% vol	Resolution 0.001%
CO_2 measuring range 0.00 – 18.00% vol	Resolution 0.01%
HC measuring range 0 – 9999 ppm vol	Resolution 1 ppm vol
O_2 measuring range 0.00 – 22.00% vol	Resolution 0.01% vol
λ measuring range 0.500 – 9.999	Resolution 0.001
NO measuring range 0 – 5000 ppm vol	Resolution <= 1 ppm vol
Degree of opacity 0 – 100%	Resolution 0.1%
Absorption coefficient 0 – 10 m^{-1}	Resolution 0.01 m^{-1}

SUMMARY AND CONCLUSIONS

The use of biofuels in engines is a growing trend. Most commonly, standard biofuels, e.g. bioethanol E85, biodiesel, biogas, are used. The use of nonstandard biofuels in engines is not widely spread since their physicochemical properties bring about several issues in the engine as well as in the fuel supply system; nevertheless, their manufacturing is less costly (Küüt, 2013). Some of the issues include the increase in the concentration of harmful components in the exhaust gas, the wearing of the fuel supply system, corrosion, excessive soot in the engine, the coking of the injectors, the injectability, ignition, etc (Courtoy et al., 2009; Ma et al., 2004). To reduce the impact of biofuels on the engine and the fuel supply system, fuel blends are taken into use as the mixing of a biofuel with a standard fuel enables to reduce the impact of biofuels. With regard to the wearing of the fuel supply system, dual-fuel supply systems have been developed as these enable the joint use of biofuels and standard fuels. For the use of nonstandard biofuels, it is rational to use either dual-fuel supply systems or additional fuel supply systems. Engines equipped with an additional fuel supply system run on two fuels whereas the standard fuel is injected into the engine by one fuel supply system and the biofuel by the other fuel supply system (examples in literature include Masahiro, 2003; Cipo & Bhana., 2009). A relevant feature in case of the given solution lies in the fact that the air-fuel mixture is formed of two fuels. It is rational to use dual-fuel supply systems in case of spark ignition engines and additional fuel supply systems in case of compression ignition engines.

The use of biofuels presents a challenge regarding the concentration of components in the exhaust gas of the engine. For example, when using diesel fuel and bioethanol in a compression ignition engine, the combustion temperature reduces and the ignition delay increases which condition the drop in the combustion pressure and the increase in the concentration of HC in the exhaust gas. To improve the combustion process, one of the possibilities would be to reduce the size of fuel droplets in the air-fuel mixture formed of bioethanol to accelerate the evaporation of bioethanol. This would enable to decrease the combustion time of the air-fuel mixture conditioned by the ignition delay. This particular solution enables the use of bioethanol in a compression ignition engine without altering the settings of the engine, e.g. injection timing (Abu-Qudais et al., 2000; Kowalewicz & Pajączek, 2003; Paper I).

The aim of the doctoral thesis was to develop a fuel supply system that would enable the dosing of different biofuels into the cylinders of spark and compression ignition engines while ensuring the formation of small fuel droplets in the air-fuel mixture as well as the resistance of the fuel supply system to the physicochemical properties of biofuels. Based on the aim, the first task was to analyse the suitability of existing fuel supply systems for using biofuels in spark and compression ignition engines. The development of the fuel supply system first required an overview of the combustion process of a compression ignition engine as well as of the impact of biofuels on the exhaust gas emission. The abovementioned overview was comprised based on bioethanol fuel. Tests were carried out with the developed fuel supply system during which the formation of the air-fuel mixture and the size of fuel droplets in the air-fuel mixture were studied. The fuel supply system was developed for use in spark and compression ignition engines. Respective tests were carried out. Engine tests were run using 96.4% bioethanol. Based on test results, the impact of the fuel supply system and bioethanol on the combustion process was analyzed.

The overall results of the doctoral thesis are as follows:

1. The existing fuel supply systems are designed for the dosing of one type of fuel into an engine. The fuel supply systems of gasoline are suitable for dosing bioethanol and biomethanol, however, their use brings about the wearing of work surfaces and the creation of corrosion. Fuel supply systems designed for the use of diesel fuel are suitable for dosing vegetable oils into the engine (Fendt, Valtra). The main issues in case of vegetable oils include their ignition, combustion, flowability, etc. The formation of the air-fuel mixture is relevant as the physicochemical properties of biofuels differ from those of standard fuels, thus, the quality formation of the air-fuel mixture ensures an effective evaporation and combustion of the air-fuel mixture in the cylinder.
2. When bioethanol is used in a compression ignition engine as an additional fuel, the exhaust gas emission of engines equipped with common rail increases (HC, CO, CO_2). In case of engines equipped with a mechanical fuel supply apparatus, the exhaust gas emission mostly decreases (except for HC). To reduce the exhaust gas emission, it is relevant to ensure the high quality air-fuel mixture in the cylinder and the stability of the combustion process. The combustion pressure p of the combustion process can be increased by reducing the size of fuel droplets in the air-fuel mixture. To calculate the combus-

tion pressure p, a model was drawn which enables to calculate the combustion pressure according to the size of droplets in the air-fuel mixture. It is relevant that in case of big fuel droplets (D_{32} = 100 µm and larger), the increase in the combustion pressure in the cylinder is slow. To be more precise, in case the size range of fuel droplets is D_{32} = 500…100 µm, the combustion pressure p doubles, respectively to the reduction in the size of fuel droplets. With regard to the droplet size range of D_{32} = 100…20 µm, the increase in the combustion pressure p is substantially quicker as compared with big fuel droplets. The combustion pressure p increases in case of fuel droplet size range of D_{32} = 100…20 µm by approximately a twice and half times. In case of fuel droplet size range of D_{32} = 20…5 µm, the combustion pressure p roughly doubles. Based on the abovementioned, it can be deduced that as the diameter of a fuel droplet is reduced, the combustion pressure p in the cylinder increases. To ensure the stabile operating of the engine and controlled combustion in the cylinder, the recommended size of fuel droplets in the air-fuel mixture is D_{32} = 15…100 µm. If the fuel droplets are too small, a detonative combustion may occur, which might damage the engine. The abovementioned calculation model also includes several other parameters that depend on the construction of the engine, environmental conditions, etc. Therefore, the combustion pressure calculated by the model may vary in different conditions from 7 – 60%.

3. During the course of the doctoral thesis, two novel fuel supply system solutions were developed (patents EE05665B1 and EE05693B1). Patent EE05665B1 describes a method of air-fuel mixture formation and a fuel supply system operating based on this particular method. The fuel supply system enables to form high quality air-fuel mixture of different fuels and it can be used as an additional or main fuel supply system. Patent EE05693B1 describes an additional fuel supply system which enables to dose liquid biofuels into an engine. This system can only be used as an additional fuel supply system. During the course of work, the solution presented in the patent document EE05665B1 was chosen and it was developed with regard to achieving the aims of the thesis. As a result, a novel fuel supply system was developed, which is more precisely described in the patent application document P201200024 (Patent III) still in process.
4. In case of the air-fuel mixture formed with the developed fuel supply system, the size of fuel droplets in the air-fuel mixture was studied. The results indicated that the size of fuel droplets is mostly affected by the working parameters of the fuel supply system (injection pres-

sure, the distance between injectors) and the viscosity of fuel. As the injection pressure increased, the size of fuel droplets generally reduced, however, the optimal injection pressure in the particular system was determined to be p_a = 2 bar. During tests, it became evident that while using diesel fuel, the size of fuel droplets in the air-fuel mixture formed by the developed fuel supply system was smaller than in the air-fuel mixture formed by the mechanical diesel fuel supply apparatus. In case of the developed fuel supply system, the average size of fuel droplets during bioethanol injection was D_{32} = 22.5 μm. In comparison to the common fuel supply systems developed for dosing gasoline (in-direct injection systems), the size of fuel droplets formed by the pulveriser fuel supply system is approximately four times smaller (the size of bioethanol fuel droplets in a regular PFI injector is $D_{32} \approx 80$ μm).

5. Using the novel fuel supply system as an additional fuel supply system of a compression ignition engine and dosing 96.4% bioethanol into the engine as an additional fuel, the following conclusions were arrived at:

   5.1. The construction and control devices of the fuel supply system are suitable for use on a compression ignition engine.

   5.2. During tests, it became evident that using bioethanol as a diesel engine fuel is rational at elevated rotational speeds on engine idle mode (the nominal rotational speed of the engine) or on engine load. The heat release from the process is too small on engine idle mode to ensure the quality combustion of bioethanol fuel.

   5.3. The stability of the combustion process, the increase in the heat release rate and the intensified heat release are ensured when an air-fuel mixture of small fuel droplet size (bioethanol proportion of up to 25%) is used at elevated rotational speeds on idle mode in a compression ignition engine. When the proportion of bioethanol in the air-fuel mixture is increased over 25%, the intensity of heat release and the combustion pressure decrease whereas the proportion of gross heat release in the combustion process increases.

   5.4. At elevated rotational speeds of the crankshaft in a compression ignition engine (an engine equipped with a mechanical fuel supply apparatus), generally, the proportion of HC in the exhaust gas increases. The proportion of HC increased in case of air-fuel mixtures with different bioethanol fuel proportions. This may have been caused by the creation of water vapour during bioethanol combustion which hinders the complete combustion of diesel fuel. This particular issue requires complementary study in further research.

6. When using the novel fuel supply system in a spark ignition engine, the following conclusions were arrived at:
   6.1. When using the pulveriser fuel supply system, fuel consumption decreased in comparison to the original fuel supply system of the test engine as follows: by ~6% in case of gasoline and by ~3% in case of bioethanol. During tests, it became evident that as engine load increased, the bioethanol consumption of the engine increased rapidly in the pulveriser fuel supply system. This was conditioned by firstly, the construction of the fuel supply system, which did not enable the sufficient air flow into the engine, and secondly, ignition timing, which conditioned the quicker combustion of the air-fuel mixture. As a result, the maximum value of combustion pressure was achieved at top dead centre of the engine or a few crank angle degrees after it, which may have caused the countermining of the combustion pressure to the upward movement of the piston.
   6.2. When using an air-fuel mixture of small fuel droplet size, the combustion pressure and heat release rate increased in the engine. In further research, it is necessary to adjust the ignition angle so it would be suitable for the engine since this would ensure the maximum of combustion pressure after the top dead centre of the piston. During the use of the pulveriser fuel supply system, the combustion pressure and heat release rate increased. In further research, it is necessary adjust the ignition angle to be suitable for the engine so that the maximum of combustion pressure after the top dead centre of the piston would be ensured.
7. During tests with the developed fuel supply system, it became evident that its use enabled to reduce fuel consumption in the engine and ensure the effective combustion of the air-fuel mixture in the engine. An increase in the combustion pressure is conditioned by several influencing factors, e.g. the size of fuel droplets, however, combustion pressure might be affected by the length of the intake manifold, the homogeneity of the air-fuel mixture and the construction of the fuel supply system. The particular thesis outlines the positive effect of the fuel supply system on the combustion process of the engine; nevertheless, it is necessary to further research which of the abovementioned influencing factors impacts the efficiency of the particular system more specifically.
8. In case of the given solution, it is first necessary to solve several constructional issues of the system before arriving at final conclusions about the effectiveness of the fuel supply system. However, these issues can be solved during the further design process of the product.

REFERENCES

Abramzon, B., Sirignano, W.A. 1989. Droplet vaporization model for spray combustion calculations. International Journal of Heat and Mass Transfer. Vol. 32. pp. 1605–1618.

Abu-Qudais, M., Haddad, O., Qudaisat, M. 2000. The effect of alcohol fumigation on diesel engine performance and emissions. Energy Conversion & Management 41, pp. 389–399.

Autodata 2005. Car diagnostic software, version 3.18.

AVL. AVL Fuel Mass Flow Meter and Fuel Temperature Control. Https://www.avl.com/fuel-massflow-meter-and-fuel-temparature-control (20.11.2013)

Chauhan, B.S., Kumar, N., Pal, S.S., Jun, Y.D. 2011. Experimental studies on fumigation of ethanol in a small capacity Diesel engine. Energy Volume 36, Issue 2, pp. 1030–1038.

Bosch BEA 350 manual. BEA Emission Analyzers. Available: http://www.gemco.co.uk/wp-content/uploads/2012/07/BEA-Emissions-.pdf (20.11.2013).

CI-2001A/B Owner Manual. Available: http://www.casturkey.com/Images/Klavuzlar/972001a-om.pdf (20.11.2013)

Cipo, D., Bhana, N. 2009. Fuelling of a compression ignition engine on ethanol with DME as ignition promoter: Effect of injector configuration. Fuel Processing Technology, Volume 90, Issue 9, pp. 1107–1113.

Courtoy, P., Smith, A., Greenhalgh, D. 2009. Multifuelling an engine. International publication number: WO2009/106647 A1. Available: http://v3.espacenet.com/publicationdetails/biblio?DB=EPODOC&adjacent=true&locale=en_EP&FT=D&date=20090903&CC=WO&NR=2009106647A1&KC=A1 (12.11.2013)

D120 technical data. Дизель Д120 техническое описание и инструкция по эксплуатации. (in Russian)

Demirbas, A. 2006. Global biofuel strateegies. Energy Edu. Sci. Tehnol. Turkey. 336 p.

Elwardany, A.E, Sazhin, S.S., Farooq, A. 2013. Modelling of heating and evaporation of gasoline fuel droplets: A comparative analysis of approximations. Fuel, Volume 111, pp. 643–647.

EVS-EN 228:2012. 2012. ISO standard. Mootorikütused. Pliivaba mootoribensiin. Nõuded ja katsemeetodid. (in Estonian)

EVS-EN 590:2009. 2009. ISO standard. Mootorikütused. Diislikütus. Nõuded ja katsemeetodid. (in Estonian)

Farouk, T., Dryer, F. L. 2011. Studies of the combustion of drops in a fuel spray the burning of single drops of fuel. Combustion Theory and Modelling, Volume 15, Issue 4, pp. 487–515.

Filippa, L., Trento, A., Įlvarez, A.M. 2012. Sauter mean diameter determination for the fine fraction of suspended sediments using a LISST-25X diffractometer. Measurement 45, pp. 364–368.

Fowlkes, W.Y. 2010. Patenting TRIZ?. Available: http://www.triz-journal.com/archives/2010/10/03/. (27.02.2012).

Gandhi, A.H., Meinhart, M.A. 2008. Comparison of Measured PFI Spray Characterizations of E85 and N-heptane Fuels for a Flex-Fuel Vehicle. ILASS Americas, 21st Annual Conference on Liquid Atomization and Spray Systems, Orlando, Florida.

GOST 18509-88. 1988. Standard. Дизели тракторные и комбайновые. Методы стендовых испытаний. (in Russian)

Govindarajan, K. 2008. Alcohol as an Automotive Fuel. http://www.cheresources.com/energy_future/ethanol_transportation_fuel.shtml (04.03.2011).

Harndorf, H., Schuemann, U., Wichmann, V., Fink, C. 2008. Motorprozessverhalten und Abgasemissionen alternativer Kraftstoffe im Vergleich mit Dieselkraftstoff, MTZ 7-8/2008, 69 Jahrgang, pp. 640–646.

HBM. Mounting instructions. Force transtrucer S2/S9. Available: http://www.hbm.com.pl/pdf/a0567.pdf (12.12.2013).

Heisler, H. 1995. Advanced engine technology. London, UK, Planta Tree.

Heisler, H. 2001. Advanced engine tehnology. – Oxford: Butterworth – Heimann, 749 p.

Heywood, J.B. 1988. Internal Combustion Engine Fundamentals. Mcgraw-Hill. 930 S.

ISO 5167. International standard. 2003. Measurement of fluid flow by means of pressure differential devices inserted in circular cross-section conduits running full. Part 1: General principles and requirements. Second editition.

ISO 8178:2006. Reciprocating internal combustion engines. Exhaust emission measurement.

Jankowski, A., Sandel, A., Seczyk, J., Sieminska-Jankowska, B. 2002. Analysis of fuel spray preparation for internal combustion engines. Journal of KONES Internal Combustion Engines. No. 1-2 ISSN 1231 - 4005, 323-332 pp.

Johnson, S.M. 1982. Venturi nozzle effects on fuel drop size and nitrogen oxide emission. NASA Technical Paper 2028. Available: http://babel.hathitrust.org/cgi/pt?id=uiug.30112101593710;view=1up;seq=7 (12.12.2013).

Kamboj, K.S., Kairimi, M.N. 2012. Effects of compression ratios, fuels and specific heats on the energy distribution in spark-ignition engine. International Journal of Emerging Technology and Advanced Engineering. ISSN 2250-2459, Volume 2, Issue 8, pp. 482–491.

Kistler. Available: http://www.intertechnology.com/Kistler/pdfs/Pressure_Model_701A.pdf (20.11.2013).

Kowalewicz, A., Pajączek, Z. 2003. Dual fuel engine fuelled with ethanol and diesel fuel. Journal of KONES Internal Combustion Engines vol. 10, 2003, No 1-2, 9.

Kuleshov, A.S. Model for predicting air-fule mixing, combustion and emissioon in DI disesel engines over whole operating range. Available: http://papers.sae.org/2005-01-2119/. (10.05.2013).

Küüt, A. 2013 Characteristics of bioethanol fuel obtained from lignocellulose biomass in internal combustion reciprocating engines with spark- and compression ignition. A Thesis for applying for the Degree of Doctor of Philosophy in Agricultural Engineering. Estonian University of Life Sciences. Tartu.

Кривенко, П.М., Федосов, И.М. 1980. Ремонт и техническое обслуживание системы питания автотракторных двигателей. Колос, Москва (in Russian).

Laaneots, R., Mathiesen, O. 2002. Mõõtmiste alused. Tallinna Raamatutrükikoda. 206 S. (in Estonian)

Laaneots, R., Mathiesen, O., Riim, J. Metroloogia. 2012. Õpik kõrgkoolidele TTÜ kirjastus, Tallinn. (in Estonian)

Labeckas, G., Slavinskas, S., Mažeika, M. 2014. The effect of ethanol–diesel–biodiesel blends on combustion, performance and emissions of a direct injection diesel engine. Energy Conversion and Management. Volume 79, pp 698–720.

Li, T. Nishida, K., Hiroyasu, H. 2011. Droplet size distribution and evaporation characteristics of fuel spray by a swirl type atomizer. Fuel, Volume 90, Issue 7, pp. 2367–2376.

Lu, X., Ma, J., Ji, L., Huang, Z. 2008. Simultaneous reduction of nox emission and smoke opacity of biodiesel-fueled engines by port injection of ethanol. Fuel 87, pp. 1289–1296

Ma, X.Q., DeCarmine, T., Xiao, T.D. 2004. Plasma Spray High Lubricity Nanocomposite Coatings. Thermal Spray 2004, Advances in Tehnology and Application.

Malvren. 2007. Accurate particle sizing of aerosols and sprays. Available: http://www.malvern.com/common/downloads/MRK690.pdf (15.11.2013)

Malvren. 2012. A Basic Guide to Particle Characterization. Available: http://golik.co.il/Data/abasicguidtoparticlecharacterization%282%29_1962085150.pdf pdf (19.11.2013)

Marchenko, A., Osetrov, A., Linkov, O., Samoilenko, D. 2012. Simulation of Biofuels Combustion in Diesel Engines. Intech, Biodiesel - Feedstocks, Production and Applications, Chapter 15, pp. 407–432.

Masahiro, K. 2003. Fuel injection system for internal combustion engine. Application number: JP2003056425. Available: http://worldwide.espacenet.com/publicationdetails/biblio?FT=D&date=20030226&DB=worldwide.espacenet.com&locale=en_EP&CC=JP&NR=2003056425A&KC=A&ND=4 (19.02.2013).

Merker, G.P., Schwarz, C., Teichmann, R. 2012. Grundlagen Verbrennungsmotoren. Funktsionsweise, Simulation, Messtechnik, Aufgabe 6. Springer Fachmedien Wiesbaden gmgh.795 S. (in German)

Norvaišiene, K. 2013. Investigation of radiant inpact on thermal transformations of sprayed water. Summary of Doctoral Dissertation Technological Sciences, Energetics and Power Engineering. Kaunas University of Tehnology, Lithuanian Energy Institute, Kaunas.

Pacek, A.W., Man, C.C., Nienow, A.W. 1998. On the Sauter mean diameter and size distributions in turbulent liquid/liquid dispersions in a stirred vessel. Chemical Engineering Science, Vol. 53, No. 11, pp. 2005–2011.

Parr, E.A. 1998. Hydraulics and preumatics. Second edition. Planta Tree, 244.

Põri, T. 2012. Pulverisaatortoitesüsteem sädesüütega mootorile. Magistritöö tootmistehnika erialal. Eesti Maaülikool, Tehnikainstituut. Juhendaja: Risto Ilves. (in Estonian)

Pulkrabek, W.W. 1997. Engineering fundamentals of the internal combustion engine. Prentice Hall, New Jersey.

Radwag. Balances & Scales. Available: http://www.radwag.com/english/1b_wlc.htm (20.11.2013)

Robert Bosch gmbh (1). 2006. Gasoline-engine management. Chichester, John Wiley & Sohn Ltd, Germany.

Robert Bosch gmbh (2). 2005. Dieselmotor Management, 4th Editor. – John Wiley & Sohn Ltd, Germany – 501 S.

Robert Bosch gmbh (3). 1999. Diesel distributor fuel-injection pumps. Tehnical Instruction. 4th Edition.

Sazhin, S.S., Qubeissi, M. Al., Kolodnytska, R., Elwardany, A.E., Nasiri, R., Heikal, M.R. 2014. Modelling of biodiesel fuel droplet heating and evaporation. Fuel, Volume 115, pp. 559–572

Sepping, R. 2011. Pulverisaatorseadme tööparameetrite karakteristikud. Magistritöö tootmistehnika erialal. Eesti Maaülikool, Tehnikainstituut. Juhendaja: Arne Küüt.

Sescu, C. 2011. Experimental and Computational Study on Liquid Atomization by Slinger Injector. Submitted to the Graduate Faculty as partial fulfillment of the requirements for the Doctor of Philosophy Degree in Engineering. The University of Toledo, Spain, Available: http://etd.ohiolink.edu/send-pdf.cgi/Sescu%20Carmen.pdf?Toledo1310163402 (19.02.2013).

Situ, R., Brown, R.J., Ristovsk,i Z., Kruger, U., Hargreaves, D.J. 2008. Analysis of dual fuel compression ignition (diesel) engine. In: The Seventh International Conference on Modeling and Diagnostics for Advanced Engine Systems. Sapporo, Japan, 9.

Starck, L., Lecointe, B., Forti, L., Jeuland, N. 2010. Impact of fuel characteristics on HCCI combustion: Performances and emissions. Fuel 89, pp. 3069–3077.

Ulrich, T.K., Eppinger, S.D. 1995. Product design and development, Second Edition. Irwin mcgraw-Hill, USA.

Wang, Z., Shuai, S.J., Wang, J.X., Tian, G.H. A computational study of direct injection gasoline HCCI engine with secondary injection. Fuel, September 2006, pp. 1831–1841.

Williams, F.A., 1985. Combustion Theory. The Fundamental Theory of Chemically Reacting Flow System. Second Edition. The Benjamin/Cummings Publishing Company, Inc. USA, 680 p.

KOKKUVÕTE

Biokütuste kasutamine mootorikütusena on üha kasvav trend. Peamiselt on kasutusel standardbiokütused, näiteks bioetanool E85, biodiislikütus, biogaas. Mittestandardsete biokütuste kasutamine mootorikütustena ei ole laialdaselt levinud, sest nende füüsikalis-keemilised omadused põhjustavad mitmeid probleeme mootorites ning toitesüsteemides, samas on nende tootmine odavam (Küüt, et al. 2013). Probleemideks on ka mootorite heitgaasides sisalduvate ühendite kontsentratsiooni suurenemine, toitesüsteemide kulumine, korrosioon, mootori tahmumine, pihustite koksistumine, pihustatavus, süttivus jne (Courtoy et al., 2009; Ma et al., 2004). Vähendamaks biokütuste mõju mootorile ning toitesüsteemile, on kasutusele võetud kütusesegud, kus biokütuse segamine tavakütusega võimaldab vähendada biokütuste mõju mootorile ning toitesüsteemile. Käsitledes ainult toitesüsteemi kulumist, on väljatöötatud ka kahesüsteemsed toitesüsteemid, mis võimaldavad biokütuste ja standardkütuste koos kasutamist. Mittestandardsete biokütuste kasutamiseks on otstarbekas kasutada kahesüsteemseid toitesüsteeme või lisatoitesüsteeme. Lisatoitesüsteemiga varustatud mootorid töötavad kahe kütusega, kus standardkütus pihustatakse mootorisse ühe toitesüsteemi abil ning biokütus teise toitesüsteemi abil (näiteid allikates (Masahiro, 2003; Cipo & Bhana., 2009)). Oluliseks tunnusteks antud lahenduse puhul on, et küttesegu moodustatakse kahest kütusest. Sädesüütega mootorite puhul on otstarbekas kasutada kahesüsteemseid toitesüsteeme, survesüütega mootorite puhul lisatoitesüsteeme.

Biokütuste kasutamisel on probleemiks mootori heitgaasides sisalduvate ühendite osakaal, sest kasutades näiteks survesüütega mootoris diislikütust ning bioetanooli, väheneb põlemise temperatuur mis tingib põlemisrõhu languse ning HC osakaalu suurenemise heitgaasides. Põlemisprotsessi parendamiseks on üheks võimaluseks vähendada bioetanoolist moodustatud küttesegus sisalduvate piiskade suurust, et kiirendada bioetanooli aurustumist. See võimaldab vähendada süüteviivisest tingitud küttesegu põlemise aega. Antud lahendus võimaldab kasutada bioetanooli survesüütega mootori kütusena, muutmata mootori seadistusi, näiteks pritsenurka (Abu-Qudais et al., 2000; Kowalewicz & Pajączek, 2003; Paper I).

Doktoritöö eesmärgiks oli välja töötada toitesüsteem, mis võimaldaks doseerida erinevaid biokütuseid säde- ja survesüütega mootori silindrisse,

tagades väikeste kütusepiiskade moodustumise küttesegus ja toitesüsteemi vastupidavuse biokütuste füüsikalis-keemilistele omadustele. Tulenevalt eesmärgist oli esimeseks ülesandeks analüüsida olemasolevate toitesüsteemide sobivust biokütuste kasutamiseks säde- ja survesüütega mootorites. Toitesüsteemi väljatöötamiseks anti ülevaade survesüütega mootori põlemisprotsessist ning biokütuse mõjust heitgaaside emisioonile. Eelmainitud ülevaade koostati bioetanoolkütuse näitel. Väljatöötatud toitesüsteemiga on läbiviidud katsetused, kus on uuritud selle küttesegu moodustamist ning küttesegus sisalduvate kütusepiikade suurust. Toitesüsteem on arendatud töötama säde- ja survesüütega mootoritel. Mootorikatsetused on läbiviidud 96.4% bioetanooliga. Katsetustel saadud andmete põhjal on analüüsitud toitesüsteemi ja bioetanooli mõju mootorite põlemisprotsessile.

Doktoritöö tulemused on kokkuvõtvalt järgmised:

1. Olemasolevad toitesüsteemid on ettenähtud ühte tüüpi kütuse doseerimiseks mootorisse. Mootoribensiini toitesüsteemid sobivad bioetanooli ja –metanooli doseerimiseks kuid nende kasutamise probleemsus seisneb peamiselt tööpindade kulumises ning korrosiooni tekkimises. Toitesüsteemid, mis on ettenähtud diislikütuse kasutamiseks, sobivad taimsete õlide doseerimiseks mootorisse (Fendt, Valtra). Peamisteks probleemideks taimsete õlide puhul on nende süttimine ja põlemine, voolavus jne. Oluline on küttesegu moodustumine, sest biokütuste füüsikalis-keemilised omadused erinevad standardkütuste omadest, mistõttu tagab kvaliteetne küttsegu moodustumine efektiivse küttsegu aurustumise ja põlemise silindris.
2. Bioetanooli kasutamisel survesüütega mootori lisakütusena, suureneb ühisanumaga varustatud mootorite heitgaaside emisioon (HC, CO, CO_2 suureneb). Mehhaanilise toiteaparatuuriga varustatud mootorite puhul heitgaaside emisioon peamiselt väheneb (va. HC). Heitgaaside emisiooni vähendamiseks on oluline tagada kvaliteetne küttesegu silindris ning põlemisprotsessi stabiilsus. Põlemisprotsessi põlemisrõhku p saab suurendada kütusepiiskade suuruse vähendamisega küttesegus. Põlemisrõhu p arvutamiseks on koostatud mudel, mis võimaldab arvutada põlemisrõhku p vastavalt piisa suurusele küttesegus. Oluline on, et suurte kütusepiiskade puhul, D_{32} = 100 µm ja suuremad, on põlemisrõhu kasv silindris aeglane. See tähendab, et näiteks kütusepiiskade suurusulatuse D_{32} = 500…100 µm puhul, suureneb põlemisrõhk p kaks korda, vastavalt piisa suuruse vähenemisele. Vaadeldes piiskade suurusulatust D_{32} = 100…20 µm, on põlemisrõhu p kasv

oluliselt kiirem võrreldes suurte kütusepiiskadega. Põlemisrõhk p kasvab kütusepiiskade suurusulatuse D_{32} = 100…20 µm puhul ligikaudu kaks ja pool korda. Kütusepiiskade suurusulatuses D_{32} = 20…5 µm suureneb põlemisrõhk p ligikaudu kaks korda. Eeltoodust saab järeldada, et kütusepiisa läbimõõdu vähenemisel suureneb põlemisrõhk p silindris. Tagamaks mootori stabiilne töö ning kontrollitud põlemine silindris, on soovitatav kütusepiiskade suurus küttesegus D_{32} = 15…100 µm. Liialt väikeste kütusepiiskade puhul võib tekkida detoneeriv põlemine, mis võib kahjustada mootorit. Eelmainitud arvutusmudel hõlmab ka mitmeid teisi parameetreid, mis sõltuvad mootori konstruktsioonist, keskkonnatingimustest jne. Seepärast võib mudeliga arvutatav põlemisrõhk muutuda erinevate tingimuste korral 7 – 60%.

3. Doktoritöö käigus on välja töötatud kaks uudset toitesüsteemi lahendust (patent EE05665B1 ja EE05693B1). Patent EE05665B1 kirjeldab küttesegu moodustamise meetodit ja antud meetodiga töötavat toitesüsteemi. Toitesüsteem võimaldab moodustada kvaliteetse küttesegu erinevatest kütustest ning seda saab kasutada nii lisa- kui põhitoitesüsteemina. Patent EE05693B1 kirjeldab lisatoitesüsteemi, mis võimaldab doseerida vedelaid biokütuseid mootorisse. Süsteemi saab kasutada ainult lisatoitesüsteemina. Töö käigus valiti patendidokumendis EE05665B1 toodud lahendus ning arendati seda vastavalt töös tood eesmärkide täitmiseks. Tulemuseks töötati välja uudne toitesüsteemi lahendus, mis on kirjeldatud täpsemalt menetluses olevas patenditaotluses P201200024.
4. Välja töötatud toitesüsteemiga moodustatud küttesegu puhul on uuritud kütusepiiskade suurust küttesegus. Tulemustest selgus, et kütusepiiskade suurust mõjutavad eelkõige toitesüsteemi tööparameetrid (pihustusrõhk, pihustite vaheline kaugus) ning kütuse viskoossus. Pihustusrõhu kasvades vähenes üldjuhul kütusepiiskade suurus, kuid optimaalseks pihustusrõhuks antud süsteemis määrati p_a = 2 bar. Katsetustes selgus, et väljatöötatud toitesüsteemi moodustatud küttesegus sisalduvate kütusepiiskade suurus on väiksem, kui tavapärase mehhaanilise diiseltoiteaparatuuriga moodustatud küttesegu. Bioetanooli pihustamisel oli välja töötatud toitesüsteemi puhul kütusepiiskade keskmiseks suuruseks D_{32} = 22.5 µm. Võrreldes tavapäraste mootoribensiini doseerimiseks väljatöötatud toitesüsteemidega on piiskade suurus ligikaudu neli korda väiksem (bioetanooli kütusepiiskade suurus tavapärase mootoribensiini pihustiga on $D_{32} \approx$ 80 µm).

5. Kasutades uudset toitesüsteemi survesüütega mootori lisatoitesüsteemina ning doseerides mootorisse lisakütusena 96.4% bioetanooli, saadi järgmised tulemused:
   5.1. Toitesüsteemi konstruktsioon ja juhtseadmed sobivad survesüütega mootoril kasutamiseks.
   5.2. Katsetustel ilmnes, et bioetanooli kasutamine diiselmootori kütusena on otstarbekas mootori kõrgendatud tühikäigu pöörlemissagedustel (mootori nimipöörlemissagedusel) või mootori koormamisel. Mootori töötamisel tühikäigul, on protsessist eralduv energia liialt väike, et tagada bioetanoolkütuse kvaliteetne põlemine.
   5.3. Survesüütega mootori kõrgendatud tühikäigupööretel, peenefraktsioonilise bioetanooli, kuni 25% osakaaluga küttesegu kasutamisel, tagatakse põlemisprotsessi stabiilsus, põlemisrõhu jäämine samasse suurusjärku mis ainult diislikütuse kasutamisel, energia vabanemise kasv mootori väntvõlli pöördenurga kohta ning vabanemise intensiivsuse suurenemine. Bioetanooli osakaalu suurenemisel küttesegus üle 25% väheneb energia eraldumise intensiivsus, põlemise rõhk ning suureneb bruto-energia osakaal põlemisprotsessis.
   5.4. Heitgaasidest suurenes peamiselt survesüütega mootori (mehhaanilise toiteaparatuuriga varustatud mootor) väntvõlli kõrgendatud pöörlemissagedustel HC osakaal. HC osakaal suurenes erinevate bioetanoolkütuse osakaaludega küttesegude puhul. Selle põhjuseks võib olla veeauru tekkimine bioetanooli põlemisel, mis pärsib diislikütuse täielikku põlemist. Antud probleem vajab täiendavat uurimist edaspidistes uurimistöödes.
6. Kasutades uudset toitesüsteemi sädesüütega mootori toitesüsteemina, saadi järgmised tulemused:
   6.1. Pulverisaatortoitesüsteemi kasutamisel vähenes kütusekulu, võrreldes katsemootori originaaltoitesüsteemiga järgmiselt: mootoribensiiniga keskmiselt ~6% ning bioetanooliga ~3%. Katsetustel ilmnes, et koormuse kasvades suurenes pulverisaatortoitesüsteemi puhul äkiliselt mootori kütusekulu. See on tingitud toiteseadme konstruktsioonist, mis ei võimalda piisavat õhu pealevoolu mootorisse ning süüte ajastusest, mis tingis küttesegu kiirema põlemise. Selle tulemusel saavutati maksimaalne põlemisrõhu väärtus mootori ülemises surnud seisus või mõned kraadid peale seda, mis põhjustab põlemisrõhu vastutöötamist kolvi tõusule.
   6.2. Toitesüsteemi kasutamisel suurenes mootoris põlemisrõhk ja energia eraldumise kiirus väntvõlli pöördenurga kohta. Edaspidistes

uurimistöödes on oluline häälestada mootorile sobiv süütenurk, mis tagaks põlemisrõhu maksimumi pärast kolvi ülemist surnud seisu.

7. Väljatöötatud toitesüsteemi katsetamisest selgub, et selle kasutamine võimaldab mootori kütusekulu vähendamist ning tagab küttesegu efektiivse põlemise mootoris. Põlemisrõhu suurenemine on tingitud mitmetest mõjuteguritest, näiteks kütusepiiskade suurusest, kuid lisaks võib mõjutad põlemisrõhku mootori sisselaskekollektori pikkus, küttesegu homogeensus ning toitesüsteemi konstruktsioon. Antud töös tuuakse välja toitesüsteemi positiivne mõju mootori põlemisprotsessile kuid täiendavalt on vajalik uurida, milline eeltoodud mõjutegur täpsemalt mõjutab antud süsteemi efektiivsust.
8. Antud lahenduse puhul on vajalik lahendada mitmeid süsteemi konstruktsioonilisi probleeme, tegemaks lõplikke järeldusi toitesüsteemi efektiivsuse kohta. Antud probleemid saab lahendada edaspidise toote disaini käigus.

ACKNOWLEDGEMENTS

The thesis has been completed thanks to the Estonian University of Life Sciences, Institute of Technology.

I would like to thank:

My supervisor, Professor Jüri Olt.

Arne Küüt, Villu Mikita, Vello Merilo, Kaie Ritslaid, Timo Kikas, Marten Madissoo, Kaarel Soots, and other colleagues from the Estonian University of Life Sciences.

Last but not least, many thanks to my family for supporting me in my studies.

CURRICULUM VITAE

Personal data

Name:	Risto Ilves
Date of birth:	26th August 1985
Address:	Estonian University of Life Sciences, Kreutzwaldi 56, Tartu
Phone:	+372 58161529
E-mail:	risto.ilves@emu.ee
Family:	Married, 1 child

Education

2010...	PhD studies, Estonian University of Life Sciences, Institute of Technology
2007–2009	Master's degree studies, Estonian University of Life Sciences, Institute of Technology
2004–2007	Bachelor's degree studies, Estonian University of Life Sciences, Institute of Technology
2001–2004	Nõo Real Gymnasium
1992–2001	Nõo Primary school

Research activity

Degree information:

2009	M.Sc. Production Engineering, (Estonian University of Life Sciences, Institute of Technology)

Honours and awards:

2010	Invention contest of Institute of Technology and College of Technology "Engineering Student Invents 2010" I place. "Additional Fuel Supply System for using bioethanol in diesel engines"
2012	Invention contest of Institute of Technology and College of Technology "Engineering Student Invents 2012" I place. "Additional Fuel Supply System for using liquid biofuels in spark and compression ignition engines"

Field of research:

Natural Sciences and Engineering, Energetic Research and Product Development

Complementary education:

2009–2010	In-service training for car engineers, Tallinn University of Technology, Estonia.
2010	In-service training for car engineers, Tallinn University of Technology, Estonia.
2011	Seminar: Overview of combustion measurement, Graz, Austria, AVL.
2013	In-service training: Bosch diagnostic software ESI[tronic] 2.0 and FSA 740. Robert Bosch OÜ.
2013	Intensive course: Current Trends in Process Type Production and Discrete Type Manufacturing. Estonian University of Life Sciences

Projects:

2012	Project: Modified fuel supply and ignition system piston engine testing, diagnosing and adjusting. Principal investigator (responsible person: Jüri Olt)
2012	Project: 8-2/T12146TEPT Addinol MZ 408 two-stroke engine oil extensive usage. Principal investigator (responsible person: Jüri Olt)

Theses supervised:

2011	Aimar Sukamägi, Master's degree, (sup) **Risto Ilves**, The electronic operating module of the pulveriser feed system.
2012	Taavi Põri, Master's degree, (sup) **Risto Ilves**, A Pulverizing Fuel Supply System for the Spark Ignition Engine.

Career

2009...	Estonian University of Life Sciences, Institute of Technology, Specialist.
2007–2009	Estonian Aviation Academy, Training coordinator.

ELULOOKIRJELDUS

Isikuandmed

Nimi:	Risto Ilves
Sünniaeg:	26. august 1985
Aadress:	Eesti Maaülikool, Kreutzwaldi 56, Tartu
Telefon:	+372 58161529
E-post:	risto.ilves@emu.ee
Perekond:	Abielus, 1 laps

Haridustee

2010…	Eesti Maaülikool, Tehnikainstituut, doktorant
2007–2009	Eesti Maaülikool, Tehnikainstituut, magister
2004–2007	Bakalaureuseõpe, Eesti Maaülikool, Tehnikainstituut
2001–2004	Nõo Reaalgümnaasium
1992–2001	Nõo Põhikool

Teadustegevus

Teaduskraadi info:

2009	Tehnikateaduste magister tootmistehnika erialal (Eesti Maaülikool)

Teaduspreemiad ja-tunnustused:

2010	EMÜ Tehnikainstituudi ja Tartu Tehnikakolledži leiutuskonkurss „Tehnikatudeng leiutab 2010“, I koht. „Lisatoitesüsteem bioetanooli kasutamiseks diiselmootorites“
2012	EMÜ Tehnikainstituudi ja Tartu Tehnikakolledži leiutuskonkurss „Tehnikatudeng leiutab 2012“, I koht. „Lisatoitesüsteem vedelate biokütuste kasutamiseks säde- ja survesüütega mootorites“.

Teadustöö põhisuunad:

Loodusteadused ja tehnika, energeetikaalased uuringud, tootearendus.

Täiendkoolitus:

2009–2010	Täiendkoolitus autodiagnostikutele, Tallinna Tehnikaülikool, Eesti
2010	Täiendkoolitus autodiagnostikutele, Tallinna Tehnikaülikool, Eesti.
2011	Seminar: Põlemisprotsessi uurimise mõõteseadmed, Graz, Austria, AVL.
2013	Täiendkoolitus: Bosch diagnostikatarkvara ESI[tronic] 2.0 and FSA 740. Robert Bosch OÜ.
2013	Kursus: Mõõtmised, modelleerimine, automatiseerimine täppispõllumajanduses (ka täppispidamisel) ja toidu tooteahelas. Eesti Maaülikool.

Projektid:

2012	Projekt Modifitseeritud toite- ja süütesüsteemiga kolbmootori testimine, diagnoosimine ja häälestamine. Põhitäitja (Vastutav täitja: Jüri Olt)
2012	Projekt 8-2/T12146TEPT Addinoli kahetaktilise mootoriõli MZ 408 kasutusvõimaluste laiendamine. Põhitäitja (Vastutav täitja: Jüri Olt)

Juhendatud väitekirjad:

2011	Aimar Sukamägi, magistrikraad, (juh) **Risto Ilves**, Pulverisaatortoitesüsteemi elektrooniline juhtmoodul.
2012	Taavi Põri, magistrikraad, (juh) **Risto Ilves**, Pulverisaatortoitesüsteem sädesüütega mootorile.

Teenistuskäik

2009…	Eesti Maaülikool, tehnikainstituut, spetsialist.
2007–2009	Eesti Lennuakadeemia, koolituskordinaator.

ETTEKANDED

Suulised ettekanded rahvusvahelistel konverentsidel:

International Scientific Conference Biosystem Engineering 2010, Tartu, Eesti, Eesti Maaülikool, Common Rail Diesel Feed System Diagnosing Tehnology, **Ilves, R.**; Mikita, V.; Traat, Ü.; Gregor, A.

International Scientific Conference Biosystem Engineering 2011, Tartu, Eesti, Eesti Maaülikool, Common Rail Diesel Feed System Diagnosing Tehnology, **Ilves, R.**; Mikita, V.; Traat, Ü.; Gregor, A.

8th International Conf. of DAAAM Baltic Industrial Engineering, 19–21 april 2012, Tallinn. **Ilves, R.**; Küüt, A.; Mikita, V.; Olt, J.

International Scientific Conference Biosystem Engineering 2012, Tartu, Eesti, Eesti Maaülikool, Study of prior art of spark ignition engine fuel supply system, **Ilves, R.**; Olt, J.

International Scientific Conference Biosystem Engineering 2013, Tartu, Eesti, Eesti Maaülikool, The forming and combustion of diesel fuel and bioethanol air fuel mixtures in a dual-fuel compression ignition engine, **Ilves, R.**; Olt, J.

10th International Scientific Conference Engineering for rural development, 26.05.2011 – 27.05.2011, Jelgava, Läti, „Impact of ethanol on the fuel injection pump of diesel engine", Olt, J.; Mikita, V.; **Ilves, R.**; Küüt, A.; Madissoo, M.

International Scientific Conference Engineering of Agricultural Tehnologies – 2013, The impact of bioethanol fuel on agricultural tractor engine's exhaust gas. **Ilves, R.**; Sakalauskas, A.; Olt, J.

International Scientific Conference Biosystem Engineering 2014, Tartu, Eesti, Eesti Maaülikool, The Influence of Bioethanol Small Fuel Drops Size Air-Fuel Mixture on Spark Ignition Engine's Combustion Process, **Ilves, R.**; Küüt, A.; Kikas, T.; Olt, J.

Stendettekanne rahvusvahelisel konverentsil:

XXXIV CIOCTA-CIGR V Conference 2011, 29.06.2011 – 01.07.2011, Viin, Austria, „Motor method evaluation of fuel-air mixtures created by using qualitative and quantitative methods", Olt, J.; Mikita, V.; **Ilves, R.**; Küüt, A., stendiettekanne.

Ettekanded kohalikel konverentsidel:

Konverents TEUK XIII, Bioetanooli kasutus diiselmootoris. 10. november 2011.

VIIS VIIMAST KAITSMIST

KATRIT KARUS

EFFECTS OF MACROPHYTES, FISH AND METAZOOPLANKTON ON A MICROBIAL FOOD WEB

VEETAIMESTIKU, KALADE JA METAZOOPLANKTONI MÕJU MIKROOBSELE TOIDUAHELALE

Vanemteadur **Priit Zingel**

28. august 2014

KAIRE LANNO

LONG-TERM CHANGES IN THE ESTONIAN FLORA AND MEASURES FOR CONSERVATION

PIKAAJALISED MUUTUSED EESTI TAIMESTIKUS JA FLOORA KAITSMISEKS SOBIVAD LOODUSKAITSEMEETMED

Vanemteadur **Marek Sammul**

28. august 2014

DIANA LAARMANN

MONITORING AND EVALUATION OF FOREST ECOSYSTEM RESTORATION

METSAÖKOSÜSTEEMI TAASTAMISE SEIRE JA ANALÜÜS

Dotsent **Henn Korjus**, juhtiv teadur **John A. Stanturf**

29. august 2014

MATS VARIK

CARBON FLUXES AND STORAGES IN A CHRONOSEQUENCE OF SILVER BIRCH STANDS

SÜSINIKU VOOD JA VARUD ERIVANUSELISTES ARUKAASIKUTES

Dotsent **Veiko Uri**, professor **Krista Lõhmus**

29. august 2014

INDREK MELTS

BIOMASS FROM SEMI-NATURAL GRASSLANDS FOR BIOENERGY

POOLLOODUSLIKE ROHUMAADE BIOMASSI KASUTAMINE BIOENERGIA TOOTMISEKS

Vanemteadur **Katrin Heinsoo**, professor **Tiiu Kull**

23. september 2014

ISBN 978-9949-536-58-0 (trükis)
ISBN 978-9949-536-59-7 (pdf)

roheline trükis
Trükitud taastoodetud paberile looduslike trükivärvidega. ©Ecoprint